Estimates of Spiral Ganglion Neuron Health in Children and Adults with Cochlear Implants

Kelly N. Jahn

A dissertation

submitted in partial fulfillment of the

requirements for the degree of

Doctor of Philosophy

University of Washington

2019

Reading Committee:

Kelly Tremblay, Chair

Julie Arenberg

Susan Norton

David Horn

Program Authorized to Offer Degree:

Speech and Hearing Sciences

University of Washington

Abstract

Estimates of Spiral Ganglion Neuron Health in Children and Adults with Cochlear Implants

Kelly N. Jahn

Chair of the Supervisory Committee:
Kelly Tremblay
Department of Speech and Hearing Sciences

Cochlear implants (CIs) can improve auditory perception for children and adults with severe to profound hearing loss, but little is known about how to optimize clinical interventions for individual patients. In fact, children and adults receive largely the same CI programming strategies despite their divergent hearing histories and auditory needs. Since CIs are designed to interface directly with the auditory nerve, knowledge of the physiological integrity of the spiral ganglion neurons (SGNs) may assist in developing patient-specific programming recommendations for children and adults. A series of experiments was conducted to quantify various aspects of SGN health in children and adults with CIs. Using the electrically evoked compound action potential (ECAP), the first two experiments determined whether local (within-ear) or global (across-ear) estimates of SGN density differ between child-implanted and adult-implanted listeners. A third experiment assessed the validity of using polarity sensitivity to infer the health of the peripheral processes in CI listeners, and a fourth experiment determined whether polarity sensitivity differed between children and adults with CIs. The results of these experiments suggested that young CI listeners who were deafened and implanted during

childhood likely have denser populations of viable SGNs than older, adult-implanted listeners. However, deaf individuals may experience some degree of peripheral process degeneration regardless of their hearing history. The knowledge gained from these experiments suggests that optimal CI programming strategies may differ for children and adults. The results of this dissertation provide several avenues for future investigation of individualized programming parameters in listeners with diverse hearing histories.

TABLE OF CONTENTS

LIST OF FIGURES

LIST OF TABLES

ACKNOWLEDGEMENTS

I would like to thank my supervisory committee members, who provided mentorship and guidance throughout the Ph.D. program: Julie Arenberg, Susan Norton, David Horn, Kelly Tremblay, and Richard Wright. I am especially appreciative of my Ph.D. advisor, Julie Arenberg, who provided the training and resources necessary to carry out these research endeavors.

I am grateful for the many friends, colleagues, and mentors who have provided valuable support and insight (scientific or otherwise) throughout the first stages of my career: Matthew Winn, Lisa Cunningham, René Gifford, Wendy Parkinson, Shae DiNino, Ashley Moore, Elle O'Brien, Molly Bergan, Katie Brown, Reva Zimmerman, Patrick Donnelly, Maggie Clarke, and Lindsay DeVries. I would also like to thank Leonid Litvak, Bob Carlyon, Christopher Long, Steven Bierer, and Tim Holden for their scientific and technical support over the years.

Finally, I am thankful for the many children and adults with cochlear implants that dedicated their time to participating in these research projects. Their devotion and interest in research are essential to scientific advancement.

This research was supported by two grants from the National Institutes of Health National Institute on Deafness and Other Communication Disorders (NIH NIDCD): T32 DC005361 (Jahn, PI: Perkel) and R01 DC012142 (Arenberg).

DEDICATION

This dissertation is dedicated to my husband, Russell Freda. Thank you for providing a consistent example of personal and professional balance, an unwavering positive outlook on life, and very good food.

CHAPTER 1. INTRODUCTION

Cochlear implants (CIs) are prosthetic devices that can improve auditory perception for children and adults with severe to profound sensorineural hearing loss by directly stimulating residual auditory nerve fibers with electric pulses. A CI consists of both externally worn and surgically implanted components. External microphones detect acoustic signals in the environment and relay them to a speech processor. Within the speech processor, a bank of bandpass analysis filters divides the acoustic signal into several frequency bands and converts it to a digital signal. An external headpiece transmits the digital signal through the skin via radio frequencies to an implanted receiver/stimulator. There, the digital signal is converted to electrical pulse trains and delivered to an array of 12-22 electrodes that are implanted in the scala tympani of the cochlea.

The cochlea is spiral-shaped and tonotopically organized such that, in acoustic hearing, high frequencies are encoded at the base and low frequencies are encoded at the apex. Taking advantage of the natural tonotopic organization of the cochlea, each CI electrode delivers a specific band of frequency information to adjacent spiral ganglion neurons (SGNs): apical electrodes transmit low frequency information and basal electrodes transmit high frequency information. Electrical pulses directly depolarize the SGNs, leading to action potential generation and transmission of the signal through the ascending neural pathway.

Because SGNs are the targets of electrical stimulation by a CI, a common assumption is that the integrity of the SGNs influences transmission of auditory information and can impact perceptual outcomes with an implant (Pfingst et al. 2015). Moreover, it is believed that within- and across-ear variation in SGN integrity may assist in developing listener-tailored programming

interventions (Zhou 2017). However, little is known about the *in vivo* status of the SGNs in CI listeners, especially in those who were deafened and implanted as children. The overall goal of the experiments in this dissertation is to characterize estimated SGN health in children and adults with CIs and to provide recommendations for using that information to investigate individualized CI stimulation strategies in listeners with diverse hearing histories.

In a deafened ear, the number of viable auditory nerve fibers is often significantly reduced relative to normal. Post-mortem human temporal bone analyses show that the density of remaining SGNs also varies as a function of patient-specific demographic characteristics that inherently differ between children and adults with CIs. Hearing loss etiology, which often differs between individuals with childhood- versus adult-onset deafness, is a strong predictor of SGN survival (Otte et al. 1978; Nadol et al. 1989; Nadol 1997). Furthermore, SGN cell counts are lowest in the temporal bones of older adults and in those who experienced relatively long durations of hearing loss or total deafness during life (Otte et al. 1978; Nadol et al. 1989; Nadol 1997; Makary et al. 2011). There is also evidence that chronic electrical stimulation in neonatally deafened animals may promote SGN survival (Lousteau 1987; Leake et al. 1991, 1992, 1999). These findings suggest that SGN density likely differs between young individuals who were deafened and implanted early in life, and older adult-deafened and implanted listeners. However, little is known about whether in vivo SGN density differs between children and adults with CIs, or whether that information could be used to improve CI programming interventions.

Experiments 1 and 2 of this dissertation determined whether global (across-channel) and local (single-channel) in vivo estimates of SGN density differ between children and adults with CIs. Both experiments estimated SGN density using the electrically evoked compound action potential (ECAP), a clinically relevant evoked potential estimate of the auditory nerve response

to electrical stimulation. The ECAP represents a synchronous response from a group of electrically stimulated auditory nerve fibers and is similar to wave I of the electrically evoked auditory brainstem response (EABR; reviewed by He et al. 2017). Electrophysiological evidence in deafened animals consistently demonstrates that morphological characteristics of the ECAP and EABR wave I are predictive of SGN density (Hall 1990; Miller et al. 1994; Shepherd and Javel 1997; Pfingst et al. 2015). Specifically, in response to electrical stimulation through a CI, animals with low SGN cell counts often have elevated evoked potential thresholds, reduced amplitudes, and shallower amplitude growth functions compared to animals with healthy SGN populations (Hall 1990; Shepherd and Javel 1997; Pfingst et al. 2015).

Furthermore, the *change* in ECAP amplitude, threshold, and amplitude growth function slope as the interphase gap of the stimulus is increased, is reflective of SGN density (Prado-Guitierrez et al. 2006; Ramekers et al. 2014). In general, when the interphase gap of the stimulus is increased, evoked potential amplitudes and slopes increase, and thresholds decrease; however, the magnitude of this change (i.e., the interphase gap effect) is smaller in animals with relatively low SGN densities than in animals with healthy SGN populations (Prado-Guitierrez et al. 2006; Ramekers et al. 2014). To date, little is known about how ECAP estimates of SGN density differ between children and adults with CIs, and the interphase gap effect has not been assessed in pediatric CI listeners.

Accordingly, Experiment 1, “Multiple evoked potential estimates of spiral ganglion density differ between younger and older listeners with cochlear implants”, assessed global differences in estimated SGN density between child- and adult-implanted listeners using standard ECAP measures (amplitude, growth function slope, and threshold) and their respective interphase gap effects. This experiment also assessed relationships between speech perception

performance and each estimate of SGN density. Experiment 2, "Differences between local and global evoked potential estimates of the cochlear implant electrode-neuron interface in younger and older listeners", built upon the findings of Experiment 1 to determine whether clinically relevant evoked potential estimates of SGN density could be used to identify CI channels with relatively good and poor electrode-neuron interfaces in both children and adults with CIs.

Notably, the status of the auditory nerve in deafened ears is likely influenced by physiological changes other than SGN density. In addition to a likely reduction in SGN cell counts with increasing auditory deprivation, residual SGNs may be physiologically compromised due to shrinkage, loss of peripheral processes, and/or demyelination (Johnsson 1974; Linthicum et al. 1991; Nadol et al. 2001). Thus, it is important to consider whether physiological differences besides SGN density vary as a function of hearing history in CI listeners, and whether that information can assist in implementing patient-specific clinical interventions. Accordingly, Experiment 3 of this dissertation assessed the validity of using polarity sensitivity, a proposed estimate of peripheral process integrity, to infer the status of the SGNs in CI listeners. Experiment 4 built upon Experiment 3 to determine whether polarity sensitivity differed between children and adults with CIs.

Cochlear implants typically stimulate the auditory nerve with trains of biphasic electrical pulses that consist of cathodic (negative polarity) and anodic (positive polarity) phases. Recent biophysical modeling evidence suggests that sensitivity to the polarity of an electrical stimulus may provide an indication of the integrity of the peripheral processes (Rattay et al. 2001a, 2001b; Joshi et al. 2017; Resnick et al. 2018). Specifically, cathodic and anodic pulse polarities are equally effective in generating action potentials when the peripheral processes of the auditory nerve are intact. However, when the peripheral processes have degenerated or demyelinated, the

cathodic polarity requires higher current levels than the anodic polarity to overcome the soma and activate the central axon. Therefore, lower behavioral thresholds in response to anodic than to cathodic stimulation, or *larger polarity effects*, are expected on electrodes near peripherally degenerated neurons.

To date, the majority of evidence characterizing the polarity effect comes from biophysical modeling studies. Little is known about whether the polarity effect correlates with SGN integrity in animals or whether its measurement is influenced by other variables that affect the electrode-neuron interface in humans. For instance, reliable in vivo estimates of neural status should vary relatively independently of electrode position within the cochlea and intracochlear bone and fibrous tissue growth. Moreover, polarity sensitivity has not been evaluated in pediatric CI listeners. Experiment 3, "Evaluating psychophysical polarity sensitivity as an indirect estimate of neural status in cochlear implant listeners" assessed the validity of using the polarity effect as an estimate of SGN health in humans. In that experiment, relationships between the polarity effect and 1) electrode-to-modiolus distance, 2) electrode scalar location, and 3) intracochlear resistance were characterized in a group of adult CI listeners. Experiment 4, "Polarity sensitivity in children and adults with cochlear implants", determined whether the polarity effect differed between children and adults with CIs, and provided recommendations for possible programming interventions based on single-channel polarity effect measurements.

Together, the experiments in this dissertation evaluate whether the estimated status of the SGNs differs between children and adults with CIs. Because CIs are designed to directly interface with the SGNs, within- and across-ear differences in SGN integrity may provide insight into optimal programming adjustments for individual CI listeners. The results of these

investigations, therefore, may lead to improved CI programming interventions for listeners with diverse hearing histories.

CHAPTER 2. MULTIPLE EVOKED POTENTIAL ESTIMATES OF SPIRAL GANGLION DENSITY DIFFER BETWEEN YOUNGER AND OLDER LISTENERS WITH COCHLEAR IMPLANTS

2.1 ABSTRACT

Objectives: The primary objective of the present study was to quantify evoked potential estimates of spiral ganglion neuron (SGN) density in younger and older individuals with cochlear implants (CIs) using the electrically evoked compound action potential (ECAP). In human temporal bone studies and in animal models, SGN density decreases with increasing age and duration of deafness. SGN density also varies as a function of hearing loss etiology. Taken together, it is likely that younger, early deafened listeners have healthier populations of SGNs than older individuals who were deafened and implanted later in life. In animal studies, large changes in ECAP amplitude, growth function slope, and threshold as the interphase gap (IPG) of the stimulus is increased (i.e., the IPG effect) are associated with relatively healthy populations of surviving SGNs. We hypothesized that younger listeners who were deafened and implanted as children would demonstrate larger IPG effects than older, adult-deafened and implanted listeners. We also predicted that individuals with larger IPG effects would have better speech perception scores than individuals with smaller IPG effects.

Design: Data were obtained from 29 implanted ears (22 individuals). Seventeen ears (11 individuals) were deafened and implanted as children (child-implanted group) and 12 ears (11 individuals) were deafened and implanted as adults (adult-implanted group). The hearing groups differed on a number of demographic variables that are implicitly related to SGN density: 1) chronological age (16.2 years versus 59.6 years), 2) age at implantation (4.9 years versus 53.2 years), and 3) duration of pre-implantation hearing loss (4.4 years versus 24.9 years). ECAP

amplitudes, amplitude growth function slopes, and thresholds were assessed on a subset of electrodes in each ear in response to two IPGs (7 and 30 μs). The IPG effect was defined as the difference in response to the 30 μs IPG minus the 7 μs IPG. Speech recognition was assessed using a medial vowel identification task.

Results: Compared to the adult-implanted listeners, individuals in the child-implanted group demonstrated larger changes in ECAP amplitude as the IPG of the stimulus was increased from 7 to 30 μs. On average, child-implanted participants also had larger amplitudes and steeper growth function slopes than the adult-implanted participants, irrespective of IPG. IPG effects for growth function slope and ECAP threshold did not differ between hearing groups. Vowel recognition performance was not correlated with any of the ECAP measures assessed in this study.

Conclusions: The results of this study enhance the growing body of literature suggesting that young CI listeners that were deafened and implanted during childhood may have healthier neural populations than older listeners that were deafened and implanted as adults. Potential between-group differences in SGN integrity emphasize a need to investigate optimized CI programming parameters for younger and older listeners.

2.2 INTRODUCTION

Although the average speech perception performance of cochlear implant (CI) listeners has greatly improved since the devices were introduced clinically, many implanted children and adults continue to experience suboptimal speech and language outcomes (e.g., Niparko et al. 2010; Holden et al. 2013). One potential reason for variable CI outcomes is that, despite having divergent hearing histories, pediatric and adult CI listeners receive largely the same clinical

programming interventions. Before we can alter our clinical recommendations, however, the differences in peripheral and central auditory processing between children and adults with CIs need to be well understood.

Given that the spiral ganglion neurons (SGNs) are the targets of electrical stimulation by a CI, a common assumption is that the integrity of the SGNs affects transmission of auditory stimuli and impacts perceptual outcomes with an implant. Available evidence suggests that the condition of the SGNs likely differs between children that were deafened and implanted early in life and adult-deafened and implanted listeners. Hearing loss etiology, which often differs between these two populations, is a strong predictor of SGN survival in post-mortem human temporal bone studies (Otte et al. 1978; Nadol et al. 1989; Nadol 1997) and in animal models (e.g., Kujawa & Liberman 2006, 2009; Zilberstein et al. 2012). Other patient-specific factors such as chronological age, duration of hearing loss and duration of total deafness, which tend to differ substantially between implanted children and adults, also predict post-mortem SGN density (Otte et al. 1978; Nadol et al. 1989; Nadol 1997; Makary et al. 2011). Specifically, SGN cell counts are lowest in the temporal bones of older individuals and in those who experienced longer durations of hearing loss or total deafness during life (Otte et al. 1978; Nadol et al. 1989; Nadol 1997; Makary et al. 2011). Finally, some studies have shown that chronic electrical stimulation in neonatally deafened animals promotes SGN survival (Lousteau 1987; Leake et al. 1991, 1992, 1999). Thus, direct estimates of SGN survival in human temporal bone and animal models suggest that neural integrity likely differs between pediatric and adult CI listeners.

Although it is impossible to directly assess neural health in vivo, electrophysiological recording techniques may assist in estimating the health of the SGNs in CI listeners. A popular in vivo estimate of neural response is the electrically evoked compound action potential (ECAP),

which is similar to wave I of the electrically evoked auditory brainstem response (EABR). The ECAP represents synchronous firing from a group of electrically stimulated auditory nerve fibers. The amplitude, amplitude growth function (AGF) slope, and threshold of the ECAP response (and EABR wave I) are all correlated with SGN survival in animal models (Smith and Simmons 1983; Hall 1990; Miller et al. 1994; Shepherd & Javel 1997; Ramekers et al. 2014; Pfingst et al. 2015). Specifically, animals with higher SGN densities tend to have larger amplitudes, steeper AGF slopes, and lower thresholds, than animals with fewer functional SGNs.

Using the ECAP, limited evoked potential evidence in humans suggests that the interface between CI electrodes and the target SGNs differs between children and adults with CIs. However, it is unclear whether this difference can be attributed, in part, to the health of the SGNs. Multiple investigations have demonstrated that children (Hughes et al. 2001; Brown et al. 2010) and young adults (Cafarelli Dees et al. 2005) have steeper ECAP AGF slopes than older individuals. However, Hughes et al. (2001) and Brown et al. (2010) showed that children not only had steeper AGF slopes, but also higher ECAP thresholds than adults. Steeper growth functions coupled with higher thresholds is inconsistent with the theory that children simply have larger populations of surviving SGNs. Instead, the authors concluded that the children in those studies may have had a larger distance between the electrodes and the auditory nerve fibers.

It is unlikely that the differences in ECAP measures between the children and adults were due to age-related differences in cochlear dimensions, as the cochlea is adult-sized at birth (e.g., Pelliccia et al. 2014). However, it is possible that the current fields within the cochlea differed between children and adults, yielding a larger effective distance between the CI electrodes and the SGNs in children. In fact, consistent with that hypothesis, Hughes et al. (2001) reported higher electrode impedances in the children than in the adults. Overall, available objective

evidence suggests that the interface between CI electrodes and the SGNs differs between younger and older CI listeners; however, it is unclear whether those findings may be attributed, in part, to differences in SGN density, or simply to differences in cochlear resistivity.

Recent behavioral evidence supports the electrophysiological data suggesting that the quality of the electrode-neuron interface differs between children and adults with CIs. DiNino et al. (2019) demonstrated that early implanted children have lower single-channel behavioral thresholds, measured in response to a spatially focused electrode configuration, compared to listeners who were deafened and implanted as adults. Across studies, electrodes with relatively low behavioral thresholds are located closer to the target SGNs (Long et al. 2014; DeVries et al. 2016; DeVries & Arenberg 2018), have higher intracochlear resistance values (Jahn & Arenberg, 2019), and have larger evoked potential amplitudes (DeVries et al. 2016) than electrodes with higher behavioral thresholds. Notably, DiNino et al. (2019) also reported that the children had significantly higher intracochlear resistance values than the adults, but that the between-group differences in cochlear resistivity did not fully explain the differences in behavioral thresholds. Because electrode position was unlikely to vary systematically between the children and the adults, it is possible that differences in behavioral thresholds could be influenced, in part, by the presence of healthier populations of SGNs in the children.

While it seems likely that children have better SGN health than adults with CIs, more evidence is needed to support that theory. The primary goal of the present study was to determine whether differences in the electrode-neuron interface between children and adults may be attributed, in part, to differences in estimated SGN density. Recent evidence suggests that the change in ECAP characteristics (i.e., amplitude, AGF slope, and threshold) as the interphase gap (IPG) of the stimulus is increased may provide insight into the health of the SGNs in addition to

being relatively independent of non-physiological conditions between the SGNs and the recording site (Ramekers et al. 2014; Schvartz-Leyzac and Pfingst 2016). Thus, of primary interest to the current study is how standard ECAP characteristics change as the IPG of the electrical stimulus is increased in pediatric and adult CI listeners.

The magnitude of the change in ECAP characteristics with increasing IPG (i.e., the IPG effect) is related to the density of the remaining SGNs in animals. In cochlear-implanted guinea pigs, the current level required to evoke an equal-amplitude ECAP is lower for stimuli with longer IPGs (Prado-Guitierrez et al. 2006; Ramekers et al. 2014). Furthermore, ECAP thresholds decrease (Prado-Guitierrez et al. 2006; Ramekers et al. 2014), and AGF slopes increase (Ramekers et al. 2014) with increasing IPG. Importantly, the magnitude of the IPG effect for amplitude and slope is smaller in animals with greater neural loss than in animals with healthier SGN populations (Prado-Guitierrez et al. 2006; Ramekers et al. 2014). Prado-Guitierrez et al. (2006) also observed larger IPG effects for threshold in animals with healthier SGN populations, but the IPG effect for threshold did not vary as a function of SGN density in the Ramekers et al. study. Overall, animal work supports a relationship between IPG effects and SGN density, wherein the magnitude of the change in ECAP amplitude, AGF slope, and possibly threshold, with increasing IPG tends to be relatively small for animals with few functional SGNs.

Assessing IPG effects may help to mitigate some of the limitations of inferring the status of the SGNs in children and adults using standard ECAP characteristics measured with a constant IPG. For instance, in response to a constant IPG, ECAP measures (i.e., amplitude, AGF slope, and threshold) are often influenced by non-physiological factors such as electrode position relative to the target SGNs and/or intracochlear bone and fibrous tissue growth. Specifically, multiple investigations suggest that individuals with perimodiolar electrode arrays or positioners,

which are designed to position the electrodes within close proximity to the SGNs, tend to have lower ECAP thresholds than individuals with lateral wall electrode arrays (e.g., Cords et al. 2000; Young & Grohne 2001; Firszt et al. 2003; Eisen and Franck 2004; Brown et al. 2010).

Moreover, Schvartz-Leyzac and Pfingst (2016) found significant relationships between ECAP measures (amplitudes and AGF slopes) and electrode impedances in 37.5% of cases. Their results suggest that in some listeners, current fields within the cochlea may influence the measurement of standard ECAP characteristics. Notably, in the same listeners, within-subject electrode impedances varied relatively independently of *changes* in ECAP amplitude and slope as the IPG was increased from 7 to 30 microseconds (μs). The authors proposed that ECAP amplitudes and AGF slopes in response to each IPG should be affected similarly by conditions near the recording electrode, and that the influence of non-physiological factors cancels out when calculating a difference score (i.e., the IPG effect). As multiple studies demonstrate differences in cochlear resistivity between children and adults with CIs, a measure that is relatively independent of non-neural factors affecting the electrode-neuron interface is crucial for evaluating potential between-group differences in SGN density (Hughes et al. 2001; Molisz et al. 2015; DiNino et al. 2019).

The primary goal of the present study was to quantify ECAP IPG effects for amplitude, AGF slope, and threshold in children and adults with CIs. To address this question, two groups of participants with divergent hearing histories were recruited: 1) younger listeners who were deafened and implanted as children (child-implanted listeners) and 2) older listeners who were deafened and implanted as adults (adult-implanted listeners). These two groups of participants differed on several important demographic characteristics that are related to SGN integrity in human temporal bone and animal studies. Specifically, the child-implanted listeners were

younger, received their implants as children (prior to age 18 years), and experienced shorter pre-implantation durations of hearing loss than the adult-implanted listeners. The contribution of between-group differences in age, age at implantation, and duration of hearing loss cannot generally be teased apart, and these hearing groups therefore represent the typical clinical presentation of younger and older CI candidates.

We predicted that individuals who were deafened and implanted as children would have larger IPG effects than adult-deafened and implanted listeners. Larger IPG effects in the child-implanted group than in the adult-implanted group would support the theory that younger listeners have healthier populations of SGNs than older listeners. Quantifying differences in the electrode-neuron interface between child-implanted and adult-implanted listeners will assist in developing programming interventions that are tailored to the unique auditory characteristics of individuals within each hearing group.

A secondary goal was to determine the relationship between ECAP IPG effects and speech perception performance in this sample of listeners with diverse hearing histories. We predicted that individuals with smaller IPG effects would have lower speech perception scores than individuals with larger IPG effects. In this study, we chose to quantify speech perception using vowel stimuli because previous literature suggests that vowels are particularly sensitive to spectral distortions resulting from degraded electrode-neuron interfaces (Friesen et al. 2001; Shannon et al. 2004; Xu et al. 2005; Nie et al. 2006; DiNino et al. 2016). It should be noted that current evidence does not overwhelmingly support relationships between ECAP measures and speech perception performance (reviewed by van Eijl et al. 2017). However, a recent study with bilateral adult CI listeners found that between-ear differences in the ECAP IPG effect for slope were predictive of between-ear differences in consonant and sentence-in-noise perception

(Schvartz-Leyzac & Pfingst 2018). Thus, further investigation of the relationship between ECAP IPG effects and speech perception in children and adults with CIs is warranted.

2.3 MATERIALS AND METHODS

2.3.1 *Participants*

Demographic information for all ears tested in this study is presented in Table 2.1. Data were obtained from a total of 29 ears (22 subjects, 7 males) that were implanted with Cochlear Ltd. (Sydney, Australia) devices. The majority of ears (n = 26) had Nucleus CI24R, CI512 or CI24RE devices with pre-curved, perimodiolar electrode arrays. Two ears (PC09R and SC08R) had Nucleus CI24M devices with straight electrode arrays. One participant (SC13) was implanted with a hybrid L24 array (straight). SC13 had low-frequency residual hearing postoperatively (audiometric thresholds in the mild loss range at 125 and 250 Hz, sloping to moderately-severe at 500 Hz and profound between 750-8000 Hz). Excluding SC13 from the analyses did not change the results of this study. No other participants had residual hearing in the implanted ear.

Table 2.1. Demographic information for each ear tested. Shaded rows indicate the participants that were deafened and implanted as children. Asterisks (*) denote participants that were tested with a 50 μsec pulse width. [+]Denotes SC09's second-implanted ear. "No responses" indicates that no measurable evoked potential responses could be obtained on any electrodes in that ear. L: left ear; R: right ear; ECAP: electrically evoked compound action potential; AGF: amplitude growth function; EVA: enlarged vestibular aqueduct; DFNB1: genetic non-syndromic hearing loss (Connexin-26 mutation)

ID	Ear	Device	Etiology	Age at Test (years)	Age Implanted (years)	Duration of Hearing Loss (years)	ECAP AGF Test Electrodes	Vowel Score (% correct)
PC01	L	CI512	EVA	18.8	11.4	11.4	18, 22	100
PC02	R	CI24RE(CA)	DFNB1	13.8	1.6	1.6	4, 10, 16, 20	95
	L	CI24RE(CA)	DFNB1	13.8	1.6	1.6	10, 16, 20	90
PC03	L	CI24RE(CA)	DFNB1	10.9	1.0	1.0	4, 8, 12, 16	98.5
	R	CI24RE(CA)	DFNB1	10.9	1.0	1.0	4, 20	80
PC05*	R	CI24RE(CA)	Unknown	10.6	0.4	0.3	6, 10, 16, 20	41.5
PC06	R	CI24RE(CA)	EVA	11.2	2.1	2.0	6, 12, 16, 20	98.5
	L	CI512	EVA	11.2	4.2	4.1	2, 4, 15, 20	83.3
PC07	R	CI24RE(CA)	Maternal measles	12.9	4.0	4.0	4, 8, 16, 20, 22	87
	L	CI24RE(CA)	Maternal measles	12.9	8.0	8.0	4, 14, 18	28.5
PC08*	L	CI24R(CS)	Unknown	18.8	2.0	0.0	1, 3	73
PC09	R	CI24M	Genetic	22.1	2.1	2.1	11, 15, 17, 21	89
	L	CI24RE(CA)	Genetic	22.1	10.5	10.5	4, 6, 16, 20	20
PC10	R	CI24RE(CA)	Unknown	17.9	11.0	8.5	4, 10, 16, 20	90
PC13	R	CI24R(CS)	DFNB1	17.9	1.1	1.1	No responses	100
	L	CI24RE(CA)	DFNB1	17.9	5.9	5.9	4, 10, 16, 20	100
SC08	R	CI24M	Genetic	23.5	3.7	2.2	8, 10, 16, 20	86.5
	L	CI24RE(CA)	Genetic	23.5	12.1	10.6	4, 10, 18, 20	67.7
SC01	R	CI512	Unknown	65.8	62.4	37.4	6, 12, 16, 20	54.3
SC04	R	CI24RE(CA)	Unknown	68.4	58.5	8.5	4, 10, 16, 20	76.5
SC06	R	CI24RE(CA)	Unknown	72.5	66.2	61.2	4, 10, 16, 20	74.3
SC09[+]	L	CI24RE(CA)	Unknown	72.5	55.4	27.4	8, 12, 16, 20	86.7
SC10	L	CI512	Unknown	34.9	33.9	33.3	4, 8, 16, 20	15
SC11	L	CI24R(CA)	Sudden/autoimmune	69.6	64.8	4.8	8, 12, 16, 20	30
SC12	L	CI512	Meningitis; head injury	31.4	30.0	28.5	4, 8, 12, 20	96.5
SC13	R	CI24RE(Hybrid)	Ototoxicity	61.5	61.2	56.2	4, 10, 14, 20	50
SC14	L	CI24RE(CA)	Meniere's disease	71.9	71.3	1.3	4,12,16,20	73.5
SC15	L	CI24RE(CA)	Unknown	58.2	51.0	15.0	4, 12, 18	98.5
SC16	L	CI24R(CA)	Autoimmune	48.7	41.7	12.7	4, 10, 16, 20	88.5
	R	CI24RE(CA)	Autoimmune	48.7	42.0	13.0	4, 10, 16, 20	90

Seventeen ears (11 individual participants, 2 males) were deafened and implanted during childhood (prior to age 18 years). Demographic characteristics of the child-implanted ears are highlighted in gray in Table 2.1. At the time of testing, participants in the child-implanted group ranged in age from 10 to 23 years (M = 16.22 years). The mean age at implantation for this group

was 4.85 years (range: 0.39 to 12.08 years) and the mean pre-implantation duration of hearing loss was 4.40 years (range: 0 to 11.37 years). Pre-implantation duration of hearing loss was defined as the time, in years, between self-reported (for adults) or parent-reported (for children) diagnosis of sensorineural hearing loss and the date of CI activation (Schvartz-Leyzac and Pfingst 2016). Seven of the 11 child-implanted participants were bilaterally implanted, and data were obtained from each ear whenever possible. In one ear (PC13R), measurable ECAP responses could not be obtained on any electrode. Subjects PC09 and SC08 are siblings. No other subjects are related to one another.

Twelve ears (11 individual participants, 5 males) were deafened and implanted as adults (age 18 years or older). At the time of testing, participants in the adult-implanted group ranged in age from 31 to 72 years (M = 59.58 years). The mean age at implantation for this group was 53.20 years (range: 30.03 to 71.30 years) and the mean duration of hearing loss was 24.93 years (range: 1.29 to 61.23 years). Three (SC04, SC09, and SC16) of the 11 adult-implanted participants were bilaterally implanted, but only SC16 was able to be tested in both ears. SC09's first-implanted ear had substantial artifact on every electrode. At the time of testing, SC04 was experiencing vestibular symptoms in the second-implanted ear, and we elected to forgo ECAP testing on that side.

All but three participants (PC08, SC11, and SC14) were native speakers of American English and all participants used spoken language to communicate. Vowel recognition scores for PC08, SC11, and SC14 were not included in the statistical analyses. Each child provided written informed assent, and his or her parents or legal guardians provided written informed consent. Each adult provided written informed consent. The use of human subjects was reviewed and approved by the University of Washington Human Subjects Division.

2.3.2 *Vowel Recognition Test Procedure*

Vowel recognition was assessed using a closed set of 10 recorded vowels presented in /h/-vowel-/d/ context (/i/, “heed”; /ɪ/, “hid”; /eɪ/, “hayed”; /ɛ/,”head”; /æ/,”had”; /ɑ/, “hod”; /u/, “who’d”; /ʊ/, “hood”; /oʊ/, “hoed”; /ʌ/, “hud”). The stimuli were spoken by a female talker native to the Pacific Northwest region of the United States. Testing was performed in a double-walled sound-treated booth (IAC RE-243). Vowel stimuli were delivered through an external A/D device (SIIF USB SoundWave 7.1) and a Crown D75 amplifier and presented via a loudspeaker positioned at 0^{o} azimuth and one meter from the participant. Stimuli were calibrated to a level of 60 dB-A.

Participants were tested with one CI at a time using their everyday listening programs. Unilateral CI users wore an earplug in the non-implanted ear during the test. SC13, who has post-operative low-frequency residual hearing, also wore an earplug in the implanted ear during speech perception testing. The test was administered via a graphical user interface programmed with custom software (ListPlayer2 version 2.2.11.52, Advanced Bionics, Valencia, CA). After each vowel token was presented, all 10 tokens were displayed on a computer screen. The listener selected each response with a computer mouse. Final percent correct scores were calculated based on six repetitions of each vowel token (10 vowels x 6 repetitions = 60 total tokens). Percent correct scores for each ear tested are presented in Table 2.1. For statistical analyses, percent correct scores were converted to rationalized arcsine units (RAUs) to normalize error variance (Studebaker 1985).

2.3.3 *Electrically Evoked Compound Action Potentials (ECAPs)*

Equipment and Stimuli • Prior to ECAP testing, electrode impedances were measured in each ear using the CustomSound EP clinical software (version 3.2; Cochlear Ltd., Sydney, Australia) to identify non-functional electrodes and to avoid stimulating above voltage

compliance limits. ECAP measurements were obtained using Advanced Neural Response Telemetry (NRT) in CustomSound EP. Stimuli were delivered through a laboratory-owned Freedom sound processor connected to a laptop computer through a programming pod. All stimuli were symmetric, biphasic, cathodic-leading pulses presented in a monopolar stimulation mode (re: MP1, the extracochlear monopolar ball electrode). Pulses were 25 μs/phase with IPGs of either 7 or 30 μs, depending on the experimental condition. Note that a 0 μs IPG is not possible with Cochlear Ltd. devices. For two subjects (PC05 and PC08), the phase duration was increased to 50 μs to achieve levels adequate for recording an ECAP response. Phase durations were constant across electrodes and ears within a subject.

Electrodes in Cochlear Ltd. devices are numbered from base to apex, with 1 denoting the most basal electrode and 22 denoting the most apical electrode. For electrodes 1-20, ECAP responses were recorded from an intracochlear electrode that was located two positions apical to the stimulating electrode. When electrodes 21 or 22 were stimulated, the recording electrode was located two positions basal (electrode 19 or 20, respectively). The extracochlear monopolar plate electrode (MP2) served as the recording-indifferent electrode. The probe repetition rate was 80 Hz. In most instances, the gain of the recording amplifier was set to 50 dB. In some cases, a gain of 60 dB was used to improve visibility of the ECAP waveform. Artifact rejection was accomplished using a forward-masking technique (Abbas et al. 1999). The masker-probe interval was 400 μs. The probe and the masker stimuli were always co-located, and the masker level was always 10 clinical units (CUs) higher than the probe level to ensure adequate masking (Hughes et al. 2001). ECAP responses were averaged across 50 to 100 sweeps.

Amplitude Measurement • First, amplitudes were measured on half of the available electrodes in response to each IPG (7 and 30 μs; hereafter, referred to as 7-IPG and 30-IPG).

When possible, the even-numbered electrodes were tested. In one ear (PC09R), the odd-numbered electrodes were tested because substantial stimulus artifact was present on the even electrodes only. For PC08, measurable ECAP responses were only present on the three most basal electrodes (1, 2, and 3). To set the upper limit of stimulation for the ECAP measurements, participants rated the loudness of 10 sweeps of the corresponding stimulus using a 10-point loudness rating scale (Advanced Bionics, Valencia, CA). Using the "Stimulate Only" feature in Advanced NRT, the current level was gradually increased from a sub-threshold level of 5 CUs up until the subject reported a loudness rating of "8", corresponding to "maximal comfort" on the loudness rating scale. Hereafter, level "8" is referred to as the "maximum stimulation level".

For amplitude testing, loudness estimates were obtained using only the 30-IPG stimulus. This was done because pilot testing revealed that when stimuli with IPGs of 7 and 30 μs were presented at equal current levels, the loudness percept of the 30-IPG stimulus was either louder than or equivalent to that of the 7-IPG stimulus. Using the maximum stimulation level for the 30-IPG stimulus, ECAP amplitudes were measured across all functional even (or odd) electrodes for each IPG (7 and 30 μs). The order of IPGs and electrodes tested was randomized for each ear. These measurements were used to calculate differences in amplitude measured at equal current levels as a function of IPG. The amplitude measurements also assisted in selecting a subset of electrodes for subsequent AGF testing.

Amplitude Growth Function (AGF) Measurement • ECAP AGFs were obtained on a subset of the electrodes for which amplitudes were assessed. Whenever possible, four electrodes that had measurable ECAP amplitudes with adequate morphology were selected for AGF testing: two basal electrodes (between 1 and 11) and two apical electrodes (between 12 and 22). For most participants, the AGF test electrodes were 4, 10, 16 and 20. If any of those electrodes were non-

functional or did not have adequate AGFs due to compliance limitations, restricted dynamic ranges, or poor waveform morphology, a different electrode within the same cochlear region (apical or basal) was selected instead. In six ears (PC01, PC03R, PC07R, PC07L, PC08, and SC15), adequate AGFs could only be obtained on 2 or 3 electrodes (out of the 11 for which amplitudes were assessed) in response to both IPGs. The electrodes selected for AGF testing in each ear are listed in Table 2.1.

Prior to measuring AGFs, the maximum stimulation levels were measured for the 7-IPG stimulus on each test channel (recall that this information had already been collected for the 30-IPG stimulus). This was done to optimize the AGF obtained in response to each IPG. To measure AGFs, the current levels for the masker and probe (offset by 10 CU) were both systematically increased from a sub-threshold current level up until the masker level reached the corresponding maximum stimulation level. The starting level of the AGF was set to 10 CU below the masker level where a visible ECAP began to emerge during maximum stimulation level testing. To obtain a sufficient number of data points for curve fitting (i.e., three or more points), current level step sizes varied depending on the dynamic range (i.e., smaller step sizes were necessary for smaller dynamic ranges).

Data Analysis • ECAP data were exported from CustomSound EP into a custom MATLAB (MathWorks, Natick, MA) program that was used to manually mark the N1 and P2 peaks and to calculate the peak-to-peak amplitudes, ECAP thresholds, and AGF slopes. Stimulus current levels were converted to dB (re: 1 μA). Peak-to-peak amplitudes (in μV) were calculated from the leading negative peak (N1) to the following positive peak (P2). AGF slopes (in μV/dB) were calculated using linear regression through all data points that were recorded above the noise floor of the system (noise floor = 20-25 μV for CI24M and CI24R devices; 2-5 μV for CI24RE

devices; Patrick et al. 2006). ECAP threshold (in dB re: 1 μA) was defined as the x-intercept of the linear regression line for each growth function. Figure 2.1 shows AGFs measured on electrode 10 in response to each IPG for A) one child-implanted participant (PC10) and B) one adult-implanted participant (SC06). Figure 2.2 shows the corresponding ECAP waveforms measured in response to the 30-IPG stimulus for the same two participants.

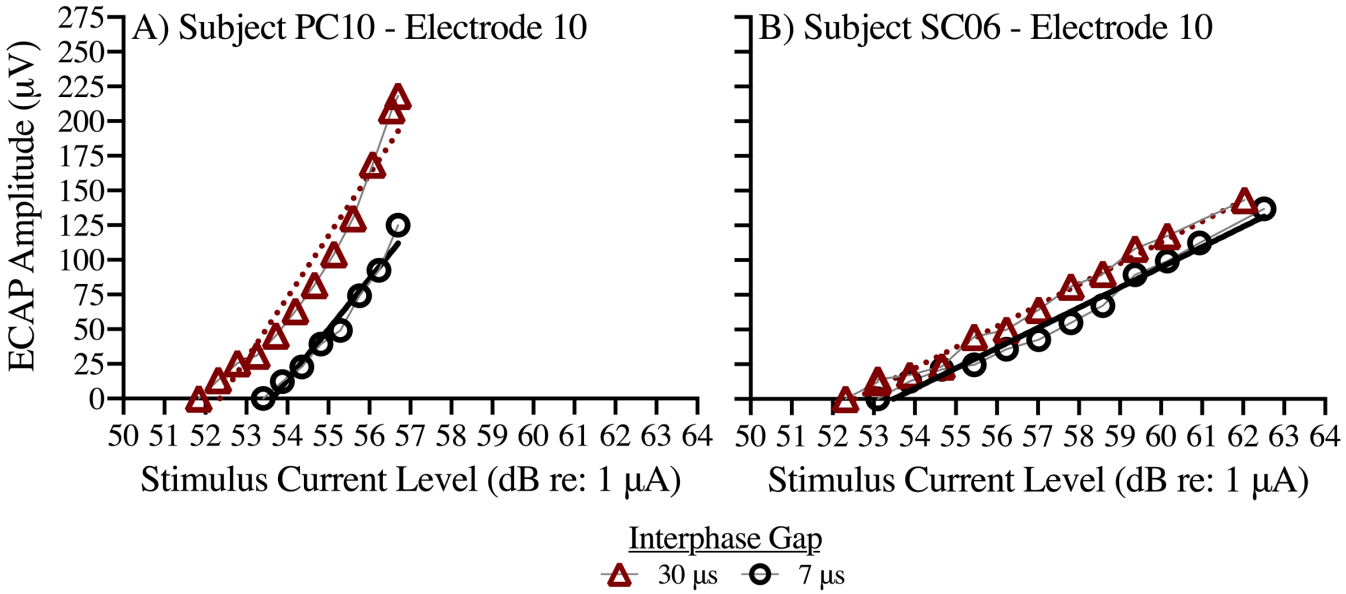

Figure 2.1. Electrically evoked compound action potential (ECAP) amplitude growth functions measured on electrode 10 for A) one child-implanted participant (Subject PC10), and B) one adult-implanted participant (Subject SC06). Black circles represent ECAP responses to the stimulus with the 7 μs interphase gap. Maroon triangles represent ECAP responses to the stimulus with the 30 μs interphase gap. Linear regression lines are shown through each growth function.

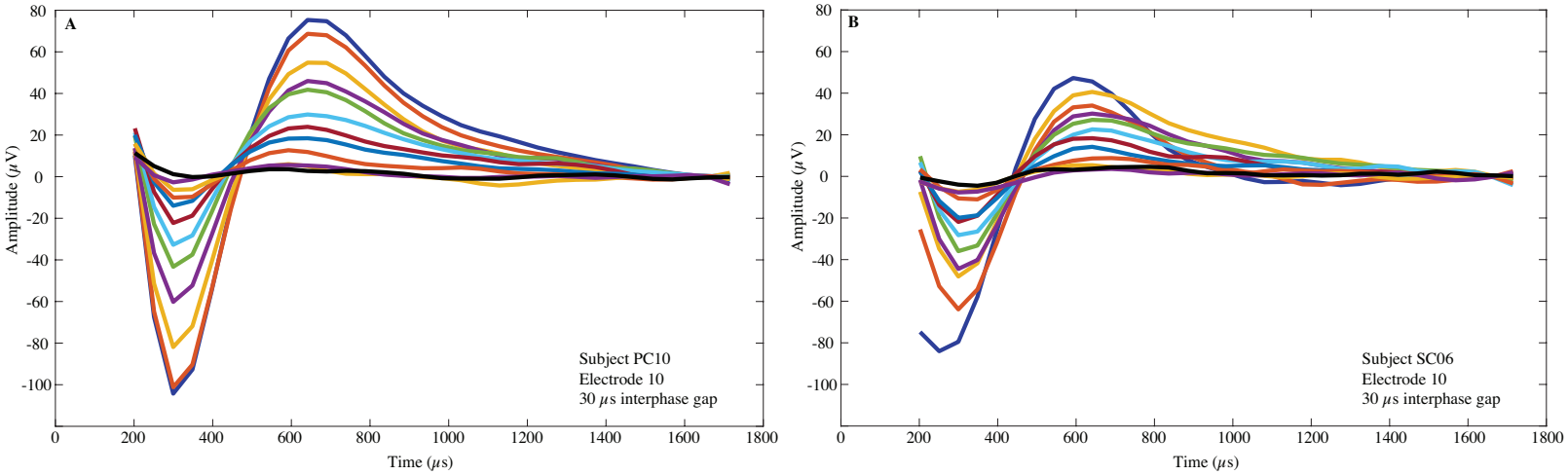

Figure 2.2. Examples of electrically evoked compound action potential (ECAP) waveforms measured on electrode 10 in A) one child-implanted participant (Subject PC10) and B) one adult-implanted participant (Subject SC06). These waveforms correspond to the growth functions shown in Figure 2.1 in response to the 30 μs interphase gap (IPG). Various colors represent different input current levels. In each panel, the dark blue tracing corresponds to the highest input current level and the black tracing corresponds to the lowest input current level.

IPG effects for amplitude, AGF slope and ECAP threshold were also calculated for each tested electrode. The IPG effect was defined as responses to the 30-IPG stimulus minus those to the 7-IPG stimulus (30 – 7 μs). Recall that the IPG effect for amplitude was calculated at equal current levels across the two IPG conditions. Additionally, for each metric, an across-site average value was calculated by averaging responses across all tested electrodes, within an ear. Across-site averages were used for comparison to vowel recognition scores and for data visualization.

2.3.4 *Statistical Analysis*

Data were analyzed using R Version 3.3.1 (R Core Team 2016). Linear mixed-effects models were used to account for clustering of electrode-specific data within ears and for clustering of

two ears within the same listener. To do so, "participant" and "ear" were included as random effects in the models where appropriate. All models were fit with restricted maximum likelihood estimation (REML) parameter estimates to minimize small sample estimation bias (McNeish 2017). An unstructured covariance matrix was used for each model. Model selection was performed using an Aikaike information criterion with a bias correction for small samples (AICc; Hurvich & Tsai 1989). As applicable, pairwise comparisons were performed using Tukey adjustments for multiple comparisons and Kenward-Roger degrees of freedom. The lmerTest (Kuznetova et al. 2017), MuMIn (Bartón 2018), emmeans (Lenth 2018), and Lattice (Sarkar 2008) packages were used to perform statistical analyses and to assess the validity of model assumptions.

2.4 RESULTS

2.4.1 *ECAP Characteristics as a Function of IPG and Hearing Group*

The primary goal of the study was to determine whether standard ECAP measures (amplitude, AGF slope, and threshold) and their respective IPG effects differ as a function of hearing group. To address this question, three separate linear mixed-effects models with dependent variables of ECAP amplitude (Model 1), AGF slope (Model 2) and ECAP threshold (Model 3) were specified. Each model predicted electrode-specific data, so random effects for "participant" and "ear" were included to account for non-independence within listeners and ears. The primary predictor variables of interest were IPG (7 or 30 μs) and hearing group (child-implanted or adult-implanted). An interaction term of IPG and hearing group (IPG*hearing group) was included to assess differences in the magnitude of the change in ECAP responses with increasing IPG (i.e., the IPG effects) between child- and adult-implanted participants.

Electrode site (apical or basal), electrode array type (perimodiolar or straight), and an interaction term for IPG and electrode site (IPG*electrode site) were included as independent variables to control for potential differences in ECAP responses as a function of electrode placement within the cochlea. Electrodes 1-11 were considered basal and electrodes 12-22 were considered apical. Model 1, which assessed predictors of ECAP amplitude, also included stimulus current level as an independent variable to control for differences in amplitude that were simply related to differences in maximum stimulation level.

Initially, duration of hearing loss was included as a predictor variable in each model to control for pre-implantation auditory deprivation. However, during the model selection procedure, the most parsimonious model fits (i.e., lowest AICc values) were obtained when duration of hearing loss was excluded. Hearing group, the primary predictor variable in this study, likely captured between-group variation in chronological age, duration of hearing loss, and age at implantation. For each IPG, descriptive statistics (means and standard deviations) for ECAP amplitude, AGF slope, and ECAP threshold as a function of hearing group and electrode site are presented in Table 2.2.

Table 2.2. Means and standard deviations for each standard ECAP measure as a function of hearing group and electrode cochlear location. Electrodes 1-11 are considered basal and electrodes 12-22 are considered apical. ECAP: electrically evoked compound action potential; AGF: amplitude growth function; IPG: interphase gap.

	Standard ECAP Measures					
	Peak Amplitude (μV)		Threshold (dB re: 1 μA)		AGF Slope (μV/dB)	
	7-IPG	30-IPG	7-IPG	30-IPG	7-IPG	30-IPG
Hearing Group						
Child-implanted	125.42 (*169.38*)	189.86 (*194.57*)	50.13 (*2.93*)	48.86 (*3.01*)	43.88 (*31.23*)	48.56 (*40.21*)
Adult-implanted	42.31 (*44.98*)	61.18 (*48.22*)	51.20 (*3.10*)	50.17 (*2.99*)	16.91 (*9.36*)	17.03 (*7.40*)
Electrode Location						
Apical	105.92 (*157.39*)	152.03 (*182.50*)	50.07 (*3.12*)	49.01 (*3.17*)	33.99 (*32.12*)	37.67 (*41.51*)
Basal	66.87 (*99.77*)	109.10 (*127.77*)	51.26 (*2.92*)	50.00 (*2.84*)	30.39 (*21.09*)	31.03 (*20.90*)

2.4.2 *ECAP Amplitude Analyses*

Figure 2.3A shows ear-specific ECAP amplitudes for the child-implanted and the adult-implanted groups. In the figure, each data point represents ECAP amplitudes averaged across all tested electrode sites within an ear. Gray lines connect data points across IPGs that correspond to the same tested ear. Figure 2.3B shows average ECAP amplitudes for each hearing group (child-implanted or adult-implanted), stratified by IPG. In the figure, each data point represents ECAP amplitudes averaged across all tested electrodes within each hearing group. Results from the linear mixed-effects analysis revealed that amplitudes increased as a function of IPG, wherein amplitudes were larger in response to the 30-IPG stimulus than in response to the 7-IPG stimulus ($F(1, 476.47) = 34.40$, $p < 0.001$). Moreover, ECAP amplitudes were larger for the child-implanted group than for the adult-implanted group ($F(1, 26.41) = 8.23$, $p = 0.008$) in response to each IPG (7-IPG: $p = 0.04$; 30-IPG: $p = 0.004$).

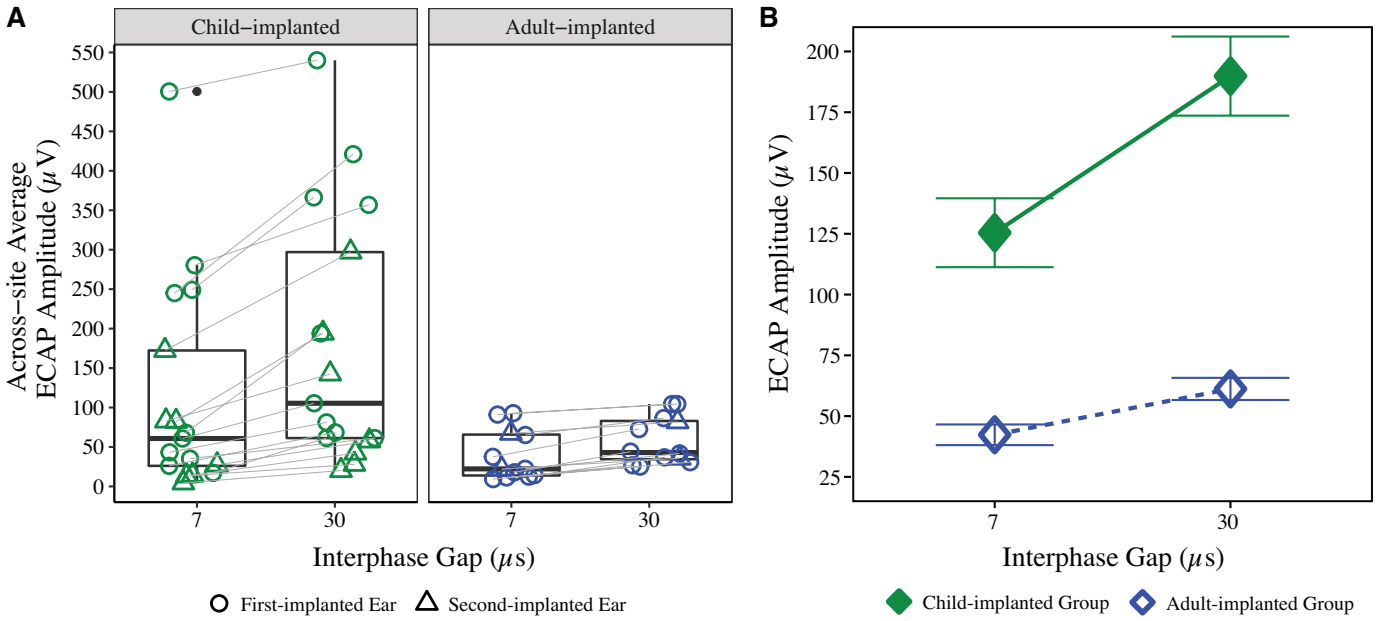

Figure 2.3. A) Across-site average electrically evoked compound action potential (ECAP) amplitudes for each ear tested. Each data point represents amplitudes averaged across all electrodes assessed within each ear. Data are stratified by interphase gap (IPG) and hearing group (child-implanted or adult-implanted). For bilaterally implanted participants, circles represent responses from first-implanted ears and triangles represent responses from second-implanted ears. Gray lines connect data points across IPGs that correspond to the same tested ear. Boxplots show the median and the first and third quartiles. B) Mean (± 1 standard error) ECAP amplitudes for each hearing group, stratified by IPG. Each data point represents amplitudes averaged across all electrodes assessed within each hearing group. Green filled diamonds represent data from the child-implanted group and blue open diamonds represent data from the adult-implanted group.

For ease of visualization, Figure 2.4 shows ear-specific IPG effects for amplitude as a function of hearing group. In the figure, IPG effects are averaged across all tested electrodes within each ear. Results indicated that there was a significant interaction between IPG and hearing group ($F(1, 476.47) = 10.71$, $p = 0.001$). Specifically, the child-implanted group exhibited a larger change in ECAP amplitude (i.e., a larger IPG effect for amplitude) than the adult-implanted group as the IPG was increased from 7 to 30 µs.

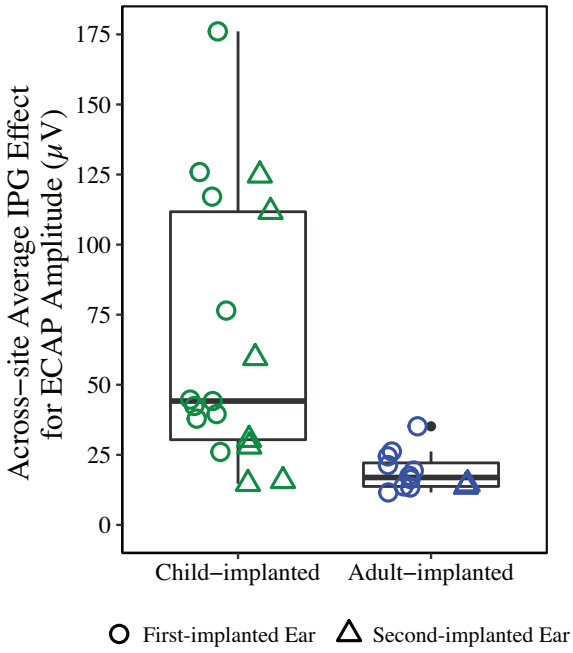

Figure 2.4. Across-site average electrically evoked compound action potential (ECAP) interphase gap (IPG) effects for amplitude for each ear tested. Each data point represents the IPG effect for amplitude averaged across all electrodes assessed within each ear. Data are stratified by hearing group (child-implanted or adult-implanted). For bilaterally implanted participants, circles represent responses from first-implanted ears and triangles represent responses from second-implanted ears. Boxplots show the median and the first and third quartiles.

Finally, the results of the linear-mixed effects model also indicated that amplitudes were smaller on basal electrodes than on apical electrodes (Table 2.2; $F(1, 480.02) = 39.35$, $p < 0.001$) in response to each IPG (7-IPG: $p < 0.001$; 30-IPG: $p < 0.001$) and that amplitudes increased with increasing stimulus current level ($F(1, 448.26) = 26.88$, $p < 0.001$). However, the IPG effect for amplitude did not differ across electrode sites (IPG*electrode site interaction; $F(1, 476.47) = 0.14$, $p < 0.71$) and amplitudes did not differ across electrode array types ($F(1, 26.35) < 0.01$, $p = 0.97$).

Because absolute ECAP amplitudes are related, in part, to the stimulus current level, a follow-up analysis was performed to assess whether probe levels differed between the child-

implanted and adult-implanted listeners. Results indicated that probe level did not differ significantly between hearing groups ($F(1, 19.89) = 0.45$, $p = 0.51$). This suggests that between-group differences in ECAP amplitude cannot be explained by systematic differences in maximum stimulation level.

2.4.3 *ECAP Amplitude Growth Function Slope Analyses*

Figure 2.5A shows ear-specific ECAP AGF slopes for the child-implanted and the adult-implanted groups. In the figure, each data point represents slopes averaged across all tested electrode sites within an ear. Gray lines connect data points across IPGs that correspond to the same tested ear. Figure 2.5B shows average ECAP AGF slopes for each hearing group (child-implanted or adult-implanted), stratified by IPG. In the figure, each data point represents slopes averaged across all tested electrodes within each hearing group. Results from the linear mixed-effects analysis revealed that AGF slopes did not differ significantly as a function of IPG ($F(1, 181.49) = 0.56$, $p = 0.45$). This indicates that a consistent IPG effect for slope was not observed in this sample. However, AGF slopes were significantly steeper for the child-implanted group than for the adult-implanted group ($F(1, 20.79) = 12.18$, $p = 0.002$) in response to each IPG (7-IPG: $p = 0.007$; 30-IPG: $p = 0.002$).

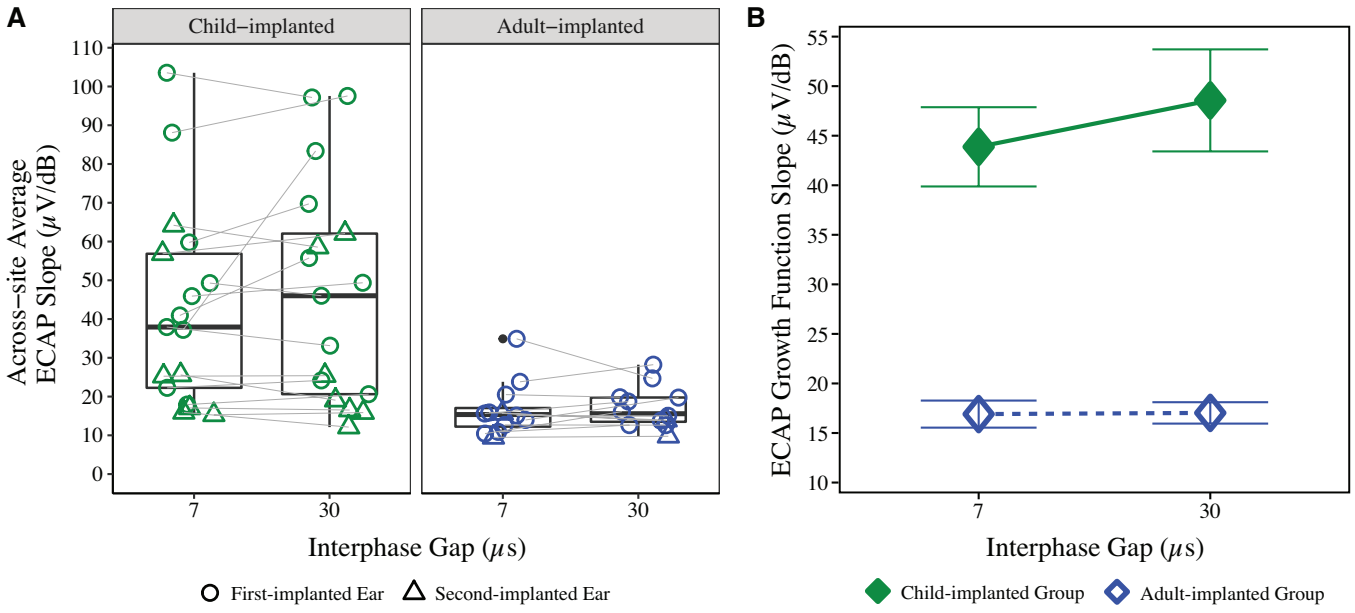

Figure 2.5. A) Across-site average electrically evoked compound action potential (ECAP) amplitude growth function slopes for each ear tested. Each data point represents slopes averaged across all electrodes assessed within each ear. Data are stratified by interphase gap (IPG) and hearing group (child-implanted or adult-implanted). For bilaterally implanted participants, circles represent responses from first-implanted ears and triangles represent responses from second-implanted ears. Gray lines connect data points across IPGs that correspond to the same tested ear. Boxplots show the median and the first and third quartiles. B) Mean (± 1 standard error) ECAP amplitude growth function slopes for each hearing group, stratified by IPG. Each data point represents slopes averaged across all electrodes assessed within each hearing group. Green filled diamonds represent data from the child-implanted group and blue open diamonds represent data from the adult-implanted group.

For ease of visualization, Figure 2.6 shows ear-specific IPG effects for AGF slope as a function of hearing group. In the figure, IPG effects are averaged across all tested electrodes within each ear. Results indicated that the interaction between IPG and hearing group was not significant, suggesting that the change in AGF slope as the IPG increased from 7 to 30 µs (i.e.,

the IPG effect for slope) did not differ between the child- and adult-implanted groups ($F(1, 181.52) = 0.73$, $p = 0.40$).

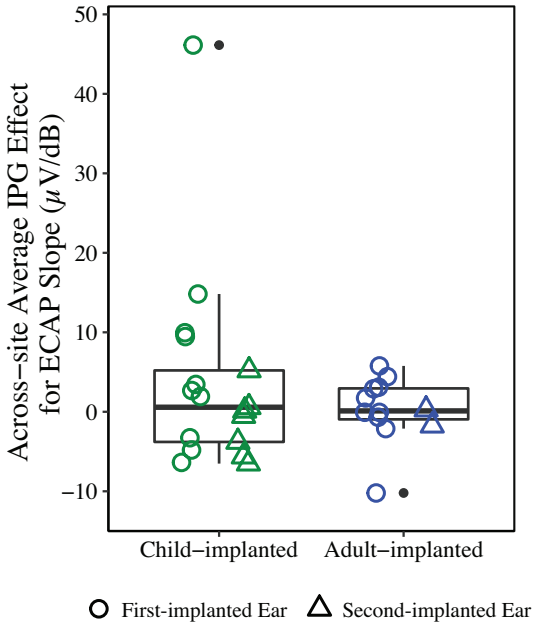

Figure 2.6. Across-site average electrically evoked compound action potential (ECAP) interphase gap (IPG) effects for amplitude growth function slope for each ear tested. Each data point represents the IPG effect for slope averaged across all electrodes assessed within each ear. Data are stratified by hearing group (child-implanted or adult-implanted). For bilaterally implanted participants, circles represent responses from first-implanted ears and triangles represent responses from second-implanted ears. Boxplots show the median and the first and third quartiles.

Finally, the results of the linear-mixed effects analysis also indicated that AGF slopes were steeper on apical electrodes than on basal electrodes (Table 2.2; $F(1, 186.60) = 4.99$, $p = 0.03$), but only in response to the 30-IPG stimulus ($p = 0.04$). The IPG effect for slope did not differ across electrode sites (IPG*electrode site; $F(1, 181.43) = 0.46$, $p = 0.50$). Slopes did not differ significantly as a function of electrode array type ($F(1, 23.90) = 1.17$, $p = 0.29$).

2.4.4 *ECAP Threshold Analyses*

Figure 2.7A shows ear-specific ECAP thresholds for the child-implanted and the adult-implanted groups. In the figure, each data point represents ECAP thresholds averaged across all tested electrode sites within an ear. Gray lines connect data points across IPGs that correspond to the same tested ear. Figure 2.7B shows average ECAP thresholds for each hearing group (child-implanted or adult-implanted) stratified by IPG. In the figure, each data point represents ECAP thresholds averaged across all tested electrodes within each hearing group. Results from the linear mixed-effects analysis revealed that ECAP thresholds decreased with increasing IPG, wherein thresholds were lower for the 30-IPG stimulus than for the 7-IPG stimulus ($F(1, 180.91) = 3.91$, $p < 0.001$). However, ECAP thresholds did not differ significantly between the child-implanted group and the adult-implanted group ($F(1, 25.48) = -1.86$, $p = 0.08$) in response to either IPG (7-IPG: $p = 0.13$; 30-IPG: $p = 0.08$).

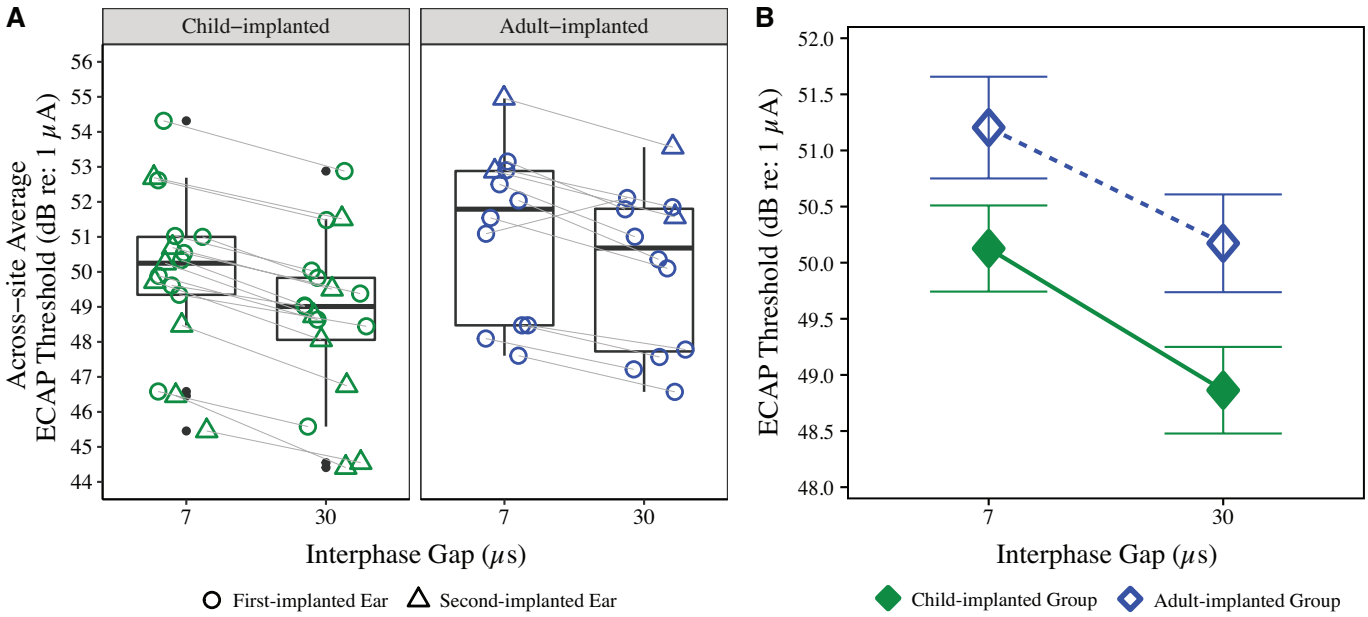

Figure 2.7. A) Across-site average electrically evoked compound action potential (ECAP) thresholds for each ear tested. Each data point represents ECAP thresholds averaged across all electrodes assessed within each ear. Data are stratified by interphase gap (IPG) and hearing group (child-implanted or adult-implanted). For bilaterally implanted participants, circles represent responses from first-implanted ears and triangles represent responses from second-implanted ears. Gray lines connect data points across IPGs that correspond to the same tested ear. Boxplots show the median and the first and third quartiles. B) Mean (± 1 standard error) ECAP thresholds for each hearing group, stratified by IPG. Each data point represents ECAP thresholds averaged across all electrodes assessed within each hearing group. Green filled diamonds represent data from the child-implanted group and blue open diamonds represent data from the adult-implanted group.

For ease of visualization, Figure 2.8 shows ear-specific IPG effects for ECAP threshold as a function of hearing group. In the figure, IPG effects are averaged across all tested electrodes within each ear. Results indicated that the interaction between IPG and hearing group was not significant, suggesting that the change in ECAP threshold as the IPG increased from 7 to 30 µs (i.e., the IPG effect for threshold) did not differ between the child- and adult-implanted groups ($F(1, 180.95) = 0.37$, $p = 0.72$).

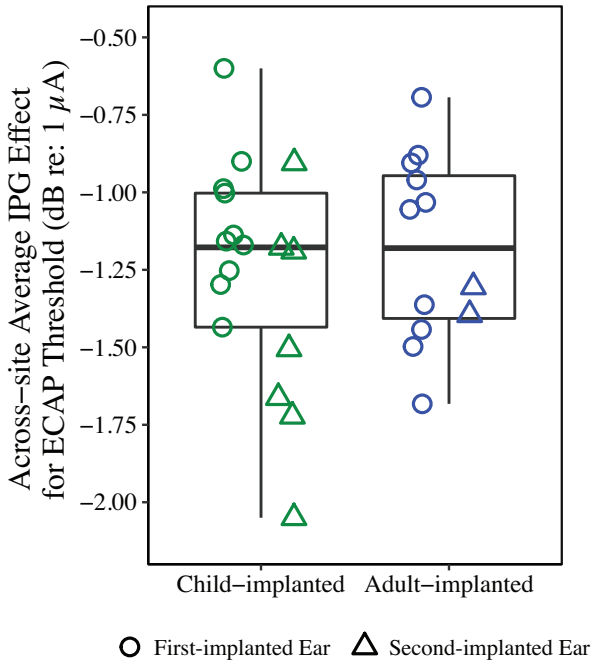

Figure 2.8. Across-site average electrically evoked compound action potential (ECAP) interphase gap (IPG) effects for thresholds for each ear tested. Each data point represents the IPG effect for ECAP threshold averaged across all electrodes assessed within each ear. Data are stratified by hearing group (child-implanted or adult-implanted). For bilaterally implanted participants, circles represent responses from first-implanted ears and triangles represent responses from second-implanted ears. Boxplots show the median and the first and third quartiles.

Finally, the results of the linear-mixed effects analysis indicated that ECAP thresholds were lower on apical electrodes than on basal electrodes (Table 2.2; $F(1, 186.51) = -3.82$, $p < 0.001$) for each IPG (7-IPG: $p = 0.004$; 30-IPG: $p = 0.01$). However, the IPG effect for threshold did not differ across electrode sites (IPG*electrode site interaction; $F(1, 180.85) = -0.27$, $p = 0.79$). Thresholds were lower in ears with perimodiolar electrode arrays compared to those with straight electrode arrays ($F(1, 24.90) = -2.59$, $p = 0.02$) in response to each IPG (7-IPG: $p = 0.03$; 30-IPG: $p = 0.03$).

Because prior literature has demonstrated differences in electrode impedances and electrical field imaging values between children and adults with CIs, a final follow-up analysis was conducted to determine whether common ground electrode impedances differed between hearing groups. Results indicated that electrode impedances did not differ significantly between child-implanted and adult-implanted listeners in this study ($F(1, 19.81) = 0.42$, $p = 0.52$).

2.4.5 *Comparison of Across-site Average ECAP Measures and Vowel Recognition Scores*

Table 2.3 shows results of linear mixed-effects analyses comparing vowel recognition scores to each of the standard ECAP responses (amplitude, AGF slope, and threshold) measured with the 7-IPG stimulus and their corresponding IPG effects. In each model, vowel recognition in RAUs (dependent variable) was compared to the respective ECAP response averaged across each tested electrode within each ear (across-site average). A random effect for "ear" was included in each model to account for clustering of two ears within the bilateral participants. A Bonferroni adjustment for six comparisons (adjusted $\alpha = 0.008$) was applied. None of the ECAP measures assessed in this study significantly predicted vowel recognition scores.

Table 2.3. Results from the linear mixed-effects models predicting vowel recognition in quiet. None of the comparisons were statistically significant after Bonferroni adjustment for multiple comparisons (adjusted $\alpha = 0.008$).

Predictor	Estimate (β)	Standard Error	*df*	*t*-value	*p*-value
Amplitude (7 µs IPG)	-0.03	0.05	24.00	-0.54	0.59
Amplitude change (30 – 7 µs)	0.02	0.13	24.00	0.12	0.91
Linear slope (7 µs)	-0.17	0.23	24.00	-0.73	0.47
Linear slope change (30 – 7 µs)	0.95	0.48	8.72	1.97	0.08
Threshold (7 µs)	5.50	2.27	16.37	2.42	0.03
Threshold change (30 – 7 µs)	24.99	18.45	23.98	1.35	0.19

2.5 DISCUSSION

The primary objective of the current study was to assess the change in ECAP amplitude, AGF slope, and threshold with increasing IPG (i.e., IPG effects) in younger and older CI listeners with divergent hearing histories. Standard ECAP measures (amplitude, AGF slope, and threshold) and their respective IPG effects were compared across two distinct hearing groups: 1) younger individuals who were deafened and implanted as children (child-implanted) and 2) older individuals who were deafened and implanted as adults (adult-implanted). These groups inherently differed on a number of demographic variables that are implicitly related to neural health including chronological age, age at implantation, and duration of pre-implantation hearing loss. By definition, it is likely that the participants within each group also broadly differed in hearing loss etiology, though many participants did not know the cause of their hearing loss.

The results of this study demonstrated that the child-implanted group had larger ECAP IPG effects for amplitude than the adult-implanted group. Amplitudes and amplitude growth function slopes measured in response to a constant IPG also differed between groups, wherein child-implanted listeners had larger amplitudes and steeper AGF slopes, on average, compared to the adult-implanted listeners. Interphase gap effects for slope and threshold did not differ systematically between hearing groups, and vowel recognition scores were not correlated with any of the ECAP measures. Overall, the results support the theory that younger individuals who received a CI during childhood may have healthier populations of SGNs than older, adult-implanted listeners.

2.5.1 *Larger Interphase Gap Effects for Amplitude in Child-implanted than in Adult-implanted Listeners*

Across listeners, ECAP amplitude consistently increased as the IPG of the stimulus was increased from 7 to 30 μs. An increase in ECAP amplitude with increasing IPG is consistent with previous studies in animals (Prado-Guitierrez et al. 2006; Ramekers et al. 2014) and in adult CI listeners (Schvartz-Leyzac & Pfingst 2016, 2018; Hughes et al. 2018). The magnitude of the IPG effect in this study was constant across electrode cochlear locations, but amplitudes were larger in the apex compared to the base. Hughes et al. (2018) and Ramekers et al. (2014) also showed that IPG effects did not vary systematically across cochlear regions in adult CI listeners or in animals, respectively. Interestingly, we observed a difference in amplitude as a function of hearing group, wherein the child-implanted group demonstrated larger amplitudes than the adult-implanted group, irrespective of IPG, electrode site, stimulus current level, and electrode array type.

In isolation, a between-group difference in amplitude may reflect between-group differences in effective distance between the recording electrode and the SGNs and/or cochlear resistivity. Systematic variation in electrode position should not underlie the between-group differences in amplitude observed in this study, since the cochlea is adult-sized at birth and ECAP amplitudes have been shown to vary independently of electrode placement relative to the modiolus (DeVries et al. 2016). However, Schvartz-Leyzac and Pfingst (2016) demonstrated that amplitudes in response to a constant IPG were correlated with electrode impedances in many of the ears tested in their study. Notably, differences in cochlear resistivity between children and adults with CIs have also been documented (Hughes et al. 2001; Molisz et al. 2015; DiNino et al. 2019). Thus, differences in amplitude between the child-implanted and adult-implanted groups in

this study could reflect between-group differences in SGN integrity and/or intracochlear bone and fibrous tissue growth.

However, the IPG effect for amplitude also differed between hearing groups in this study, lending support to the theory that SGN integrity does differ between the child-implanted and adult-implanted listeners. Specifically, compared to the adult-implanted listeners, the child-implanted group demonstrated larger changes in ECAP amplitude as the IPG of the stimulus was increased from 7 to 30 μs (i.e., a larger IPG effect for amplitude). Animal studies consistently demonstrate that the magnitude of the IPG effect for ECAP amplitude is larger in animals with healthier populations of SGNs compared to animals with fewer functional SGNs (Prado-Guitierrez et al. 2006; Ramekers et al. 2014). Importantly, IPG effects for amplitude are believed to vary largely independently of non-physiological conditions near the recording electrode such as electrode position and tissue impedances (Ramekers et al. 2014; Schvartz-Leyzac & Pfingst 2016). Moreover, we did not observe differences in electrode impedances between hearing groups in this study.

There are several possible reasons why an ear with greater SGN density might have a larger IPG effect than an ear with fewer surviving SGNs. Introducing or increasing an IPG between opposing phases of a biphasic stimulus increases the probability that a neuron will fire before the charge is removed by the second hyperpolarizing phase (Shepherd and Javel 1999; Ramekers et al. 2014). In a deafened ear, a reduction in SGN density is typically accompanied by increased demyelination and degeneration of the peripheral processes, which can increase the neural membrane time constant (Tasaki 1955; Koles & Rasminsky 1972; Prado-Guitierrez et al. 2006). Degenerated neurons may need a longer time to reach the threshold charge necessary for action potential initiation. Moreover, in ears with high SGN density, many neurons are activated

by each pulse, and a higher proportion of those neurons will be closer to their individual thresholds than in an ear with fewer functional SGNs (Prado-Guitierrez et al. 2006).

Thus, the observation of a larger IPG effect for amplitude in the child-implanted ears compared to the adult-implanted ears is consistent with the theory that children may have a healthier population of SGNs than adults. Child-implanted and adult-implanted listeners differ in several demographic characteristics that likely influence the integrity of the SGNs. Specifically, compared to individuals in the adult-implanted group, listeners in the child-implanted group were much younger, received their CIs during childhood, and experienced shorter periods of auditory deprivation prior to cochlear-implantation. In human temporal bone studies and in animal models, the integrity of the SGNs tends to decrease with increasing age and duration of hearing loss (e.g., Otte et al. 1978; Nadol et al. 1989; Nadol 1997; Kujawa & Liberman 2006, 2009; Makary et al. 2011; Zilberstein et al. 2012; Ramekers et al. 2014). Moreover, hearing loss etiology is a strong predictor of post-mortem SGN density (Nadol 1997). Though etiology was unknown for many participants in this sample, child-implanted and adult-implanted listeners inherently tend to present with different etiologies. In fact, 10 of the child-implanted ears reported genetic causes of deafness (six with confirmed Connexin-26 mutations), whereas none of the adult-implanted listeners reported etiologies of genetic origin.

2.5.2 *Steeper ECAP Growth Function Slopes in Child-implanted than in Adult-implanted Listeners*

Across participants and electrodes, ECAP AGF slope did not change predictably as the IPG was increased from 7 to 30 μs. Our observation is consistent with that of Hughes et al. (2018), who did not find a significant effect of IPG on AGF slope in adult CI listeners with either Cochlear Ltd. or Advanced Bionics devices. However, Schvartz-Leyzac and Pfingst (2016) found that

AGF slopes increased as the IPG was increased from 7 to 30 μs in adult CI listeners, which is consistent with the animal data obtained by Ramekers et al. (2014).

Across-study differences in the influence of IPG on AGF slope may be related to several limitations inherent in measuring ECAP responses in humans. For instance, slope measurements in animal models are dependent upon the use of high current levels that are not possible in un-anaesthetized humans (Ramekers et al. 2014). In this study, and in most human ECAP studies, the upper limit of stimulation is based on a subjective perception of loudness, which varies across subjects and across the electrode array within the same subject. Unfortunately, it is impossible to know which point in the neural dynamic range corresponds to each listener- and electrode-specific stimulus current level. In fact, despite the relationship between each IPG effect measure and SGN density in animal models, Schvartz-Leyzac and Pfingst (2016) demonstrated that within-subject IPG effects for slope and amplitude are often not correlated with each other in human CI listeners.

Given the lack of an IPG effect for slope in this study, it is unsurprising that the IPG effect for slope did not differ as a function of hearing group. However, AGF slopes measured in response to a constant IPG were steeper for child-implanted listeners than for adult-implanted listeners, irrespective of IPG, electrode location, and electrode array type. This finding is consistent with previous studies that demonstrated steeper slopes for younger listeners than for older listeners (Cafarelli Dees et al. 2005; Hughes et al. 2001; Brown et al. 2010). As discussed, steeper slopes may reflect healthier populations of SGNs and/or differences in cochlear resistivity between the child-implanted and adult-implanted groups. Of note, AGF slope is one of the most consistent electrophysiological predictors of neural integrity across animal studies (Hall 1990; Ramekers et al. 2014). Together with the amplitude results, it is likely that differences in

neural integrity, in part, contributed to the differences in ECAP measures observed between the child-implanted and the adult-implanted listeners.

Finally, across electrodes and participants, ECAP threshold decreased as the IPG of the stimulus was increased from 7 to 30 μs. This finding is consistent with prior human (Hughes et al. 2018) and animal data (Prado-Gutierrez et al. 2006; Ramekers et al. 2014) showing a decrease in ECAP thresholds with increasing IPG. The IPG effect for threshold did not vary as a function of electrode cochlear location, but thresholds were higher for basal electrodes than for apical electrodes. Across studies, ECAP thresholds are often higher in the base than in the apex, possibly reflecting better neural survival or a smaller distance between the electrodes and stimulated neurons in the apex (Eisen and Franck 2004; Gordon et al. 2004; Nehme et al. 2014).

Moreover, neither absolute ECAP thresholds nor the IPG effect for threshold differed between child-implanted and adult-implanted listeners. This finding is consistent with Ramekers et al. (2014), who showed that although amplitude and slope were reduced in guinea pigs with low SGN counts, ECAP threshold did not differ as a function of SGN density. Additionally, the relationship between IPG effects for threshold and SGN density are inconsistent across animal studies (Prado-Guitierrez et al. 2006; Ramekers et al. 2014). Taken together, these findings may suggest that ECAP threshold is a less reliable correlate of neural health than ECAP AGF slope and amplitude measures.

2.5.3 *ECAP Measures and Vowel Recognition*

A secondary goal of this study was to determine whether ECAP measures were predictive of speech perception scores in children and adults with CIs. None of the ECAP responses (amplitude, AGF slope, or threshold), nor their respective IPG effects, were related to vowel recognition scores in this sample of participants. Notably, clear relationships between post-

mortem SGN density and speech perception performance during life have not been demonstrated (Nadol et al. 2001; Khan et al. 2005; Fayad & Linthicum 2006). Furthermore, consistent evidence of a relationship between standard ECAP measures (amplitude, AGF slope, and threshold) and speech perception abilities does not exist (reviewed by van Eijl et al. 2017).

Two previous studies evaluated the relationship between ECAP IPG effects and speech perception. Kim et al. (2010) did not find a relationship between the IPG effect for slope and monosyllabic word or sentence-in-noise perception. However, Schvartz-Leyzac and Pfingst (2018) demonstrated that, for adults with bilateral CIs, between-ear differences in the IPG effect for slope predicted between-ear differences in consonant and sentence-in-noise perception. Interestingly, similar evidence suggests that between-ear differences in a psychophysical estimate of neural density (multipulse integration slope; Zhou & Pfingst 2014) and between-ear differences in post-mortem SGN density (Seyyedi et al. 2014) are predictive of between-ear differences in speech perception abilities. It is well-known that factors beyond the status of the SGNs, such as cognitive abilities, influence speech perception outcomes (e.g., Heydebrand et al. 2007; Holden et al. 2013; Finke et al. 2016). It is possible that the impact of peripheral neural degeneration on speech perception scores is better elucidated by within-subject comparisons that reduce the confounding influence of non-physiological factors on speech outcomes.

2.5.4 *Clinical Implications and Future Directions*

The current results support the theory that young listeners who were deafened and implanted during childhood may have healthier populations of SGNs compared to older adult-deafened and implanted listeners. Potential between-group differences in SGN density warrants investigation of different programming parameters in children and adults with CIs. It is particularly important

to optimize programming parameters for children, as individuals who are deafened early in life must develop speech and spoken language using the degraded input from a CI.

In fact, a recent study by Jahn et al. (2019) showed that CI channel interaction may be more detrimental to the speech perception performance of children than it is for adults. In that study, children and adults with normal hearing showed significant improvements in phoneme recognition performance when the degree of simulated CI channel interaction was reduced. Most notably, however, children's phoneme recognition performance continued to improve with reductions in simulated channel interaction beyond where adult performance plateaued or reached ceiling. This difference between children and adults persisted through late adolescence (at least up to age 17 years). The Jahn et al. study emphasizes the importance of optimizing spectral information for CI listeners, and especially for children.

If young listeners with CIs have healthier or denser populations of SGNs compared to older listeners, they may benefit from programming strategies that stimulate the auditory nerve using a spatially focused electrode configuration. Modern CI programming strategies use a spatially broad electrode configuration (i.e., monopolar), which likely results in substantial overlap of current between adjacent channels (Jolly et al. 1996; Kral et al. 1998). In adults with CIs, current focusing yields improved speech perception performance for some listeners (Berenstein et al. 2008; Srinivasan et al. 2013; Bierer & Litvak 2016; Arenberg et al. 2018). Results from Jahn et al. (2019) and the present study suggest that current focusing is worth investigating in young, child-implanted listeners.

Additionally, site selection strategies that deactivate electrodes near regions of poor neural health, or that stimulate relatively healthy neural regions with a spatially focused electrode configuration, may benefit children and young adults. Previous research has shown that

deactivating electrodes near cochlear regions with estimated poor neural function leads to improved speech perception performance in some postlingually deafened adult listeners (Garadat et al. 2013; Zhou 2017). To date, only one study has attempted to optimize programming for children with CIs using a site selection strategy (Noble et al. 2016). Noble et al. (2016) demonstrated that some children received speech perception benefit when poorly-positioned electrodes were deactivated. In children, continued investigation of site selection strategies that deactivate or employ current focusing based on the presumed status of the local electrode-neuron interface are warranted. In a companion study, we evaluate the utility of the ECAP in distinguishing between CI channels with estimated good and poor electrode-neuron interfaces in listeners with diverse hearing histories (Jahn & Arenberg, companion paper).

CHAPTER 3. DIFFERENCES BETWEEN LOCAL AND GLOBAL EVOKED POTENTIAL ESTIMATES OF THE COCHLEAR IMPLANT ELECTRODE-NEURON INTERFACE IN YOUNGER AND OLDER LISTENERS

3.1 ABSTRACT

Objectives: The primary objective of the present study was to quantify local (within-ear) and global (between-ear) differences in electrically evoked compound action potential (ECAP) estimates of the electrode-neuron interface in younger and older listeners with cochlear implants (CIs). In animals, evoked potential amplitudes, amplitude growth function slopes, and thresholds are predictive of spiral ganglion neuron (SGN) density and electrode placement relative to the target neurons. Moreover, large changes in ECAP characteristics as the interphase gap (IPG) of the stimulus is increased (i.e., the IPG effect) are associated with relatively healthy SGN populations. We tested the hypothesis that, within an ear, ECAP measures can be used to identify implant channels with presumed good and poor electrode-neuron interfaces, which may be influenced by a combination of SGN health, electrode position, and cochlear resistivity. We also hypothesized that differences in ECAP responses between younger and older listeners likely reflect global between-group differences in SGN integrity.

Design: Data were obtained from 18 implanted ears (13 individuals) with Advanced Bionics HiRes 90K devices. Eight ears (6 individuals) were children or young adults (age range: 14 to 32 years) and 10 ears (7 individuals) were older adults (age range: 54 to 88 years). In each ear, single-channel auditory detection thresholds were measured on channels 2-15 in response to a spatially focused electrode configuration (steered quadrupolar; focusing coefficient = 0.9). ECAP amplitudes, amplitude growth function slopes, and thresholds were assessed on a subset

of channels in each ear in response to three interphase gaps (0, 7 and 30 μs). Amplitudes were assessed on all available channels between 2 and 15. Amplitude growth functions and ECAP thresholds were assessed on the two non-adjacent channels with the lowest and highest focused behavioral thresholds in each ear. Interphase gap (IPG) effects were defined as the change in ECAP amplitude, growth function slope, and threshold with increasing stimulus IPG. Standard ECAP responses (amplitudes, slopes, and thresholds) and their respective IPG effects were compared across low- and high-threshold channels and between younger and older CI listeners.

Results: Channels that were estimated to interface poorly with the auditory nerve (i.e., high-focused-threshold channels) had steeper ECAP amplitude growth function slopes and higher ECAP thresholds than channels with low focused thresholds, irrespective of stimulus IPG. IPG effects did not differ as a function of implant channel. Younger listeners had steeper ECAP amplitude growth function slopes, irrespective of stimulus IPG. Moreover, younger listeners had larger IPG effects for amplitude than older listeners.

Conclusions: ECAP responses may be used to identify both local (within-ear) and global (between-ear) differences in the quality of the electrode-neuron interface. Results of this study support future investigation into the use of ECAP responses in site-selection CI programming strategies. The present results also support a growing body of evidence suggesting that children and young adults with CIs may have healthier populations of functional SGNs relative to older adults. Potential differences in global SGN integrity between younger and older listeners warrants investigation of optimal CI programming interventions based on their divergent hearing histories.

3.2 INTRODUCTION

Optimal auditory outcomes with a cochlear implant (CI) depend, in part, upon achieving appropriate patient-specific device settings. Yet, little is known about how to objectively customize CI programming interventions for individual listeners (Vaerenberg et al. 2014). Available evidence suggests that the fidelity of information transfer between each CI channel and local auditory neurons (i.e., the electrode-neuron interface) may influence auditory performance with an implant (Pfingst et al. 2004; Bierer 2007; Long et al. 2014; DeVries et al. 2016). Additionally, there is growing evidence that the electrode-neuron interface differs globally between younger and older listeners with CIs, likely resulting from their divergent hearing histories (Cafarelli Dees et al. 2005; Brown et al. 2010; DiNino et al. 2019).

In a companion study, we provided evidence that differences in the quality of the CI electrode-neuron interface as a function of age may be explained, in part, by the presence of healthier spiral ganglion neuron (SGN) populations in younger listeners than in older listeners (Jahn and Arenberg, companion paper). In the present study, we evaluate whether the electrically evoked compound action potential (ECAP) may be used to both identify relatively poor CI channels and distinguish global, across-listener differences in electrode-neuron interface quality. The ability to evaluate both local (within-ear) and global (across-ear) variation in the electrode-neuron interface may lead to the development of improved patient-centered programming interventions.

The ECAP, which is similar to wave I of the electrically evoked auditory brainstem response (EABR), represents a synchronized response from a group of electrically stimulated auditory nerve fibers (reviewed by He et al. 2017). Previous work in animal models suggests that ECAPs and EABRs may provide insight into the integrity of the spiral ganglion neurons (SGNs).

Specifically, animals with higher global SGN densities tend to have larger evoked potential amplitudes, steeper amplitude growth function (AGF) slopes, and lower thresholds than animals with fewer functional SGNs (Hall 1990; Miller et al.,1994; Shepherd & Javel 1997; Ramekers et al. 2014; Pfingst et al. 2015a,b). Across animal studies, AGF slope is the strongest correlate of global neural loss (Hall 1990; Shepherd & Javel 1997; Pfingst et al. 2015a,b).

In addition to standard amplitude and threshold measures, the magnitude of the change in ECAP characteristics with increasing stimulus interphase gap (IPG) reflects SGN density in animals. A change in ECAP characteristics with increasing stimulus IPG is hereafter referred to as an *IPG effect*. In cochlear-implanted guinea pigs, ECAP thresholds decrease (Prado-Guitierrez et al., 2006; Ramekers et al., 2014), and AGF slopes increase (Ramekers et al. 2014) with increasing IPG. Moreover, the current level required to evoke an equal-amplitude ECAP is lower for stimuli with longer IPGs (Prado-Guitierrez et al. 2006; Ramekers et al. 2014). Most importantly, in animals with few surviving SGNs, the magnitude of these IPG effects is smaller than in animals with a relatively healthy population of SGNs (Prado-Guitierrez et al. 2006; Ramekers et al. 2014).

Based on animal data, CI listeners with healthier populations of SGNs should theoretically demonstrate ECAP and EABR responses with larger amplitudes, steeper AGF slopes, lower thresholds and larger IPG effects than listeners with reduced SGN densities. Emerging evidence consistently demonstrates that younger CI listeners have steeper AGF slopes than older listeners (Cafarelli Dees et al. 2005; Brown et al. 2010). In the companion study, we demonstrated that, in addition to having steeper ECAP AGF slopes, younger listeners who were deafened and implanted during childhood have larger IPG effects for amplitude than older, adult-implanted listeners (Jahn & Arenberg, companion paper).

Children and young adults with CIs tend to differ from older adults in several demographic characteristics that are implicitly related to neural health. In particular, younger listeners are often implanted early in life and experience shorter durations of pre-implantation auditory deprivation than older adults. By definition, younger listeners also tend to have different hearing loss etiologies than older listeners. Each of those demographic characteristics, including chronological age, is correlated with SGN density in human temporal bones studies. Specifically, the number of remaining SGNs varies as a function of hearing loss etiology and is lowest in older individuals and in those who experienced long durations of deafness during life (Otte et al. 1978; Nadol et al. 1989; Nadol 1997; Makary et al. 2011). Taken together, differences in ECAP characteristics between younger and older CI users align with the findings from animal models, suggesting that younger listeners may have healthier global populations of SGNs than older listeners.

However, within a listener, single-channel evoked potential estimates seem to tell a different story. Bierer et al. (2011) measured EABRs on CI channels that were identified as having good or poor electrode-neuron interfaces, estimated via focused (tripolar) behavioral thresholds. Results suggested that high-threshold channels, which reflect a poor electrode-neuron interface, had *steeper* EABR amplitude growth functions than low-threshold channels. In a related study, Bierer and Nye (2014) demonstrated that high-threshold channels had steeper loudness growth functions and narrower dynamic ranges than low-threshold channels. Taken together, those results would suggest that steeper evoked potential and loudness growth functions are associated with degraded local electrode-neuron interfaces. This appears to contrast with the aforementioned animal and human data suggesting that steep evoked potential growth functions are expected in subjects with healthy populations of SGNs.

In support of the data presented by Bierer et al. (2011) and Bierer and Nye (2014), computational modeling evidence suggests that imposing discrete regions of local SGN loss leads to elevated thresholds and steeper growth of neural recruitment with increasing current levels (Goldwyn et al. 2010). Moreover, one animal study has demonstrated that EABR thresholds and AGF slopes decrease with increasing physical proximity of the electrode array to the inner wall of the cochlea (Shepherd et al. 1993). These findings suggest that within-subject patterns of evoked potential responses may be influenced by both local SGN integrity and electrode position, two important factors that influence the quality of the electrode-neuron interface.

Thus, evoked potential growth function characteristics that reflect degraded interfaces on a local level may differ, in part, from those that distinguish global, across-listener differences in SGN integrity. The goal of the present study was to assess characteristics of the ECAP response both within- and across-listeners in a group of participants with diverse hearing histories. Within each ear, ECAPs were measured on the two channels with the lowest and highest focused behavioral thresholds, representing estimated good and poor electrode-neuron interfaces, respectively (Bierer & Faulkner 2010; Bierer et al. 2011; Bierer & Nye 2014; Bierer et al. 2015c). We propose that, within a listener, ECAP responses can assist in identifying channels that interface poorly with the auditory nerve. In line with previous evoked potential data in humans and animals, we predict that channels with high focused behavioral thresholds will have smaller ECAP amplitudes, steeper AGFs, higher thresholds, and smaller IPG effects than channels with low behavioral thresholds. If the results of this study are consistent with those of Bierer et al. (2011), the ECAP would provide a more clinically feasible method than EABR for

estimating the local electrode-neuron interface and may assist in developing patient-specific site selection programming strategies.

In addition, across-listener differences in estimated SGN integrity will be evaluated by comparing responses across two groups of young and older CI listeners with divergent hearing histories. We propose that, across listeners, ECAP measures may assist in distinguishing global differences in SGN density. However, we predict that the pattern of ECAP responses associated with global variation in SGN density will differ from responses that distinguish between good and poor local electrode-neuron interfaces. Specifically, we hypothesize that younger listeners will have larger ECAP amplitudes, steeper AGFs, lower thresholds, and larger IPG effects than older listeners. Between-group differences in ECAP responses, which presumably reflect global differences in the electrode-neuron interface, can lead to the development of programming recommendations tailored to groups of patients with similar demographic characteristics.

3.3 MATERIALS AND METHODS

3.3.1 *Participants*

Demographic information for all ears tested in this study is presented in Table 3.1. Data were obtained from a total of 18 ears (13 subjects, 7 males) that were implanted with Advanced Bionics HiRes 90K devices (Valencia, CA). All participants had bilateral severe-to-profound sensorineural hearing loss. Because chronological age was bimodally distributed in this sample, the participants were divided into two age groups (younger and older) based on the mean chronological age (46.94 years). The younger group consisted of subjects younger than the mean age (< 46.94 years), whereas the older group was comprised of subjects older than the mean age (> 46.94 years). Duration of deafness, defined as the length of time (in years) between diagnosis

of severe-to-profound hearing loss and CI activation, was used as a proxy for pre-implantation auditory deprivation.

Table 3.1. Demographic information for all ears tested. H: high-focused-threshold channel; L: low-focused-threshold channel; ECAP: electrically evoked compound action potential; EVA: enlarged vestibular aqueduct; DFNB1: genetic non-syndromic hearing loss (Connexin-26 mutation); HF1J: HiFocus 1J electrode array; MS: Mid-Scala electrode array. Asterisks (*) denote participants that were tested with a 50 μs pulse width. The term "No responses" indicates that no measurable evoked potential responses could be obtained on any electrodes in that ear. Shaded rows indicate participants in the younger age group.

ID	Ear	Electrode Array	Etiology	Age at Test (years)	Age Implanted (years)	Duration of Deafness (years)	ECAP AGF Test Electrodes
P04	R	HF1J	Unknown	15.7	1.7	1.7	4 (L), 10 (H)
	L	HF1J	Unknown	15.7	4.7	4.7	2 (L), 6 (H)
P09	L	HF1J	Unknown	15.7	2.6	1.3	No responses
	R	HF1J	Unknown	15.7	3.9	2.7	2 (L), 9 (H)
P16	L	HF1J	DFNB1	14.6	1.0	1.0	5 (L), 9 (H)
	R	HF1J	DFNB1	14.6	4.5	4.5	6 (H), 15 (L)
P17*	R	HF1J	Unknown	15.5	1.3	1.3	2 (H), 9 (L)
S59	L	MS	Genetic; ototoxicity	32.4	30.9	18.9	2 (L), 7 (H)
S60	R	MS	Meningitis	22.5	19.2	19.1	4 (L), 14 (H)
S22	R	1J Helix	Unknown	78.6	66.7	11.8	7 (L), 13 (H)
S23*	L	1J Helix	Unknown	73.8	62.0	3.9	5 (H), 9 (L)
	R	HF1J	Unknown	73.8	64.6	6.5	11 (H), 13 (L)
S29	L	HF1J	Noise exposure	88.3	76.8	30.3	10 (H), 13 (L)
	R	MS	Noise exposure	88.3	85.7	39.2	8 (H), 13 (L)
S39	R	HF1J	Genetic	54.9	30.1	8.0	2 (H), 12 (L)
	L	HF1J	Genetic	54.9	40.1	18.0	6 (H), 12 (L)
S40	L	HF1J	EVA	56.7	50.4	46.4	3 (H), 9 (L)
S46	R	HF1J	Unknown	69.9	64.2	25.1	2 (L), 9 (H)
S52	R	HF1J	Unknown	71.7	66.0	6.1	11 (H), 13 (L)

Demographic information for the younger participants is highlighted in gray in Table 3.1. The younger participants (n = 8 ears, 6 subjects) ranged in age from 14.56 to 32.41 years (mean age = 19.38 years). The mean age at implantation of the younger participants was 9.67 years (range: 1.00 to 30.91 years) and the mean duration of deafness was 6.72 years (range: 1.00 to 19.07 years). Four of the younger participants (P04, P09, P16, and S59) were bilaterally

implanted, and each ear was tested separately whenever possible. S59's second-implanted ear was not able to be tested as part of this study due to time constraints, and one of P09's ears (left) did not have measurable ECAP responses on any electrode. All of the younger listeners were deafened during childhood (prior to age 18 years), and all but two (S59 and S60) were implanted as children.

The older participants (n = 10 ears, 7 subjects) ranged in age from 54.88 to 88.26 years (mean age = 70.56 years). The mean age at implantation for the older participants was 59.44 years (range: 30.12 to 76.80) and the mean duration of pre-implantation deafness was 19.53 years (range: 3.92 to 46.40 years). One older listener (S40) was deafened during childhood and received an implant as an adult. All other older listeners were deafened and implanted as adults (after age 18 years). Three of the older participants (S23, S29 and S39) were bilaterally implanted, and each ear was tested separately.

All participants were native speakers of American English and used spoken language to communicate. Each child provided written informed assent, and his or her parents or legal guardians provided written informed consent. Each adult provided written informed consent. The use of human subjects was reviewed and approved by the University of Washington Human Subjects Division.

3.3.2 *Channel Selection Procedure*

Single-channel focused behavioral thresholds were measured prior to ECAP testing. The two non-adjacent channels with the lowest and highest focused behavioral thresholds were selected in each ear for subsequent ECAP growth function measurement. Stimuli were biphasic, cathodic-leading pulse trains (102 μs/phase, 0-μs interphase gap, 200.4 ms duration, 997.9 pps) presented in a steered quadrupolar (sQP) stimulation mode. In sQP stimulation, a channel is comprised of

four adjacent intracochlear electrodes: two middle electrodes serve as active electrodes and two flanking electrodes serve as return electrodes. In this study, a current focusing coefficient of 0.9 was used, where 90% of the return current was delivered through the intracochlear return electrodes (45% to each return electrode) and the remaining 10% was delivered through an extracochlear ground. This highly focused stimulation mode was selected to capture as much within-subject variability in behavioral thresholds as possible, while stimulating below voltage compliance limits (Bierer 2007).

Thresholds were assessed using a modified Békésy style sweep procedure (based on Sék et al. 2005; Bierer et al. 2015a). The reader is referred to Bierer et al. (2015a) for a detailed description of the sweep procedure. Briefly, current steering was used to sweep the stimuli across the electrode array. This is accomplished by dividing the electrical current between two adjacent intracochlear electrodes and varying the steering coefficient, alpha (α), which specifies the proportion of return current delivered through each electrode. When $\alpha = 0$, all current is delivered through the more apical active electrode. When $\alpha = 1$, all current is delivered through the more basal active electrode. On electrodes 3-15, integer channel numbers refer to the basal active electrode when $\alpha = 1$; on channel 2, an α value of 0 is used to center the current on electrode 2. Due to the need for four adjacent intracochlear electrodes, sQP thresholds can only be obtained on channels 2-15. However, note that Advanced Bionics devices have 16 intracochlear electrodes.

To measure thresholds, the upper limit of stimulation on each electrode was set to the listener's most comfortable listening level (MCL), which was defined as a subjective loudness rating of "6" ("most comfortable") on the Advanced Bionics clinical loudness rating scale (Advanced Bionics, Valencia, CA). The pulse trains were presented starting at 6 dB below MCL

and swept across the electrode array by varying alpha from 0 to 1 in step sizes of 0.1. The participant continuously pressed a spacebar on a standard computer keyboard whenever he or she could hear the stimulus and released the spacebar when he or she could no longer perceive the stimulus. Each participant completed one basal sweep (progressing from channels 2 to 15) and one apical sweep (progressing from channels 15 to 2). Single-channel threshold estimates represent the weighted average of consecutive current levels at integer channel numbers along the basal and apical sweeps (see Bierer et al. 2015b for further details). After threshold measurement, the two non-adjacent channels with the lowest and highest sQP (focused) thresholds were identified in each ear for ECAP AGF testing.

3.3.3 *Electrically Evoked Compound Action Potentials (ECAPs)*

Equipment and Stimuli • Prior to ECAP testing, electrode impedances were measured in each ear using the SoundWave clinical software (Advanced Bionics, Valencia, CA) to identify non-functional electrodes and to avoid stimulating above voltage compliance limits. ECAP measurements were obtained using the Bionic Ear Data Collection System (BEDCS) version 1.18.315 (Advanced Bionics, Valencia, CA). Stimuli were delivered through a Platinum Series Processor (PSP). All stimuli were symmetric, biphasic, cathodic-leading pulses presented in a monopolar stimulation mode. Pulses were 25 μs/phase with IPGs of either 0, 7, or 30 μsec, depending on the experimental condition. Interphase gaps of 7 and 30 μs were used to remain consistent with the methods used in the companion paper, which evaluated ECAP responses in listeners with Cochlear Ltd. (Sydney, Australia) implants (Jahn & Arenberg, companion paper). An IPG of 0 μsec was also tested because it is a more clinically relevant IPG for Advanced Bionics devices. For two subjects (P17 and S23), the phase duration was increased to 50 μs to

achieve levels adequate for recording an ECAP response. Phase durations were constant across electrodes and ears within each subject.

Electrodes in Advanced Bionics devices are numbered from apex to base, with 1 denoting the most apical electrode and 16 denoting the most basal electrode. In this study, electrodes 1 and 16 were never tested because channel selection for AGFs was based on sQP thresholds, which cannot be evaluated on electrodes 1 and 16. For electrodes 3-15, ECAP responses were recorded from an intracochlear electrode that was located two positions apical to the stimulating electrode. When electrode 2 was stimulated, the recording electrode was located two positions basal (electrode 4). The extracochlear monopolar electrode served as the recording-indifferent electrode. The probe repetition rate was 20 Hz. A gain of 1000 (equivalent to 60 dB) was used. Artifact rejection was accomplished using a forward-masking technique (Abbas et al. 1999, 2004). The masker-probe interval was 400 μsec. The probe and the masker stimuli were always co-located, and the masker level was always 10% higher than the probe level to ensure adequate masking. ECAP responses were averaged across 50 to 100 sweeps and sampled at a rate of 56 kHz.

Amplitude Measurement • First, amplitudes were measured on electrodes 2 through 15 in response to each IPG (0, 7 and 30 μs; hereafter, referred to as 0-IPG, 7-IPG and 30-IPG, respectively). To set the upper limit of stimulation for the ECAP measurements, participants rated the loudness of 10 sweeps of the corresponding stimulus using a 10-point loudness rating scale (Advanced Bionics, Valencia, CA). The current level was manually increased from a sub-threshold level of 50 μA up until the subject reported a loudness rating of "8", corresponding to "maximal comfort" on the loudness rating scale. Hereafter, level "8" is referred to as the "maximum stimulation level".

For amplitude testing, loudness estimates were obtained using only the 30-IPG stimulus. This was done because pilot testing revealed that when stimuli with IPGs of 0, 7 and 30 μs were presented at equal current levels, the loudness percept of the 30-IPG stimulus was either louder than or equivalent to that of the 0-IPG and 7-IPG stimuli. Using the maximum stimulation level for the 30-IPG stimulus, ECAP amplitudes were measured across all functional electrodes between 2 and 15 in response to each IPG (0, 7 and 30 μs). The order of IPGs and electrodes tested was randomized for each ear. These measurements were used to evaluate differences in amplitude measured at equal current levels as a function of IPG. This procedure also assisted in identifying channels with measurable ECAPs for subsequent AGF testing.

Amplitude Growth Function (AGF) Measurement • Following amplitude testing, amplitude growth functions (AGFs) were assessed on the two non-adjacent channels with the highest and lowest focused (sQP) behavioral thresholds within each ear. If a desired channel did not have a measurable or adequate ECAP response during prior amplitude testing, the next-lowest or next-highest threshold channel was selected instead. Six out of the original 36 selected channels (17%) did not exhibit adequate ECAP responses for AGF testing and needed to be switched out for the next-lowest or next-highest threshold channels; four out of the six channels (67%) that had absent or poor ECAP morphology were high-threshold channels. The electrodes selected for AGF testing in each ear are listed in Table 3.1.

Prior to measuring AGFs, maximum stimulation levels were measured for the 0-IPG and the 7-IPG stimuli on each test channel using the loudness scaling procedure described in the previous section (recall that this information had already been collected for the 30-IPG stimulus). This was done to optimize the AGF obtained in response to each IPG. To measure AGFs, the current levels for the masker and probe (offset by 10%) were both systematically increased from

a sub-threshold current level up until the masker level was equivalent to the maximum stimulation level of the corresponding IPG. The starting level for AGF measurement was estimated based on the current level where the participant first heard the stimulus during the loudness scaling procedure. To obtain a sufficient number of data points for curve fitting, current level step sizes varied depending on the dynamic range (i.e., smaller step sizes were necessary for smaller dynamic ranges). A minimum of three data points was required for curve fitting. Note that an adequate AGF could not be obtained for subject P09R on channel 2 (low-threshold channel) in response to the 0-IPG stimulus. That data point is missing from the AGF slope and threshold analyses.

Data Analysis • ECAP data were exported from BEDCS into a custom MATLAB (MathWorks, Natick, MA) program that was used to manually mark the N1 and P2 peaks and to calculate the peak-to-peak amplitudes, AGF slopes, and thresholds. Stimulus current levels were converted from μA to dB re: 1 μA. Peak-to-peak amplitudes (in μV) were calculated from the leading negative peak (N1) to the following positive peak (P2). Amplitude growth function slopes (in μV/dB re: 1 μA) were calculated using linear regression through all data points that were recorded above the noise floor of the system (20 μV). ECAP threshold (in dB re: 1 μA) was defined as the x-intercept of the linear regression line for each growth function. Figure 3.1 shows AGFs measured on a low-threshold channel and a high-threshold channel in response to each IPG for one participant (P16L). Figure 3.2 shows the corresponding ECAP AGF waveforms measured in response to the 30-IPG stimulus for the same participant (P16L).

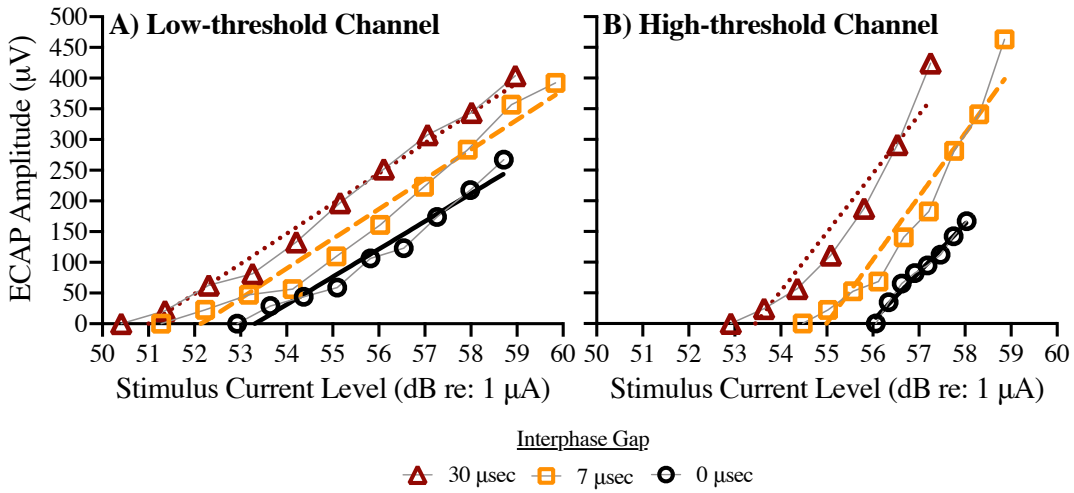

Figure 3.1. Examples of electrically evoked compound action potential (ECAP) amplitude growth functions measured on two channels within one ear (P16L). In each panel, three growth functions measured in response to stimuli with interphase gaps of 0, 7, and 30 μs are shown. Best-fit lines are included for each growth function. Various colors represent different input current levels. A) Low-threshold channel (electrode 5). B) High-threshold channel (electrode 9).

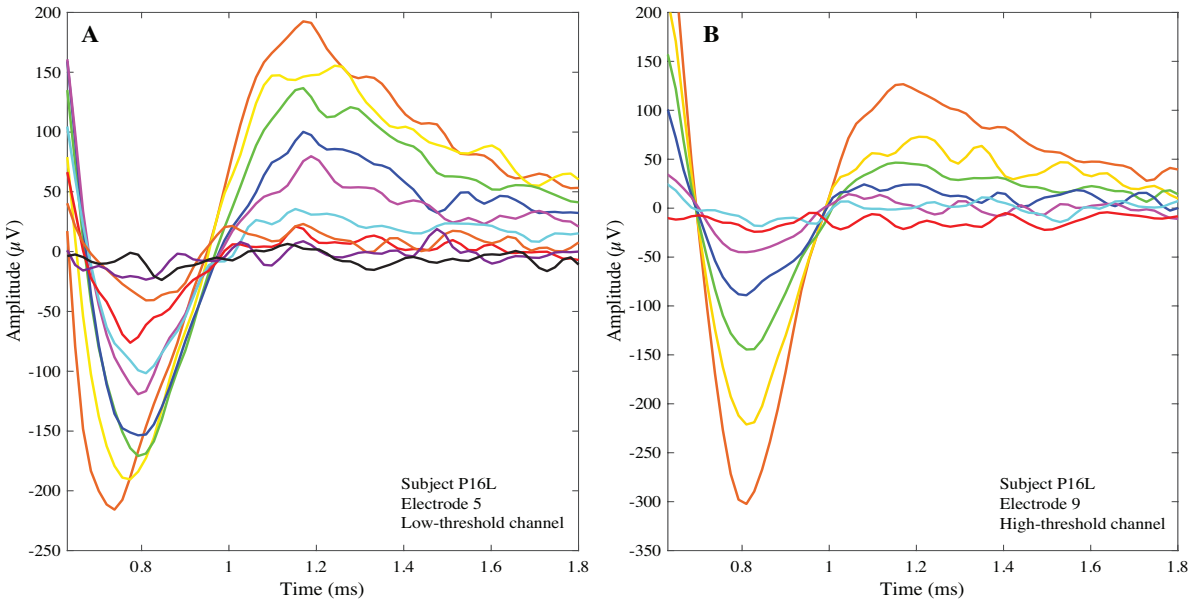

Figure 3.2. Examples of electrically evoked compound action potential (ECAP) waveforms measured on two electrodes within one ear (P16L) in response to an interphase gap (IPG) of 30 μs. Varying colors correspond to different input current levels. These waveforms correspond to the growth functions shown in Figure 3.1 in response to the 30 μs IPG. Note the differing y-axes in each panel. A) Low-threshold channel (electrode 5). B) High-threshold channel (electrode 9).

3.3.4 *Statistical Analysis*

Data were analyzed using R Version 3.3.1 (R Core Team 2016). Linear mixed-effects models with random effects for "participant" and "ear" were used to account for clustering of electrode-specific data within ears and for clustering of two ears within the bilateral listener. Models were fit with restricted maximum likelihood estimation (REML) parameter estimates to minimize small sample estimation bias (McNeish 2017). An unstructured covariance matrix was specified for each model. An Aikaike information criterion with a bias correction for small samples (AICc) was used for model selection (Hurvich & Tsai 1989). Where appropriate, Tukey's pairwise comparisons were performed using the Kenward-Roger degrees of freedom method. The lmerTest (Kuznetova et al. 2017), MuMIn (Bartón 2018), emmeans (Lenth 2018), and Lattice (Sarkar 2008) packages were used to perform the linear mixed-effects analyses and to assess the validity of the model assumptions.

3.4 RESULTS

3.4.1 *ECAP Characteristics as a Function of Interphase Gap and Cochlear Implant Channel*

The first goal of the study was to determine whether standard ECAP measures (amplitude, AGF slope, and threshold) and their respective IPG effects differ as a function of implant channel. Three separate linear mixed-effects models with dependent variables of amplitude (Model 1), AGF slope (Model 2) and ECAP threshold (Model 3) were specified to address the research question. Each model included random effects for "participant" and "ear". The primary predictor variables of interest were IPG (0, 7 or 30 μs) and channel (low- or high-threshold). An interaction term for IPG and channel (IPG*channel) was included to assess differences in the magnitude of the change in ECAP response with increasing IPG (i.e., IPG effect) between low-

and high-threshold channels. Electrode array was included in each model to control for potential differences in ECAP responses as a function of electrode placement relative to the modiolus. Model 1, which assessed predictors of ECAP amplitude, also included stimulus current level as an independent variable to account for differences in amplitude related to probe level.

Table 3.2 shows descriptive statistics (means and standard deviations) for ECAP amplitude, AGF slope, and ECAP threshold as a function of IPG and implant channel (low- versus high-threshold). Figure 3.3A shows average ECAP amplitudes $\pm$ 1 SE as a function of IPG and implant channel. Results of the linear mixed-effects model analysis revealed a significant main effect of IPG on ECAP amplitude (Figure 3.3A; $F(2, 84.27) = 19.86$, $p < 0.001$). Pairwise comparisons (Tukey) showed that amplitudes progressively increased with increasing stimulus IPG. Specifically, amplitudes were larger in response to the 30-IPG stimulus than in response to both the 7-IPG ($p = 0.003$) and the 0-IPG stimuli ($p < 0.001$). Amplitudes were also larger for the 7-IPG stimulus than for the 0-IPG stimulus ($p = 0.01$).

Table 3.2. Means and standard deviations for each standard ECAP measure as a function of cochlear implant channel (low- or high-threshold) and age group. Amplitude data as a function of age group is averaged across all available channels between 2 and 15. All other values are averaged across the two channels with the lowest and highest focused behavioral thresholds in each ear. ECAP: electrically evoked compound action potential; AGF: amplitude growth function; IPG: interphase gap.

	Standard ECAP Measures								
	Amplitude (μV)			AGF Slope (μV/dB re: 1 μA)			Threshold (dB re: 1 μA)		
	0-IPG	7-IPG	30-IPG	0-IPG	7-IPG	30-IPG	0-IPG	7-IPG	30-IPG
Channel									
Low-threshold	164.41 (*193.83*)	200.88 (*202.71*)	238.58 (*202.46*)	41.32 (*17.18*)	40.56 (*17.09*)	39.84 (*17.14*)	52.82 (*3.26*)	51.97 (*3.05*)	50.79 (*2.99*)
High-threshold	137.59 (*165.55*)	183.42 (*185.92*)	242.35 (*202.14*)	51.84 (*20.54*)	51.68 (*21.04*)	52.53 (*19.63*)	54.36 (*3.02*)	53.56 (*2.85*)	52.57 (*2.93*)
Age Group									
Younger	192.76 (*251.89*)	245.64 (*272.43*)	316.07 (*273.20*)	61.57 (*16.02*)	58.21 (*20.55*)	58.26 (*19.10*)	53.45 (*2.61*)	52.43 (*2.35*)	51.24 (*2.33*)
Older	117.59 (*75.77*)	149.36 (*70.06*)	179.98 (*75.16*)	35.60 (*13.54*)	36.44 (*12.68*)	36.53 (*13.23*)	53.73 (*3.63*)	53.03 (*3.50*)	52.04 (*3.55*)

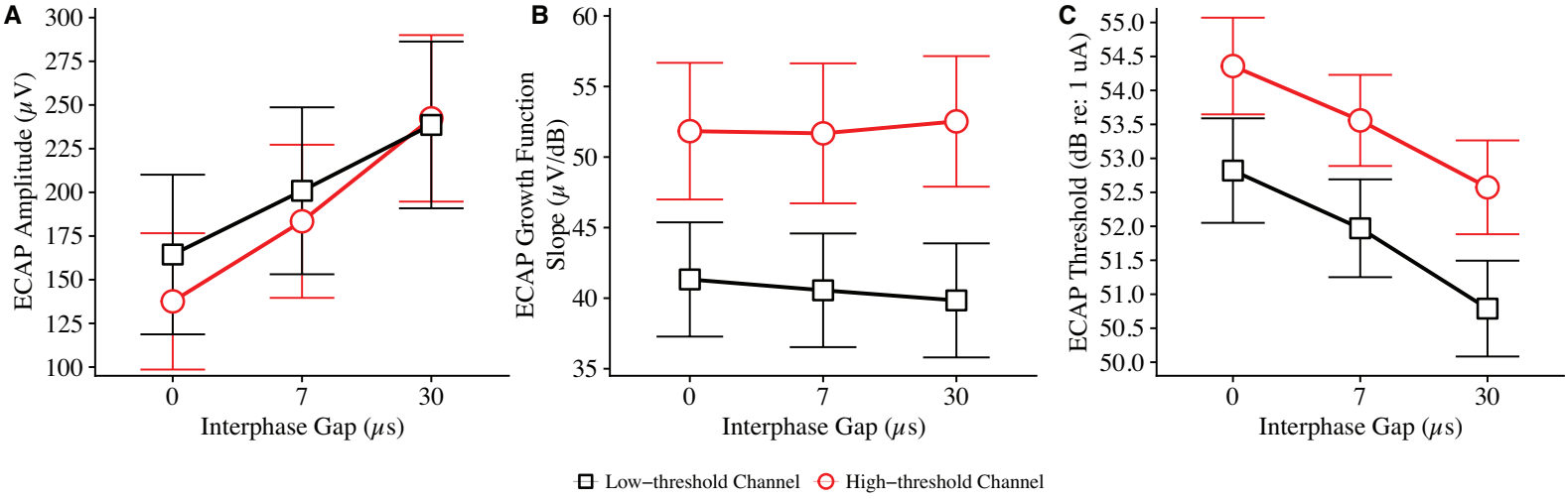

Figure 3.3. Mean (± 1 standard error) electrically evoked compound action potential (ECAP) characteristics as a function of implant channel and interphase gap (IPG): A) ECAP amplitude, B) ECAP amplitude growth function slope, C) ECAP threshold. Black squares denote data from low-behavioral-threshold channels and red circles denote data from high-behavioral-threshold channels.

On average, amplitudes also differed as a function of implant channel, wherein low-threshold channels had larger amplitudes than high-threshold channels ($F(1, 85.20) = 4.76$, $p = 0.03$). However, pairwise comparisons revealed that amplitudes did not differ significantly between low- and high-threshold channels in response to any one IPG in isolation (all ps > 0.05). Moreover, the interaction between IPG and channel was not significant, indicating that the magnitude of the change in amplitude with increasing IPG (i.e., the IPG effect for amplitude) was constant across low- and high-threshold channels ($F(2, 84.27) = 0.61$, $p = 0.55$). Across electrodes and IPGs, larger amplitudes were associated with higher stimulus current levels ($F(1, 62.23) = 40.50$, $p < 0.001$). Amplitudes did not differ across electrode array types ($F(2, 3.49) = 4.13$, $p = 0.12$).

Because absolute ECAP amplitudes are related, in part, to the stimulus current level, a follow-up analysis was performed to assess whether probe levels differed between the low- and high-threshold channels. Results indicated that probe level did not differ significantly between channels ($F(1, 89) = 1.99$, $p = 0.16$). This suggests that the average across-channel difference in ECAP amplitude cannot be explained by systematic differences in probe level.

Figure 3.3B shows average ECAP AGF slopes $\pm$ 1 SE as a function of IPG and implant channel. Results indicated that AGF slopes did not change systematically as a function of stimulus IPG (Figure 3.3B; $F(2, 84.06) = 0.03$, $p = 0.97$). However, high-threshold channels had significantly steeper AGF slopes than low-threshold channels ($F(1, 84.06) = 28.98$, $p < 0.001$). Pairwise comparisons (Tukey) revealed that slopes were steeper on high-threshold channels than on low-threshold channels in response to each IPG (0-IPG: $p = 0.007$; 7-IPG: $p = 0.003$; 30-IPG: $p < 0.001$). However, the interaction between channel and slope was not significant, indicating that the magnitude of the change in slope with increasing IPG (i.e., the IPG effect for slope) was

constant across low- and high-threshold channels ($F(2, 84.06) = 0.12$, $p = 0.90$). Slope did not differ across electrode array types ($F(2, 7.31) = 2.74$, $p = 0.13$).

Figure 3.3C shows average ECAP thresholds ± 1 SE as a function of IPG and implant channel. A significant main effect of IPG on ECAP threshold was observed (Figure 3.3C; $F(2, 84.04) = 16.07$, $p < 0.001$). Pairwise comparisons (Tukey) revealed that ECAP thresholds progressively decreased with increasing stimulus IPG. Specifically, ECAP thresholds were lower in response to the 30-IPG stimulus than in response to both the 7-IPG ($p = 0.005$) and the 0-IPG stimuli ($p < 0.001$). ECAP thresholds were also lower for the 7-IPG stimulus than for the 0-IPG stimulus ($p = 0.04$).

On average, ECAP thresholds also differed as a function of implant channel, wherein low-threshold channels had lower ECAP thresholds than high-threshold channels ($F(1, 84.04) = 34.84$, $p < 0.001$). Pairwise comparisons revealed that ECAP threshold differed significantly between low- and high-threshold channels in response to each IPG (0-IPG: $p = 0.002$; 7-IPG: $p = 0.001$; 30-IPG: $p < 0.001$). However, the interaction between IPG and channel was not significant, indicating that the magnitude of the change in ECAP threshold with increasing IPG (i.e., the IPG effect for threshold) was constant across low- and high-threshold channels ($F(2, 84.04) = 0.08$, $p = 0.92$). ECAP threshold did not differ across electrode array types ($F(2, 5.43) = 0.24$, $p = 0.79$).

Figure 3.4 shows single-channel ECAP characteristics measured in response to the 30-IPG stimulus: A) ECAP amplitude, B) ECAP AGF slope, C) ECAP threshold. Lines connect data points across channels that correspond to the same tested ear. Data are shown for the 30-IPG stimulus because amplitudes were measured at current levels that corresponded to the maximum stimulation level of the 30-IPG stimulus. Recall that ECAP amplitudes did not differ

significantly between low- and high-threshold channels in response to any one IPG in isolation. Accordingly, individual data show that only 10 out of 18 ears tested (56%) had larger ECAP amplitudes on the low-threshold channel than on the high-threshold channel in response to the 30-IPG stimulus (Figure 3.4A).

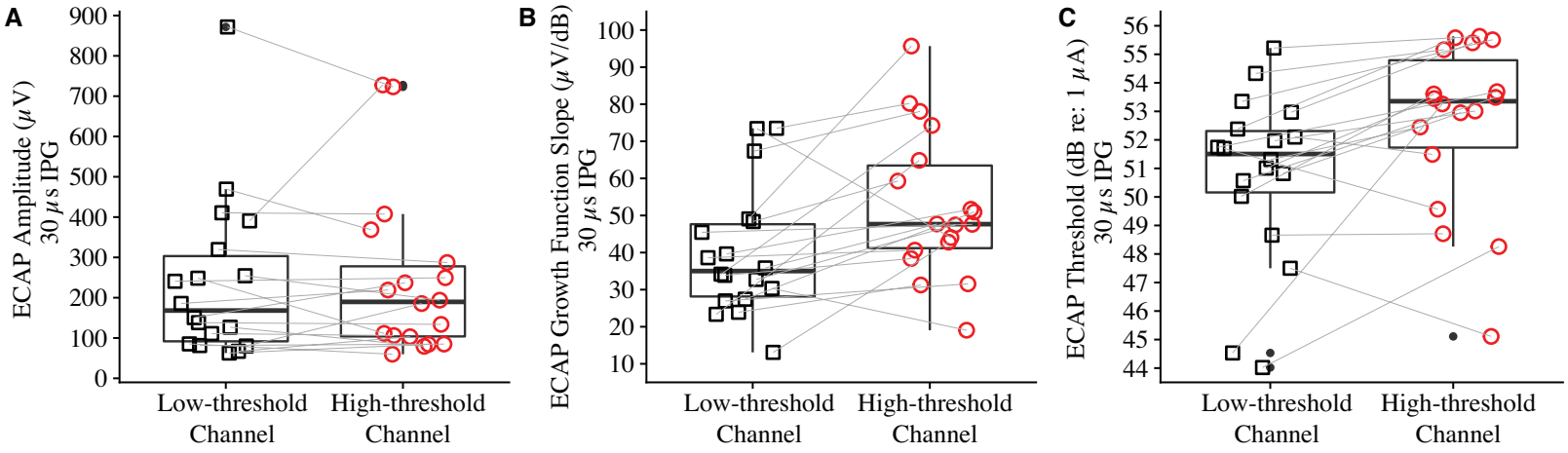

Figure 3.4. Single-channel electrically evoked compound action potential (ECAP) characteristics measured in response to the 30 µs interphase gap (IPG), stratified by implant channel: A) ECAP amplitude, B) ECAP amplitude growth function slope, C) ECAP threshold. Gray lines connect data points across channels that correspond to the same tested ear. Black squares denote data from low-behavioral-threshold channels and red circles denote data from high-behavioral-threshold channels. Boxplots show the median and the first and third quartiles.

On the other hand, only two out of the 18 ears (11%; Subjects P04R and S23L) did not show the expected within-subject pattern of a shallower ECAP AGF slope on the low-threshold channel compared to the high-threshold channel (Figure 3.4B; 30-IPG stimulus). Similarly, three out of 18 ears (17%; Subjects S23L, S39R and S60) did not show the expected within-subject pattern of a lower ECAP threshold on the low-threshold compared to the high-threshold channel (Figure 3.4C; 30-IPG stimulus). Notably, P04R and S23L were two of the original six ears that required a channel swap for ECAP testing due to poor or absent ECAP responses on the true

high-threshold (P04R) or low-threshold (S23L) channel (Table 3.1). Thus, P04's high-threshold channel and S23L's low-threshold channel do not represent the two channels with the most extreme focused thresholds across their respective electrode arrays. Still, only one subject (S23L) had between-channel differences in *both* ECAP slope and threshold that diverged from the group data. Taken together, the individual and group data suggest that, in most ears, within-subject ECAP AGF slopes and ECAP thresholds may reliably capture local differences in the electrode-neuron interface, whereas ECAP amplitudes may not.

3.4.2 *ECAP Characteristics as a Function of Age Group*

The second goal of the study was to determine whether standard ECAP measures (amplitude, AGF slope, and threshold) and their respective IPG effects differ as a function of age group. Like before, three separate linear mixed-effects models with dependent variables of ECAP amplitude (Model 4), AGF slope (Model 5) and ECAP threshold (Model 6) were specified to address the research question. Each model included random effects for "participant" and "ear". The primary predictor variables of interest were IPG (0, 7 or 30 μs) and age group (younger or older). An interaction term for IPG and age group (IPG*age group) was included to assess differences in the magnitude of the change in ECAP response with increasing IPG (i.e., IPG effect) between younger and older listeners. Again, Model 4, which assessed predictors of ECAP amplitude, also included stimulus current level as an independent variable to account for differences in amplitude related to probe level. Electrode array was not included in these models, as it was previously determined that electrode array did not significantly contribute to observed differences in the ECAP responses in this sample.

Initially, duration of deafness was included as a predictor variable in each model to control for pre-implantation auditory deprivation. However, during the model selection

procedure, it was determined that the most parsimonious model fits (i.e., lowest AICc values) were obtained when duration of deafness was excluded. This is likely because duration of deafness co-varied with chronological age.

Table 3.2 shows descriptive statistics (means and standard deviations) for standard ECAP measures (amplitude, AGF slope, and threshold) as a function of age group. Recall that amplitudes were assessed on all available channels between 2 and 15 in each ear. Figure 3.5 shows ECAP amplitudes averaged across all available channels between 2-15 (i.e., across-site average amplitudes) for each ear tested. Data are stratified by IPG and age group, and lines connect data points across IPGs that correspond to the same tested ear. Figure 3.6A shows single-channel ECAP amplitudes assessed on only the low- and high-threshold channels, stratified by IPG and age group. Lines connect data points across IPGs that correspond to the same tested ear and channel. Figure 3.6B shows average ECAP amplitudes $\pm$ 1 SE as a function of IPG and age group.

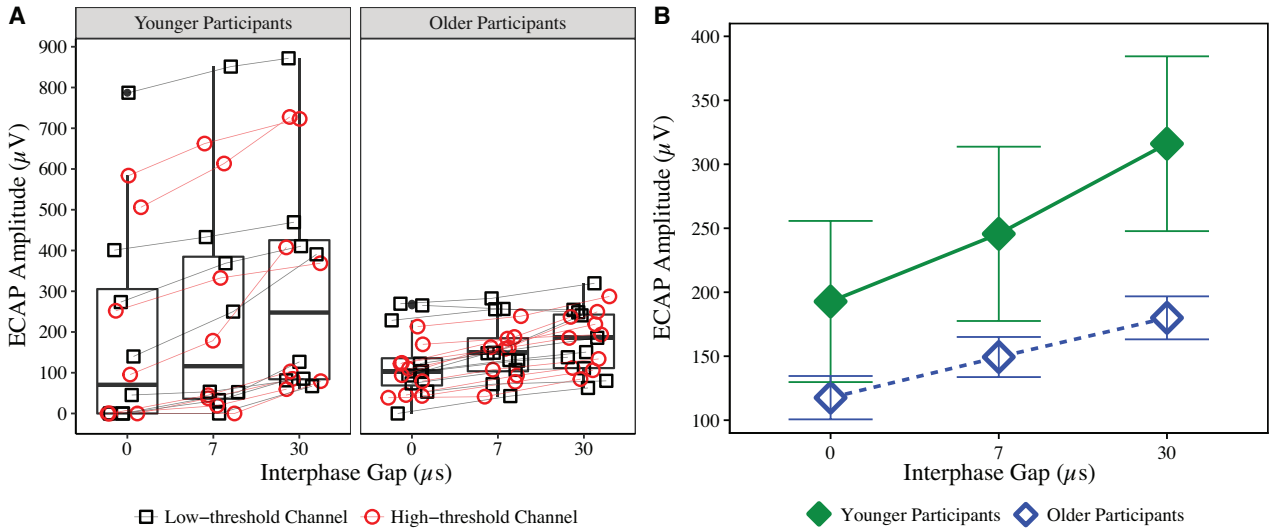

Figure 3.5. Across-site average electrically evoked compound action potential (ECAP) amplitudes in each ear as a function of age group. Amplitudes are averaged across all functional channels between 2 and 15 in each ear. Gray lines connect data points across interphase gaps (IPGs) that correspond to the same tested ear. For bilaterally implanted participants, circles represent first-implanted ears and triangles represent second-implanted ears. Boxplots show the median and the first and third quartiles.

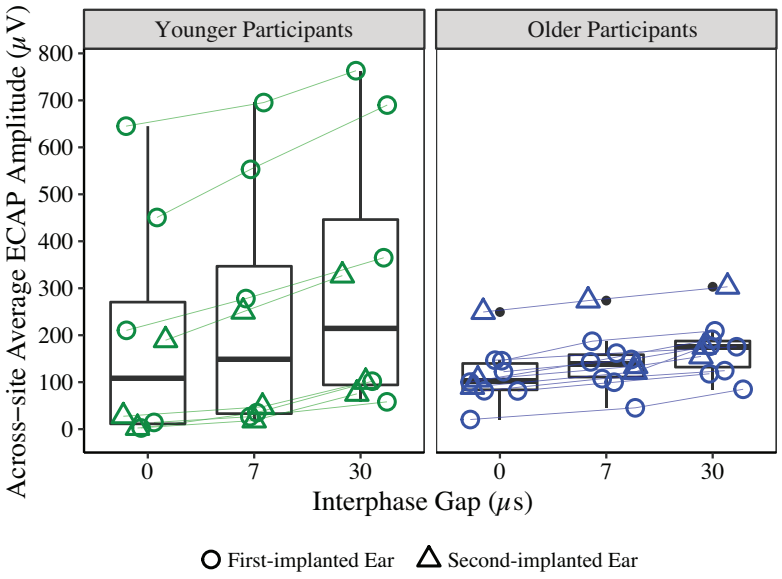

Figure 3.6. A) Single-channel electrically evoked compound action potential (ECAP) amplitudes. Data are stratified by interphase gap (IPG) and age group (younger and older participants). Black squares denote data from low-behavioral-threshold channels and red circles denote data from high-behavioral-threshold channels. Lines connect data points across IPGs that correspond to the same tested ear and channel. Boxplots show the median and the first and third quartiles. B) Mean (± 1 standard error) ECAP amplitudes for each age group, stratified by IPG. Each data point represents amplitudes averaged across all electrodes assessed within each age group. Green filled diamonds represent data from the younger participants and blue open diamonds represent data from the older participants.

The linear mixed-effects model predicting ECAP amplitude included electrode-specific data for all available channels between 2 and 15. Results suggested that, on average, ECAP amplitudes did not differ between the younger and older groups ($F(1, 10.77) = 3.82$, $p = 0.08$). However, pairwise comparisons revealed that younger listeners had larger amplitudes than older listeners in response to the 30-IPG stimulus ($p = 0.04$). Recall that amplitudes were assessed at equal current levels for all three IPGs, and that the current level corresponded to the maximum stimulation level for the 30-IPG stimulus. Thus, amplitudes in response to the 30-IPG condition more closely reflect true peak amplitudes for that stimulus, whereas those in response to 0-IPG and 7-IPG may not. Additionally, the interaction between age group and IPG was significant,

indicating that younger listeners exhibited a larger IPG effect than the older listeners, or a larger increase in ECAP amplitude as the IPG of the stimulus was increased ($F(2, 676.03) = 12.73$, $p < 0.001$).

Again, probe current level was significantly related to ECAP amplitude, wherein larger absolute amplitudes were associated with higher stimulus levels ($F(1, 687.95) = 254.71$, $p < 0.001$). So, a follow-up analysis was performed to assess whether probe levels differed as a function of age group. Results indicated that probe level did not differ significantly between younger and older listeners ($F(1, 11.07) = 0.51$, $p = 0.49$). This suggests that larger ECAP amplitudes for younger listeners than for older listeners cannot be explained by systematic between-group differences in stimulus current level.

Figure 3.7A shows single-channel ECAP AGF slopes assessed on the low- and high-threshold channels, stratified by IPG and age group. Lines connect data points across IPGs that correspond to the same tested ear and channel. Figure 3.7B shows average ECAP amplitudes $\pm$ 1 SE as a function of IPG and age group. Results from the linear mixed-effects model suggested that, on average, AGF slopes were significantly steeper for younger listeners than for older listeners ($F(1, 9.14) = 14.21$, $p = 0.004$) across all tested IPGs (0-IPG: $p = 0.002$; 7-IPG: $p = 0.006$; 30-IPG: $p = 0.006$). The interaction between slope and age group was not significant, indicating that the IPG effect for slope did not differ between younger and older listeners ($F(1, 85.10) = 0.26$, $p = 0.77$).

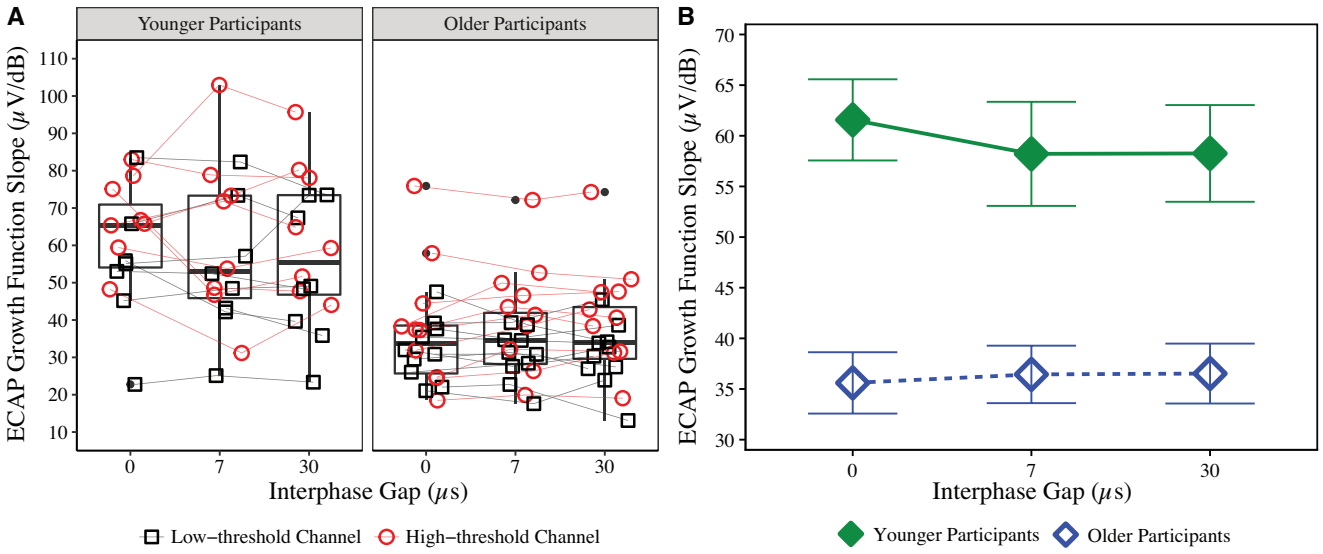

Figure 3.7. A) Single-channel electrically evoked compound action potential (ECAP) amplitude growth function slopes. Data are stratified by interphase gap (IPG) and age group (younger and older participants). Black squares denote data from low-behavioral-threshold channels and red circles denote data from high-behavioral-threshold channels. Lines connect data points across IPGs that correspond to the same tested ear and channel. Boxplots show the median and the first and third quartiles. B) Mean (± 1 standard error) ECAP slopes for each age group, stratified by IPG. Each data point represents slopes averaged across all electrodes assessed within each age group. Green filled diamonds represent data from the younger participants and blue open diamonds represent data from the older participants.

Figure 3.8A shows single-channel ECAP thresholds assessed on the low- and high-threshold channels, stratified by IPG and age group. Lines connect data points across IPGs that correspond to the same tested ear and channel. Figure 3.8B shows average ECAP thresholds ± 1 SE as a function of IPG and age group. Results indicated that ECAP thresholds did not differ significantly between age groups ($F(1, 11.23) = 0.84$, $p = 0.38$). The interaction between ECAP threshold and age group was also not significant, indicating that the IPG effect for threshold did not differ between younger and older listeners ($F(2, 90.25) = 0.26$, $p = 0.77$).

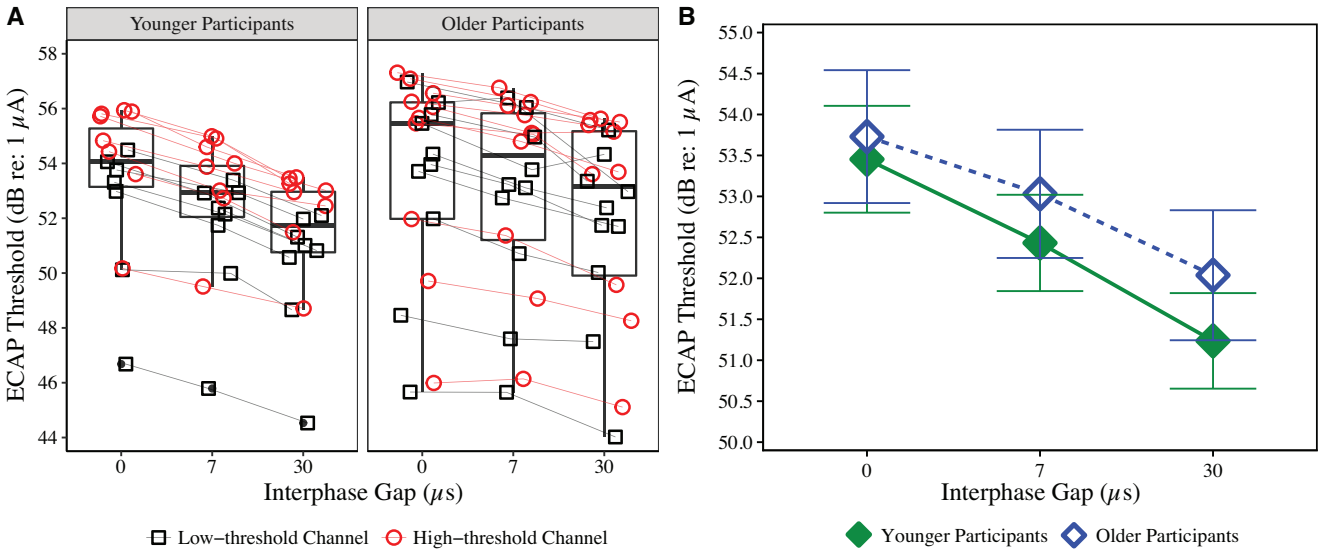

Figure 3.8. A) Single-channel electrically evoked compound action potential (ECAP) thresholds. Data are stratified by interphase gap (IPG) and age group (younger and older participants). Black squares denote data from low-behavioral-threshold channels and red circles denote data from high-behavioral-threshold channels. Lines connect data points across IPGs that correspond to the same tested ear and channel. Boxplots show the median and the first and third quartiles. B) Mean (± 1 standard error) ECAP thresholds for each age group, stratified by IPG. Each data point represents ECAP thresholds averaged across all electrodes assessed within each age group. Green filled diamonds represent data from the younger participants and blue open diamonds represent data from the older participants.

3.4.3 *ECAP Characteristics in Relation to Electrode Impedances*

Follow-up analyses were conducted to assess whether the ECAP measures in this study were related, in part, to electrode impedances. Three separate models were specified with electrode-specific ECAP amplitude, AGF slope, and ECAP threshold as dependent variables. In each model, IPG, electrode impedance, and an interaction term for IPG and impedance (IPG*impedance) were included as independent variables. Random effects for subject and ear were specified.

Results indicated that electrode impedances were inversely related to ECAP amplitude ($F(1, 722.74) = 66.50$, $p < 0.001$), AGF slope ($F(1, 88.69) = 9.14$, $p = 0.003$), and ECAP thresholds ($F(1, 83.33) = 13.45$, $p < 0.001$). Specifically, relatively large ECAP amplitudes, steep AGF slopes, and high ECAP thresholds measured in response to a constant IPG were associated with relatively low electrodes impedances. However, the IPG*impedance interactions were not significant in any model [Amplitude: $F(2, 723.99) = 0.87$, $p = 0.42$); Slope: $F(1, 81.08) = 0.54$, $p = 0.58$; Threshold: $F(2, 84.34) = 0.09$, $p = 0.91$]. This suggests that IPG effects varied relatively independently of electrode impedances.

Because ECAP amplitudes, AGF slopes, and thresholds measured in response to a constant IPG were correlated with electrode impedance in this study, a final follow-up analysis was performed to assess the relation between electrode impedances (dependent variable) and 1) CI channel and 2) age group. Electrode impedances were significantly lower on the high-threshold channels than on the low-threshold channels ($F(1, 89) = 40.30$, $p < 0.001$). However, electrode impedances did not differ between the younger and older listeners ($F(1, 11.76) = 1.65$, $p = 0.23$) in this sample.

3.5 DISCUSSION

The present study assessed the utility of ECAP measures in characterizing both local (within-ear) and global (across-ear) variation in the quality of the electrode-neuron interface. Results demonstrated that ECAP characteristics that reflect the local quality of the electrode-neuron interface may differ from those that reveal across-listener differences in global SGN integrity. Specifically, CI channels estimated to interface relatively poorly with the SGNs (i.e., high-behavioral-threshold channels) had steeper AGFs, higher ECAP thresholds, and smaller ECAP amplitudes than presumed higher-functioning channels. Across subjects, however, younger

listeners had steeper AGFs, larger ECAP amplitudes, and larger IPG effects than older listeners. Overall, results support the use of ECAPs to identify presumed low- and high-functioning CI channels within an ear. Moreover, the data enhance the growing body of literature suggesting that younger, early deafened and implanted listeners likely have healthier populations of SGNs than older adults.

3.5.1 *ECAPs Can Assist in Identifying Channels with Poor Electrode-Neuron Interfaces*

Variation in the quality of the electrode-neuron interface is influenced by several underlying factors including the radial distance between the CI electrodes and the target SGNs, the numbers and distribution of viable SGNs, and bone and tissue growth within the scala tympani (Goldwyn et al. 2010; Bierer 2010). The results of the present study suggest that, within an ear, ECAP measures are sensitive to the local quality of the electrode-neuron interface, and they may be used to identify relatively high- and low-functioning channels. Differences in ECAP AGF slope and threshold may be particularly useful metrics for identifying local channels that interface poorly with the auditory nerve. Specifically, channels with high focused behavioral thresholds had consistently steeper AGF slopes and higher ECAP thresholds than channels with low focused behavioral thresholds, irrespective of the IPG of the stimulus.

Prior animal data suggest that evoked potential AGF slopes decrease with increasing neural loss (Smith & Simmons 1983; Hall 1990; Miller et al. 1994; Pfingst et al. 2015a,b). On the surface, this seems to contrast with our results showing steeper slopes on channels that are presumed to interface poorly with the auditory nerve. However, our findings are consistent with those of Bierer et al. (2011), who demonstrated steeper EABR slopes on channels with high focused behavioral thresholds than on channels with low focused behavioral thresholds. Similarly, Bierer and Nye (2014) showed that channels with high focused thresholds have

steeper loudness growth functions and smaller dynamic ranges than channels with low focused thresholds.

Notably, animals in the evoked potential studies are deafened with ototoxic drugs administered uniformly throughout the basal turn of the cochlea, likely inducing a relatively global loss of neurons (Hall 1990; Shepherd et al. 1993). In contrast, human CI listeners likely have a combination of global and localized neural loss (Nadol 1997). Modeling data suggest that a reduced local neuron count leads to relatively fast growth of neural recruitment with increasing current level (Goldwyn et al. 2010). In the same modeling study, a large radial distance between CI electrodes and local SGNs also resulted in fast neural recruitment. Moreover, Shepherd et al. (1993) demonstrated progressively steeper evoked potential AGF slopes as the electrode array was moved closer to the modiolus in implanted cats. Previous data, therefore, suggest that growth of evoked potential amplitude with increasing current on a single channel can reflect either a loss of local SGNs, a large distance between the electrode and the modiolus, or a combination of both factors.

In fact, several studies have demonstrated that, within- and across-subjects, electrode-to-modiolus distance is one of the strongest factors influencing variation in focused behavioral thresholds (Long et al. 2014; DeVries et al. 2016; DeVries & Arenberg 2018; Jahn & Arenberg 2019). In the present study, ECAP AGFs were assessed on two channels that were selected based on the relative within-ear magnitude of focused behavioral thresholds. Thus, it is likely that electrode position relative to the modiolus strongly co-varied with the selection of channels. Steeper ECAP AGF slopes on the high-threshold channels than on the low-threshold channels likely reflect, to a large extent, relatively suboptimal positioning of the electrodes relative to the target SGNs.

Though local SGN integrity presumably influences focused behavioral thresholds and ECAP measures to some extent, it is likely that the channel selection procedure in this study yielded channels that differed widely in electrode position, and less so in neural integrity. This idea is corroborated by our finding that IPG effects did not differ between low- and high-threshold channels. It has been proposed that examining how ECAP characteristics change as the IPG of the stimulus increases can provide an estimate of neural health that is relatively independent of non-physiological conditions between the neurons and the electrodes (Ramekers et al. 2014; Schvartz-Leyzac & Pfingst 2016). In fact, Schvartz-Leyzac and Pfingst (2016) demonstrated that ECAP slopes and amplitudes measured in response to a constant IPG were significantly correlated with electrode impedances in 37.5% of cases. However, in the same subjects, IPG effects for slope and amplitude varied relatively independently of the impedance environment surrounding the electrodes.

In the present study, the local impedance environment influenced ECAP responses measured with a constant IPG, whereas IPG effects were not related to electrode impedances. Specifically, relatively small ECAP amplitudes, shallow AGF slopes, and low ECAP thresholds were associated with relatively high electrode impedances, consistent with Schvartz-Leyzac and Pfingst (2016). Additionally, channels with low focused behavioral thresholds had higher electrode impedances than channels with high focused behavioral thresholds, which is consistent with previous electrical field imaging data (Jahn & Arenberg 2019). Taken together, these findings suggest that local differences in the impedance environment contribute, in part, to across-channel differences in ECAP responses measured in with a constant IPG.

Overall, the results of this study suggest that ECAP AGF slopes and thresholds may be used to identify CI channels within an ear that interface relatively poorly with the auditory nerve.

In isolation, ECAP amplitudes are not sensitive enough to distinguish good and poor interfaces, due to their strong relationship with probe level, which is based on subjective loudness percepts. Differences in AGF slopes and thresholds as a function of implant channel in this study were likely driven, in part, by the radial distance of the electrodes from the modiolus and local cochlear resistivity. Though SGN integrity can presumably differ between channels with low and high behavioral thresholds, the lack of IPG effect and the robust across-study relationship between electrode position and focused thresholds suggest that the health of the auditory nerve may not play a substantial role in local ECAP measures assessed with a constant IPG in humans. Channel-to-channel variability in SGN health may be better elucidated by assessing ECAP IPG effects across the entire electrode array (Schvartz-Leyzac & Pfingst 2016, 2018).

3.5.2 *Differences in ECAP Responses between Younger and Older Listeners*

A second objective of the present study was to compare ECAP responses between younger and older listeners who presumably differed in global SGN integrity. In the companion study, we demonstrated that younger listeners who were deafened and implanted during childhood had steeper ECAP AGF slopes and larger IPG effects for amplitude than older, adult-implanted listeners (Companion paper). In a different sample of participants with Advanced Bionics devices, the present study also demonstrated that younger listeners had steeper ECAP AGF slopes and larger IPG effects for amplitude than older listeners. Together, these findings support a growing body of literature suggesting that the electrode-neuron interface differs systematically between younger, early deafened and implanted listeners and older adults with CIs (Hughes et al. 2001; Cafarelli Dees et al. 2005; Brown et al. 2010; DiNino et al. 2019).

In this study, we showed that, within an ear, relatively steep ECAP AGF slopes reflect relatively poor electrode-neuron interfaces and are likely influenced by combined differences in

electrode placement within the cochlea, cochlear resistivity, and SGN health. It is unlikely that between-group differences in AGF slope were due to systematic differences in electrode position because the cochlea is adult-sized at birth (e.g., Pelliccia et al. 2014). Furthermore, although not all participants in this study had the same electrode array, we demonstrated that differences in electrode array type did not significantly influence the ECAP measures.

It is possible that between-group differences in ECAP characteristics could result from systematic differences in cochlear resistivity. Prior research has demonstrated that children tend to have higher tissue impedances than adults with CIs (Hughes et al. 2001; Molisz et al. 2015; DiNino et al. 2019). But, if similar systematic differences in intracochlear resistance contributed to the between-group differences in slope, then slopes would have been shallower in the younger listeners than in the older listeners (Schvartz-Leyzac & Pfingst 2016). We observed the opposite relationship here, and in the companion study.

Thus, steeper slopes in the younger listeners than in the older listeners likely reflect, in part, healthier populations of SGNs in the younger group. This is corroborated by the finding that IPG effects for amplitude were also significantly larger for the younger listeners than for the older listeners. In animals, relatively large changes in ECAP amplitudes with increasing stimulus IPG are associated with relatively robust global populations of SGNs (Prado-Guitierrez et al. 2006; Ramekers et al. 2014). Of note, IPG effects for slope and threshold did not differ between groups in this study or in the companion study. Similarly, previous reports in humans and in animals have not found consistent IPG effects for ECAP thresholds (Prado-Guitierrez et al. 2006; Ramekers et al. 2014; Hughes et al. 2018) or slopes (Ramekers et al. 2014; Hughes et al. 2018; Schvartz-Leyzac & Pfingst 2016, 2018). It is possible that AGF slopes measured in response to a

constant IPG and IPG effects for amplitude are more robust predictors of neural health in humans than IPG effects for slope and threshold.

In fact, steeper AGF slopes (Cafarelli Dees et al. 2005; Brown et al. 2010; Companion paper) and larger IPG effects for amplitude (Companion paper) between younger and older listeners are now robust findings across multiple investigations. The present results are thus consistent with prior ECAP data in humans and provide increasingly strong support that SGN density differs between younger and older listeners with CIs. Moreover, to our knowledge, the present report is the first to demonstrate this relationship in listeners with Advanced Bionics devices, as previous work, including the companion study, was conducted in those with Cochlear Ltd (Sydney, Australia) implants (Cafarelli Dees et al. 2005; Brown et al. 2010; Companion paper). Differences in ECAP AGF slope and the IPG effect for amplitude between younger and older listeners appear to be consistent across device types.

Despite being grouped by chronological age, the younger and older listeners in this study, in the companion study, and in others (Cafarelli Dees et al. 2005; Brown et al. 2010) differed in several demographic characteristics that are implicitly related to SGN integrity. The younger listeners were all deafened during childhood and experienced shorter durations of pre-implantation auditory deprivation compared to the older listeners. On the other hand, all but one participant in the older group (subject S40) were deafened as adults. Although most participants did not know the cause of their hearing loss, etiologies associated with childhood hearing impairment often differ from those associated with adult-onset deafness. Importantly, human temporal bone studies indicate that global SGN density varies as a function of hearing loss etiology and decreases with increasing chronological age and duration of deafness during life (Otte et al. 1978; Nadol et al. 1989, 1997; Makary et al. 2011). There is also some evidence that

chronic electrical stimulation by a CI in neonatally deafened animals may contribute to SGN survival (Lousteau 1987; Leake et al. 1991, 1992, 1999). Taken together, the present study and others suggest that, overall, children and young adults with CIs likely have more robust populations of healthy SGNs compared to older adults.

3.5.3 *Clinical Implications and Future Directions*

Prior evidence suggests that deactivating CI electrodes that are presumed to interface poorly with the auditory nerve may improve speech perception outcomes for some CI listeners (Garadat et al. 2013; Noble et al. 2013, 2014, 2016; Bierer & Litvak 2016; Zhou 2017). In those investigations, the deactivated channels were selected based on poor psychophysical performance (temporal modulation detection: Garadat et al. 2013; behavioral thresholds: Bierer & Litvak 2016; multipulse integration: Zhou 2017) or poor electrode position estimated via computed tomography (CT) imaging (Noble et al. 2013, 2014, 2016). However, estimating psychophysical performance on every available CI electrode is generally not clinically feasible due to time or attention constraints. Difficult psychophysical tasks are also not practical for young children or patients with limited cognitive resources. Moreover, CT imaging can be cost-prohibitive and exposes patients to radiation.

Alternatively, the present study suggests that ECAP responses can be used to identify local CI channels with poor electrode-neuron interfaces. ECAP measures are attractive clinical tools because they can be assessed with existing clinical software and equipment. They are also relatively time and cost effective, robust to muscle artifact and sleep state, and do not require the patient's sustained attention. A caveat to ECAP measures, however, is that some patients do not have measurable responses within their comfortable listening range (e.g., P09L in the present dataset and PC13R in the companion study). In such cases, ECAPs would not be useful for

distinguishing between channels with relatively good and poor electrode-neuron interfaces. Nevertheless, future investigations should assess the efficacy of site-selection programming strategies based on ECAP responses in children and adults with CIs.

Additionally, potential differences in global SGN health between younger and older adults with CIs may portend differences in optimal CI stimulation strategies between the two populations. For instance, if children and young adults have relatively healthy or dense populations of SGNs, they may benefit from a focused electrode configuration that restricts electrical current spread relative to the traditional monopolar mode. In fact, recent evidence suggests that children with normal hearing may receive more speech perception benefit than adults when simulated CI channel interaction is reduced (Jahn et al. 2019). Future work may assess potential benefits of current focusing in children with CIs.

CHAPTER 4. EVALUATING PSYCHOPHYSICAL POLARITY SENSITIVITY AS AN INDIRECT ESTIMATE OF NEURAL STATUS IN COCHLEAR IMPLANT LISTENERS

Published in the *Journal of the Association for Research in Otolaryngology* (2019)

DOI: 10.1007/s10162-019-00718-2

4.1 ABSTRACT

The physiological integrity of spiral ganglion neurons is presumed to influence cochlear implant (CI) outcomes, but it is difficult to measure neural health in CI listeners. Modeling data suggest that, when peripheral processes have degenerated, anodic stimulation may be a more effective neural stimulus than cathodic stimulation. The primary goal of the present study was to evaluate the emerging theory that polarity sensitivity reflects neural health in CI listeners. An ideal in vivo estimate of neural integrity should vary independently of other factors known to influence the CI electrode-neuron interface, such as electrode position and tissue impedances. Thus, the present analyses quantified the relationships between polarity sensitivity and 1) electrode position estimated via computed tomography imaging, 2) intracochlear resistance estimated via electrical field imaging, and 3) focused (steered quadrupolar) behavioral thresholds, which are believed to reflect a combination of local neural health, electrode position, and intracochlear resistance. Eleven adults with Advanced Bionics devices participated. To estimate polarity sensitivity, electrode-specific behavioral thresholds in response to monopolar, triphasic pulses where the central high-amplitude phase was either anodic (CAC) or cathodic (ACA) were measured. The polarity effect was defined as the difference in threshold response to the ACA compared to the CAC stimulus. Results indicated that the polarity effect was not related to electrode-to-modiolus distance,

electrode scalar location, or intracochlear resistance. Large, positive polarity effects, which may indicate SGN degeneration, were associated with relatively high focused behavioral thresholds. The polarity effect explained a significant portion of the variation in focused thresholds, even after controlling for electrode position and intracochlear resistance. Overall, these results provide support for the theory that the polarity effect may reflect neural integrity in CI listeners. Evidence from this study supports further investigation into the use of polarity sensitivity for optimizing individual CI programming parameters.

4.2 INTRODUCTION

Cochlear implants (CIs) stimulate the auditory system by directly depolarizing spiral ganglion neurons (SGNs), and the physiological integrity of the SGNs may contribute to a patient's success with a CI. In fact, variability in phoneme, word, and sentence perception scores across CI listeners is partially explained by demographic variables that are implicitly related to neural health, such as duration of deafness, age, and hearing loss etiology (Friedland et al. 2010; Lazard et al. 2012; Holden et al. 2013). In post-mortem temporal bone studies, total SGN counts decrease with increasing age and duration of deafness and vary as a function of etiology (Nadol et al. 1989; Nadol 1997). Moreover, some investigations have shown that in vivo estimates of SGN density relate to speech perception performance in CI listeners (e.g., Kim et al. 2010; Zhou and Pfingst 2014; DeVries et al. 2016; Scheperle 2017; Schvartz-Leyzac and Pfingst 2018). While SGN density constitutes an important aspect of neural health, the status of the peripheral processes may also contribute to CI outcomes. However, less is understood about how to quantify peripheral process integrity in vivo.

Recent evidence suggests that sensitivity to stimulus polarity may provide insight into the health of the peripheral processes. The polarity effect represents the difference in psychophysical

or electrophysiological responses to positive (anodic) and negative (cathodic) electrical current. Biophysical modeling data show that the site of spike initiation differs for anodic and cathodic polarities (Rattay et al. 2001a,b; Joshi et al. 2017; Resnick et al. 2018). Specifically, anodic current is more effective at exciting the central axon, whereas cathodic current is more effective at exciting the peripheral processes. When the peripheral processes have degenerated, anodic stimulation generates action potentials at lower current levels than cathodic stimulation (Rattay et al. 2001a,b; Joshi et al. 2017; Resnick et al. 2018). If this theory holds true in CI listeners, then large, positive polarity effects may suggest degeneration of adjacent SGNs.

In CI listeners, better sensitivity to anodic than to cathodic stimulation is consistently observed at suprathreshold levels, which may reflect a proximal shift in spike initiation at high current levels (Macherey et al. 2006, 2008; van Wieringen et al. 2008; Undurraga et al. 2010, 2013; Macherey et al. 2017; Hughes et al. 2017, 2018). Polarity sensitivity at low current levels, however, may provide more insight into the variation in local neural status than suprathreshold measurements. In fact, recent evidence suggests that the polarity effect at threshold varies both across- and within- ears (Macherey et al. 2017; Carlyon et al. 2018). Although neural health also varies across the electrode array, so do non-physiological factors such as electrode position relative to the SGNs and intracochlear bone and tissue growth (reviewed by Bierer 2010).

An ideal in vivo estimate of neural status would vary independently of electrode placement and tissue impedances. However, it is unknown whether polarity effect measurements are influenced by electrode position or intracochlear resistance in CI listeners. The primary goal of the present study was to evaluate the theory that polarity sensitivity reflects neural status by quantifying its relationship with electrode-to-modiolus distance, electrode scalar location, and intracochlear resistance. Because computational studies have used highly simplified models to

describe polarity sensitivity, there was no a priori expectation of whether the polarity effect would correlate with electrode position or intracochlear resistance.

A secondary goal was to evaluate the relationship between the polarity effect and behavioral thresholds measured in response to a spatially-focused electrode configuration (i.e., focused thresholds). Focused threshold levels are believed to reflect the cumulative contributions of local electrode placement, bone and tissue growth, and neural health (Bierer 2010). Specifically, channels with relatively high focused thresholds are often located farther from target neurons (Long et al. 2014; DeVries et al. 2016; DeVries and Arenberg 2018a) and have lower intracochlear resistance values (Bierer et al. 2015b) and smaller evoked potential amplitudes (DeVries et al. 2016) than channels with lower focused thresholds. In line with the theory that polarity sensitivity reflects neural health, we hypothesized that the polarity effect would explain a significant portion of the variation in focused thresholds, even after controlling for the contributions of electrode position and intracochlear resistance. The results of this study will provide evidence either in support of or against the use of polarity sensitivity as an estimate of neural status in CI listeners. Ultimately, in vivo estimates of peripheral process integrity may improve our understanding of how aspects of neural health other than SGN density relate to CI performance, and whether that information can be used to optimize device programming.

4.3 METHODS

4.3.1 *Subjects*

Eleven adults (6 males) who were unilaterally implanted with Advanced Bionics HiRes90K devices participated (Table 4.1). Subjects ranged in age from 27 to 87 years (M = 62.00 years, SD = 18.32). Two subjects (S49 and S53) were pre-lingually deafened (diagnosed with severe to profound sensorineural hearing loss before the age of 4 years) and one (S40) was peri-lingually

deafened (diagnosed with severe to profound sensorineural hearing loss at age 4). The remaining eight subjects became deaf in adulthood. All subjects were fluent English speakers and used spoken language to communicate. One subject (S54) learned English as a second language. Each subject provided written informed consent and all procedures were approved by the University of Washington Human Subjects Division.

Table 4.1. Demographic information for all eleven subjects including ear implanted, chronological age, age diagnosed with a profound hearing loss, age at implantation, duration of deafness, etiology (if known), and electrode array type. EVA: enlarged vestibular aqueduct.

ID	*Ear*	*Age (years)*	*Age at profound HL (years)*	*Age Implanted (years)*	*Duration of deafness (years)*	*Etiology*	*Electrode array*
S22	R	78	55	66	11	Suspected genetic	1-J Helix
S29	L	87	46	76	30	Noise exposure	HiFocus 1J
S40	L	56	4	50	46	EVA	HiFocus 1J
S43	R	72	49	67	18	Noise exposure	Mid-scala
S46	R	69	40	64	24	Suspected genetic	HiFocus 1J
S47	R	40	26	36	10	Unknown	Mid-scala
S49	R	45	1.5	44	42.5	Genetic	Mid-scala
S50	R	76	18	71	53	Unknown	HiFocus 1J
S52	R	71	59	65	6	Unknown	HiFocus 1J
S53	R	56	1	44	43	Meningitis	1-J Helix
S54	L	27	7	23	16	EVA	Mid-scala
Mean *(SD)*		62.0 *(18.3)*	27.9 *(22.8)*	55.5 *(16.8)*	27.6 *(16.3)*		

4.3.2 *Computed Tomography Imaging*

Electrode position was estimated using computed tomography (CT) imaging. Subjects enrolled in a series of CT-based studies in our laboratory between the years 2013 and 2016. CT scans were obtained at the time of enrollment. Imaging was not repeated, as substantial electrode migration is rare (Rader et al. 2016; Dietz et al. 2016), and no subjects demonstrated clinical signs of array migration over the course of the experiments; that is, electrode impedances, behavioral thresholds, and speech perception scores were stable over time (Rader et al. 2016).

Thus, the risks of obtaining serial CT scans (e.g., exposure to radiation, financial costs) outweighed the benefits. All other psychophysical and objective measures were obtained simultaneously at the time of each experiment. Nine of the 11 subjects participated in more than one experiment in our laboratory that incorporated these CT images (DeVries et al. 2016; DeVries and Arenberg 2018a). Subjects S50 and S52 were not included in the prior publications.

CT scans of the implanted and non-implanted ears of each subject were performed at the University of Washington Medical Center in Seattle, Washington. The scans were analyzed at Washington University in St. Louis, Missouri using a technique developed by Skinner et al. (2007) and validated by Teymouri et al. (2011). Images of the non-implanted ear were obtained because pre-operative CT scans were not available, and because metal artifact contamination in the implanted ear interferes with the ability to accurately identify individual electrodes and cochlear anatomy. Using ANALYZE software (Mayo Clinic, Rochester; Robb 2001), the image of the non-implanted ear was co-registered with the image of the implanted ear to identify structural anatomy and to optimize resolution of the electrodes. To further improve visualization of the scalar position of the electrode array and the individual electrodes, each of 11 cochlear atlases were aligned, through translation, rotation, and scaling, to find a best fit to the cochlear wall of the composite CT (Figure 4.1). The atlases assist in the localization of non-bony cochlear structures and were derived from 10 Micro CTs and 1 orthogonal-plane fluorescence optical sectioning (OPFOS) (Voie et al. 1993) obtained from cadaveric temporal bones. The composite CT images from all eleven ears are shown in Figure 4.2 (see Results section for descriptive analyses of electrode position).

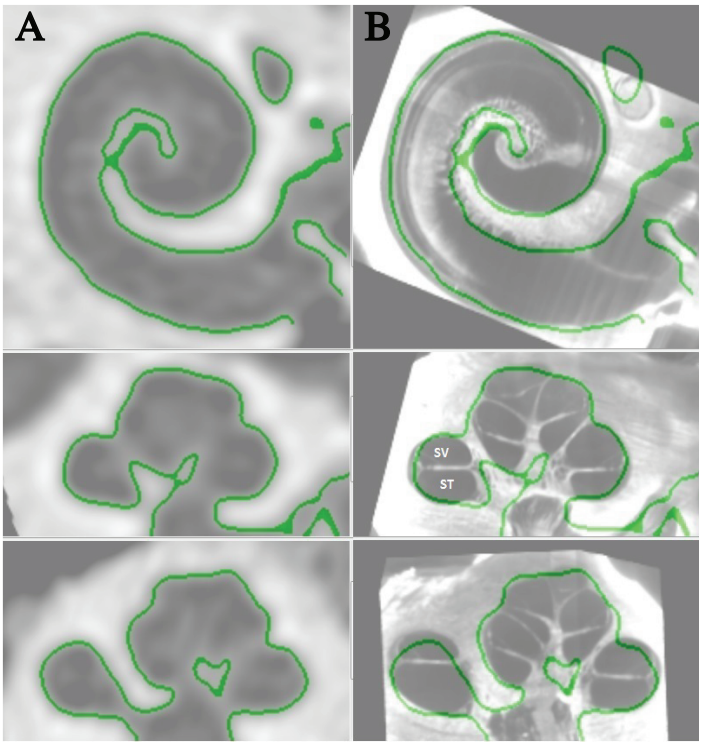

Figure 4.1 Cochlear wall as defined by the computed tomography (CT) scan (column A) and an atlas selected from 10 Micro CTs and 1 OPFOS (orthogonal-plane fluorescence optical sectioning) that was aligned by rigid registration to create best fit (column B). SV denotes the estimated location of scala vestibuli and ST denotes the estimated location of scala tympani.

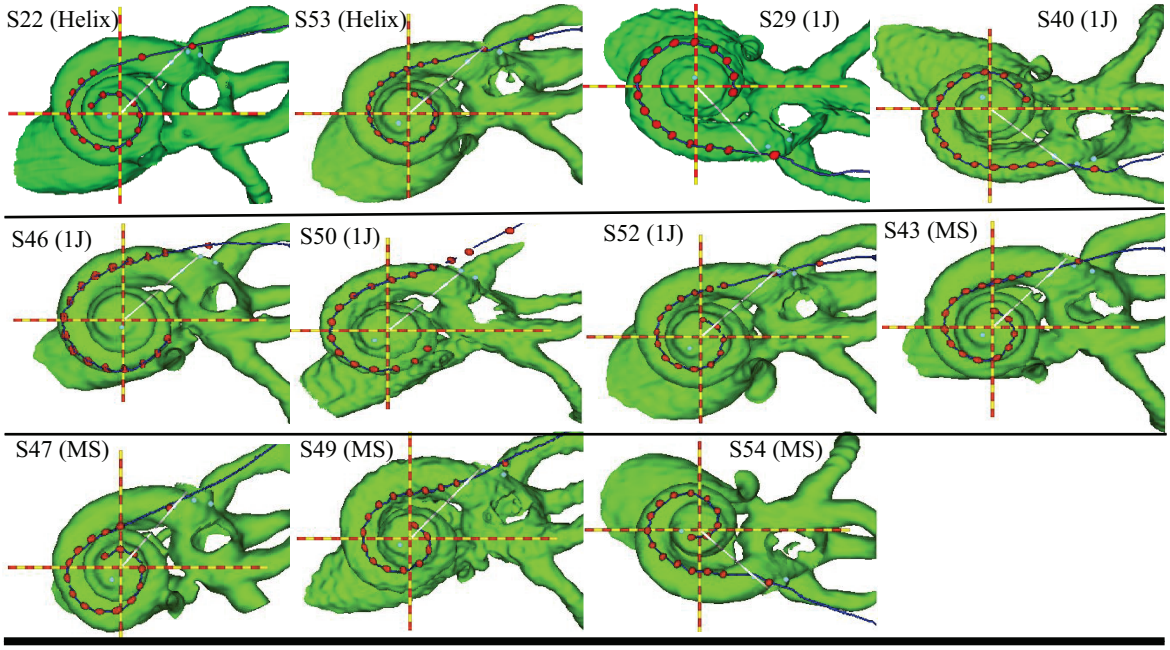

Figure 4.2. 3D cochlear reconstructions from all 11 subjects, arranged in order of electrode array type (Helix followed by 1J followed by Mid-scala). MS represents the Mid-scala array. Red dots represent the electrodes, with the outermost dot representing the insertion depth marker. The red and yellow lines represent the X and Y axes that are used to determine the insertion angle from the white 0º insertion line.

Two CT-estimated metrics of electrode position were used in the present study: electrode-to-modiolus distance and scalar location. Electrode-to-modiolus distance was calculated as the lateral distance, in millimeters (mm), of an electrode from the inner wall of the cochlea. Scalar location refers to the location of each electrode within the cochlear compartments: scala tympani (ST), intermediate, or scala vestibuli (SV). Given the relatively small cross-sectional area of the scala media, the intermediate position refers to those electrodes that approximate the position of the basilar membrane and that could not be definitively localized to either the ST or the SV.

4.3.3 *Electrical Stimulation*

All electrical stimuli were presented and controlled using the Bionic Ear Data Collection System (BEDCS) version 1.18.315 (Advanced Bionics, Valencia, CA). Custom MATLAB scripts controlled the BEDCS software (Mathworks, Inc. Natick, MA). Stimuli were verified using a reference implant and digital storage oscilloscope.

4.3.4 *Polarity Effect*

Polarity sensitivity was assessed on each available cochlear implant channel in each subject. This was accomplished by measuring single-channel behavioral thresholds in response to each of two triphasic pulses, in which the high-amplitude central phase was either anodic (CAC) or cathodic (ACA). Several investigations have demonstrated that asymmetric pulse shapes (e.g., pseudomonophasic, triphasic, or quadruphasic) are more effective than symmetric biphasic pulses for studying polarity sensitivity in human behavioral experiments (Macherey et al. 2006, 2008; Carlyon et al. 2013; Macherey et al. 2017). Recently, Carlyon and colleagues (2018) studied psychophysical polarity sensitivity at threshold using triphasic pulses in which the central high-amplitude phase of each pulse was twice the amplitude of the first and third phases. This type of asymmetric pulse shape concentrates the charge of the polarity of interest into a short time window, while maintaining the necessary charge balance. The stimuli used in the present study were identical to those used by Carlyon and colleagues (2018). Stimuli were 99 pulse-per-second (pps) trains presented in a monopolar stimulation mode (43 μs/phase, 0-μs interphase gap, 400 ms duration).

The polarity effect was defined as the difference between ACA and CAC thresholds on each channel (polarity effect, in dB = ACA minus CAC). A positive polarity effect indicated that

behavioral thresholds in response to the ACA stimulus were higher (i.e., worse) than those in response to the CAC stimulus. A negative polarity effect indicated the inverse.

Prior to threshold testing, most comfortable listening levels (MCLs) were obtained on each channel, in response to each polarity. This was done to avoid presenting uncomfortable stimulation levels, and to determine an appropriate starting level for threshold measurements. To measure MCL, the experimenter gradually increased the current level from a subthreshold level of 50 microamps (μA) up until the subject reported a loudness rating of "6", corresponding to "most comfortable" on the Advanced Bionics clinical loudness scale (Advanced Bionics, Valencia, CA). The MCL ratings served as the maximum stimulus levels for the threshold procedures.

Single-channel signal detection thresholds were measured for each polarity on each available channel using an adaptive one-up/one-down staircase tracking procedure. Two adaptive tracks were completed for each polarity on each electrode, and the two values were averaged together to arrive at the final threshold estimation. If the thresholds estimated on the first two runs differed by 1 decibel (dB) or more, a third and fourth run were completed. In that case, the thresholds from each of the four runs were averaged together. The testing order of channels and polarities was randomized for each subject.

For each adaptive track, the initial presentation level was set to 90% of MCL. For subsequent tracks, the initial presentation level was set to 50 to 98% of MCL. On electrodes with relatively large dynamic ranges, a lower percentage of MCL was used as the starting level to reduce the number of steps necessary to estimate threshold. Conversely, a higher starting level was selected for electrodes with small dynamic ranges to ensure that the subject could adequately hear the stimulus before reaching the first reversal.

The subject indicated when he or she heard a sound by pressing the spacebar on a standard computer keyboard. If the subject responded within three seconds after stimulus presentation, the presentation level decreased. If the subject did not respond within three seconds, the level increased. The initial step size was 0.5 dB. After the first reversal, the step size reduced to 0.2 dB. Random delays ranging from 0.1 to 0.6 seconds were implemented prior to each stimulus presentation. The adaptive procedure terminated after eight reversals, and threshold level was estimated as the average of the last six reversals.

4.3.5 *Focused Behavioral Thresholds*

Single-channel focused behavioral thresholds were estimated for channels 2-15 using a sweep procedure (based on Sek et al. 2005; Bierer et al. 2015a). Stimuli were biphasic, cathodic-leading pulse trains (102 μs/phase, 0-μs interphase gap, 200.4 ms duration, 997.9 pps) presented in a steered quadrupolar (sQP) stimulation mode with a current focusing coefficient of 0.9. Across studies, focused thresholds measured with cathodic-leading biphasic pulses reflect variation in CT-estimated electrode position (Long et al. 2014; DeVries et al. 2016; DeVries and Arenberg 2018a), EFI-estimated intracochlear resistance (Bierer et al. 2015b), and evoked potential estimates of SGN density (Bierer et al. 2011; DeVries et al. 2016). We thus maintained a pulse shape consistent with prior investigations (biphasic, cathodic-leading).

In sQP stimulation, a channel is comprised of four adjacent intracochlear electrodes. Two middle electrodes serve as active electrodes, whereas two outer electrodes serve as return electrodes. The current coefficient, sigma (σ), specifies the fraction of current delivered through the return electrodes. Higher sigma values indicate greater current focusing, such that $\sigma = 1$ represents the highest possible degree of current focusing. In the present study, a highly focused current fraction of $\sigma = 0.9$ was selected to capture local variability in the ENI while maintaining

perceptible current levels that were below voltage compliance limits (Bierer 2007). Note that Advanced Bionics devices have 16 intracochlear electrodes; however, sQP thresholds cannot be measured on channels 1 and 16 due to the need for two intracochlear return electrodes.

A fast threshold measurement procedure based on a variation of the Bekesy tracking technique was used to obtain sQP thresholds across the electrode array (Bierer et al. 2015a). Current was steered between the two active electrodes by changing the steering coefficient, alpha (α). When $\alpha = 0$, all current was delivered through the more apical of the two active electrodes; when $\alpha = 1$, all current was steered through the most basal active electrode. By convention, an electrode channel number is equivalent to the basal active electrode when $\alpha = 1$. This convention can be maintained for electrodes 3 to 15. However, because the sQP configuration requires four electrodes, it is not possible to steer current for electrode 2 in the same manner as for electrodes 3-15. Instead, the same set of electrodes must be used for both channel 2 and channel 3, but an α value of 0 is specified to center the current on electrode 2. This arrangement is referred to as "channel 2".

Prior to initiating the threshold sweep procedure, MCLs were measured for the sQP stimuli across channels 2-15 using the Advanced Bionics loudness rating scale and the same procedure described in the previous section. MCL was then set as the upper limit of stimulation for the threshold measurements. To measure threshold, pulse trains were presented starting at 6 dB below MCL and swept across the electrode array with alpha increasing from 0 to 1 in steps of 0.1. Each 200.4 ms pulse train was followed by a 300 ms silent interval, resulting in a repetition rate of approximately 500 ms. The alpha value changed every 1,000 ms, such that two successive presentations of the same electrode and alpha combination occurred during each sweep. This

process repeated uninterrupted for each successive set of electrodes until all available sets (active electrodes 2-15) had been tested, constituting a single run.

During the sweep, the listener was instructed to continuously depress the spacebar when he or she could perceive a sound, and to release the spacebar when he or she could no longer perceive a sound. The current changed in step sizes of 1 dB. When the spacebar was depressed, the current level decreased by 1 dB on each stimulus presentation. Conversely, when the spacebar was released, the current level increased by 1 dB on each stimulus presentation. Two successive pulse trains were presented for each alpha value. Because the task is based on Bekesy tracking principles, both the alpha value and the current level change while the spacebar is depressed in order to continuously sweep the stimulus across the electrode array. The reader is referred to Figure 2 of Bierer et al. (2015a) for a visual representation of this procedure.

Participants completed two forward runs, sweeping from channels 2 to 15 (apical to basal), and two reverse runs, sweeping from channels 15 to 2 (basal to apical). Final threshold estimates were obtained by calculating a weighted average of consecutive current levels along the forward and reverse sweeps at integer channel numbers (as in Bierer et al. 2015a). Thresholds were calculated for integer channel numbers for direct comparison to the other measures in this study. This current steering method also provides threshold data in 0.1 alpha increments in-between the integer channel numbers; however, despite the extra data collection, thresholds across the electrode array are still obtained up to four times faster with this procedure compared to traditional two-alternative forced-choice methods (Bierer et al. 2015a).

4.3.6 *Electrical Field Imaging*

Stimuli were single biphasic, anodic-leading pulses (100 μs duration, either 50 or 100 μA in amplitude) presented in a monopolar stimulation mode at a rate of 16.6 per second. EFI uses

low-level pulses to estimate the distribution of electrical current in the cochlea. Note that the leading polarity of the EFI stimulus does not affect the voltage measures, and that the low-level stimuli were sub-threshold for all subjects in this study. Ten pulses were presented on each electrode consecutively, progressing from electrode 1 to electrode 16 (apical to basal). While the pulses were presented, voltage was recorded on every electrode at a 56 kHz sampling rate. Data analysis was performed offline with a custom MATLAB program. The analysis was modeled after that of Vanpoucke and colleagues (2004). Briefly, the voltage that was measured at each recording electrode in response to each of the ten pulses was averaged. Voltage was then scaled to resistance units (Ohms) by dividing by the applied current. Signal amplitude at each recording electrode was calculated as half the difference between the positive and negative voltage excursions.

The 16x16 impedance matrix was transformed to solve a lumped parameter resistor network. The solution yielded 16 transversal resistances (R_{trans}), 15 longitudinal resistances (R_{long}), and 16 total resistances (R_{total}). R_{long} and R_{trans} values were estimated using least squares optimization and a localized weighting scheme to improve the EFI profile fit. R_{long} represents localized current flow along the length of the cochlea, whereas R_{trans} includes resistance pathways through the osseous spiral lamina. R_{total} was calculated as the peak of the reconstructed EFI profile, which was based on the solution to the ladder network. A detailed explanation of these analyses is discussed by Vanpoucke and colleagues (2004). All three resistance measurements are highly correlated with one another, so only R_{long} was used in the present analyses. R_{long} was selected because it has been hypothesized that the majority of current from an electrode flows longitudinally along the cochlear duct (Jolly et al. 1996; Briare and Frijns 2000).

4.3.7 *Statistical Analyses*

Data were analyzed using R Version 3.3.1 (R Core Team 2016). To account for repeated measurements within the same subjects, either repeated measures correlations (Bakdash and Marusich 2017) or linear mixed-effects models were used for all analyses that involved electrode-specific data. In such cases, subjects were included in the models as random factors. To minimize small sample bias in estimation, all linear mixed-effects models were fit using restricted maximum likelihood (REML) parameter estimates (McNeish 2017). Repeated measures analyses were performed using the lme4 (Bates et al. 2015), lmerTest (Kuznetsova et al. 2017), MuMIn (Bartón 2018), and rmcorr (Bakdash and Marusich 2018) packages in R.

4.4 RESULTS

4.4.1 *Comparisons of Polarity Effect, Electrode Position, and Intracochlear Resistance*

Figure 4.1 shows the 3D cochlear reconstructions of all subjects, arranged in order of electrode array type. Two subjects had a 1J-Helix array (S22 and S53), five subjects had a 1J array (S29, S40, S46, S50, and S52), and four subjects had a Mid-scala array (S43, S47, S49, and S54). Each of the three types of electrode arrays is designed to achieve a different position within the cochlea (Dhanasingh and Jolly 2017). The standard 1J array has a lateral wall design. The 1J-Helix and the Mid-scala arrays are both pre-curved. The 1J-Helix should achieve a more medial position relative to the 1J, whereas the Mid-scala is designed for placement in the middle of the ST. Of the 176 total electrodes in the sample, 104 electrodes (59.1%) were located in ST, 62 electrodes (35.2%) were located in the intermediate position, and 8 electrodes (5.5%) were located in SV. Two of Subject S50's electrodes were extracochlear (electrodes 15 and 16).

Across electrodes, electrode-to-modiolus distance ranged from 0.18 to 2.2 mm (*M* = 1.14 mm, *SD* = 0.52; see Table 4.2).

Table 4.2. Means and standard deviations for sQP threshold, polarity effect, electrode-to-modiolus distance (EMD), and intracochlear resistance. Data are averaged across electrodes 2-15.

ID	*sQP Threshold (dB)* Mean *(SD)*	*Polarity effect (dB)* Mean *(SD)*	*EMD (mm)* Mean *(SD)*	*Resistance (Ohms)* Mean *(SD)*
S22	44.30 *(5.90)*	-0.45 *(2.08)*	1.14 *(0.35)*	208.03 *(62.63)*
S29	47.76 *(3.00)*	0.61 *(0.57)*	1.50 *(0.24)*	333.75 *(90.58)*
S40	55.76 *(1.37)*	2.29 *(0.59)*	1.80 *(0.22)*	595.44 *(607.13)*
S43	43.73 *(3.68)*	-0.06 *(1.06)*	0.88 *(0.45)*	274.58 *(68.53)*
S46	51.69 *(1.53)*	0.08 *(0.57)*	1.79 *(0.34)*	583.70 *(186.62)*
S47	35.29 *(4.04)*	0.66 *(0.97)*	0.93 *(0.46)*	237.57 *(135.58)*
S49	50.71 *(2.15)*	-0.03 *(1.36)*	0.94 *(0.47)*	1122.99 *(642.40)*
S50	45.82 *(5.08)*	1.05 *(1.83)*	1.37 *(0.27)*	567.82 *(646.46)*
S52	39.01 *(1.92)*	-0.48 *(1.03)*	0.71 *(0.30)*	345.00 *(185.68)*
S53	45.55 *(2.62)*	0.34 *(1.20)*	0.66 *(0.17)*	274.57 *(127.61)*
S54	47.14 *(5.77)*	0.09 *(1.55)*	0.89 *(0.46)*	1064.25 *(1002.10)*
Mean *(SD)*	46.01 *(6.51)*	0.36 *(1.42)*	1.14 *(0.52)*	496.95 *(518.07)*

Figure 4.3 shows individual site-specific thresholds in response to the ACA and CAC stimuli. Black squares indicate responses to the ACA stimulus, whereas red circles indicate responses to the CAC stimulus. Higher (i.e., worse) thresholds in response to the ACA stimulus compared to the CAC stimulus indicate a positive polarity effect. Conversely, higher (i.e., worse) thresholds in response to the CAC stimulus compared to the ACA stimulus indicate a negative polarity effect. The polarity effect could not be measured on electrodes 15 and 16 for subject S50, because those electrodes were extracochlear and stimulation did not result in auditory percepts.

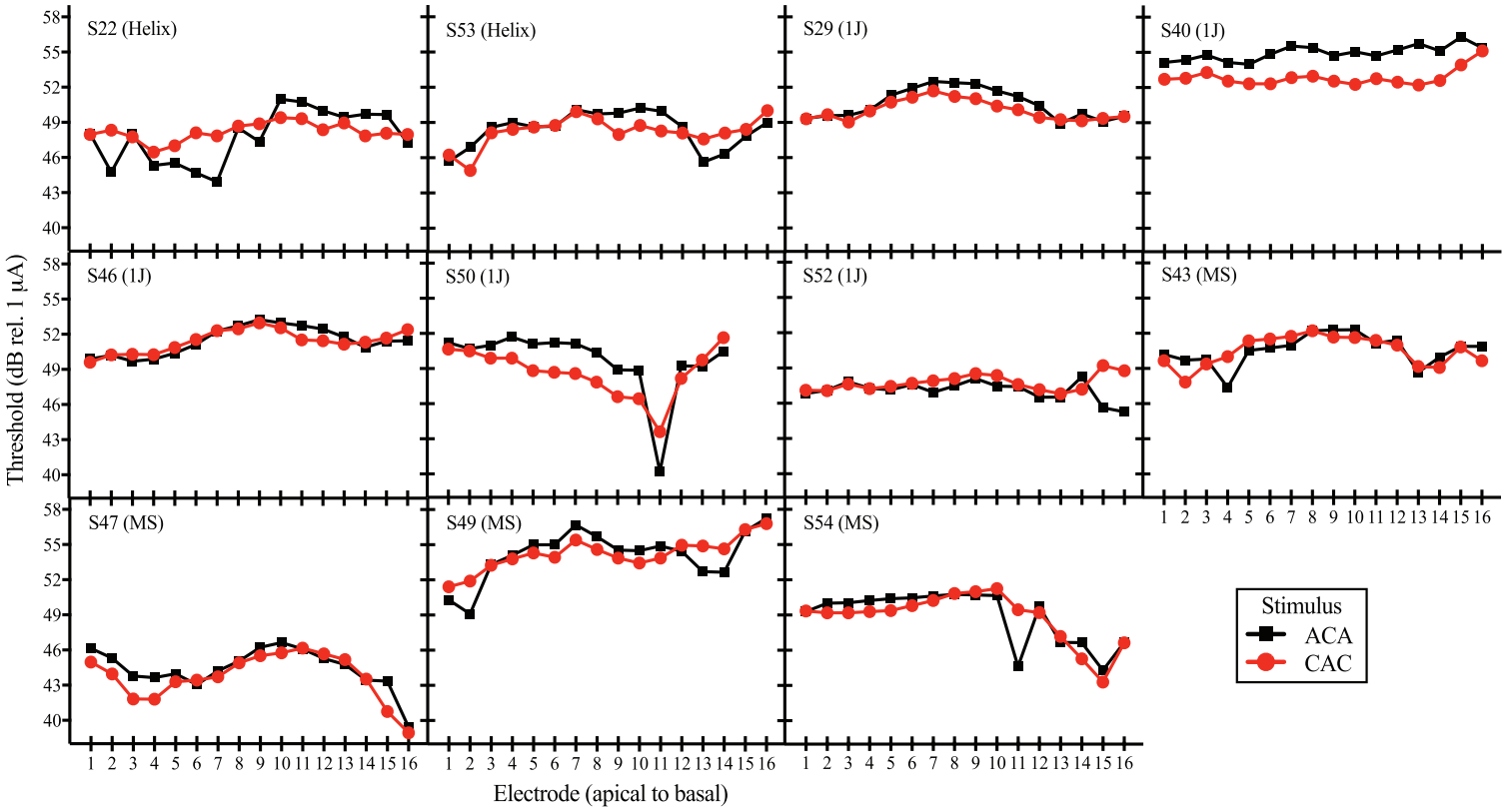

Figure 4.3. Individual subjects' electrode-specific thresholds in response to each of the two triphasic monopolar stimuli. ACA refers to the stimulus with a cathodic central phase and CAC refers to the stimulus with an anodic central phase. Thresholds in response to the ACA stimulus are depicted by black squares. Thresholds in response to the CAC stimulus are depicted by red circles. Threshold (in dB relative to 1 µA) is shown on the ordinate and electrode number (ordered from apical to basal) is shown on the abscissa. Subjects are arranged in order of electrode array type, with the electrode array displayed in parentheses. MS represents the Mid-scala array. The order of subjects is the same as in Figure 4.2.

Across electrodes, the polarity effect ranged from -4.83 dB to 3.54 dB (M = 0.36 dB, SD = 1.42; see Table 4.2). The polarity effect varied both across subjects, and across the electrode array within the same subject. For example, subject S40 shows consistently large, positive polarity effects at most electrode sites (Figure 4.3). Conversely, Subject S22 tends to have

negative polarity effects in the apical portion of the electrode array, and positive polarity effects in the basal portion of the electrode array (Figure 4.3).

Intracochlear resistance also varied across- and within-subjects, ranging from 91.71 Ohms to 2718.57 Ohms (M = 496.95 Ohms, SD = 518.17; see Table 4.2). Prior to data analysis, histograms were plotted to determine whether the data were normally distributed. This analysis revealed that R_{long} values were highly skewed. To reduce skew, the R_{long} data were log-transformed prior to data analysis and for visualization purposes. Of note, the size of the electrode contacts differs slightly between the three electrode arrays, which may influence electrode impedances (Hughes 2012). However, R_{long} did not differ as a function of electrode array type in this study (β = 2.36, $F_{(2,8)}$ = 1.45, $P > 0.05$).

The first analysis assessed the relationship between the polarity effect and 1) electrode position and 2) intracochlear resistance. Figure 4.4 shows electrode-specific polarity effect plotted against (A) electrode-to-modiolus distance, and (C) intracochlear resistance. Individual subjects are distinguished by color and shape. The right-hand panels of Figure 4.4 (B and D) show the best-fit lines for each individual. Results from a linear mixed-effects analysis showed that, across subjects, the polarity effect was not significantly predicted by electrode-to-modiolus distance (β = 0.11, $F_{(1,103.23)}$ = 0.15, P = 0.70), electrode scalar location (β = -0.15 for intermediate, 0.45 for SV, $F_{(2, 145.48)}$ = 0.50, P = 0.61), or intracochlear resistance (β = -0.39, $F_{(1, 106.62)}$ = 0.86, P = 0.36). As a complement to the multilevel model, repeated measures correlations (r_{rm}) indicated very small effect sizes for each comparison: 1) polarity effect and electrode-to-modiolus distance ($r_{rm(162)}$ = -0.02, 95% CI [-0.17, 0.14], P = 0.80) and 2) polarity effect and intracochlear resistance ($r_{rm(151)}$ = -0.13, 95% CI [-0.28, 0.03], P = 0.11). These results

suggest that the polarity effect varies independently of both CT-estimated electrode position and EFI-estimated longitudinal intracochlear resistance.

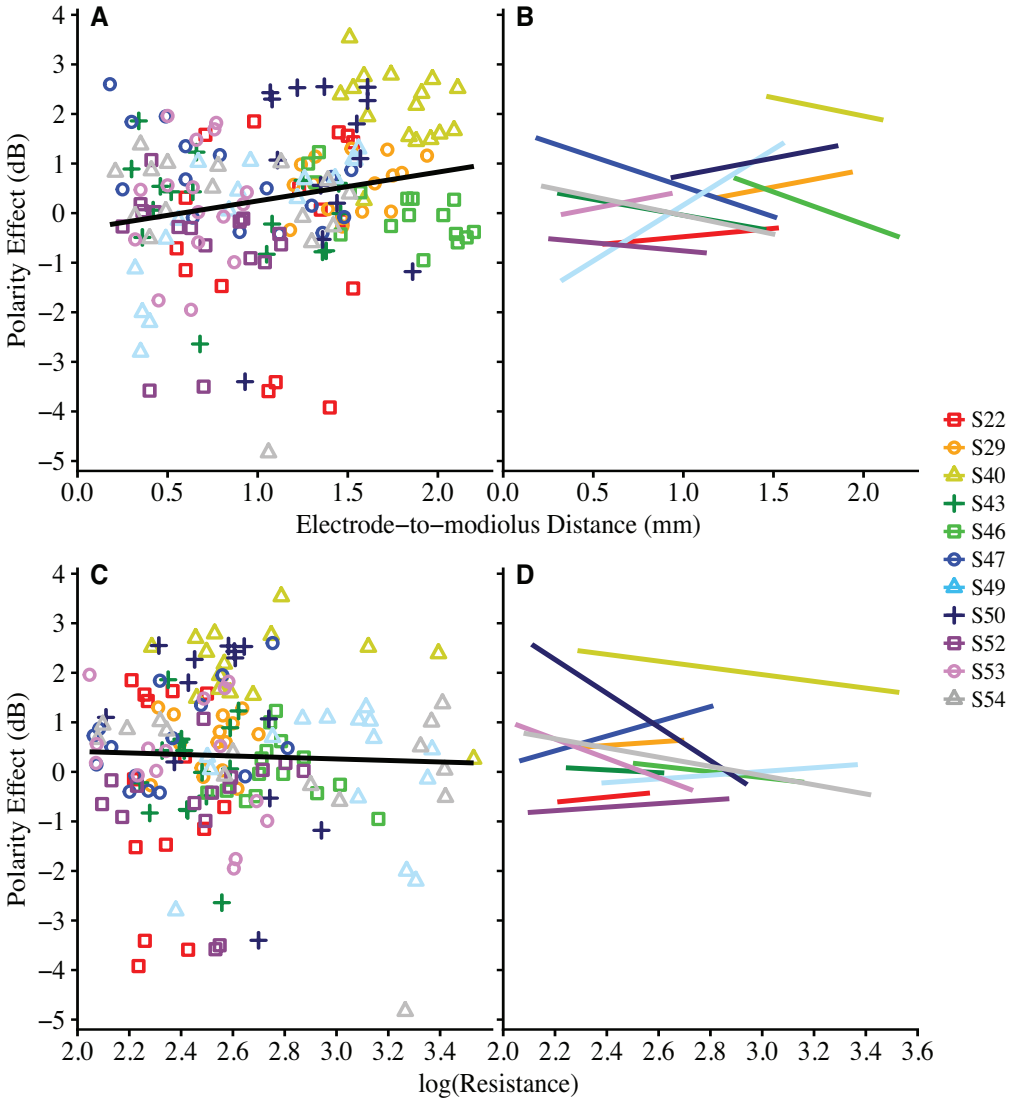

Figure 4.4. Polarity effect (in dB) as a function of A,B) electrode-to-modiolus distance (in mm) and, C,D) log-transformed intracochlear resistance values. Individual subjects are represented by different colors and shapes. In panels A and C, a group regression line is shown in black for ease of visualization. However, note that the black regression line does not account for non-independence of within-subject data. Panels B and D show best-fit lines for individual subjects.

4.4.2 *Predicting Focused Behavioral Thresholds*

The second analysis assessed the relationship between the polarity effect and sQP thresholds and whether the polarity effect explains a significant portion of the variation in sQP thresholds after accounting for CT-estimated electrode position and EFI-estimated intracochlear resistance. Recall that sQP thresholds are believed to reflect the cumulative contributions of local neural health, electrode position relative to the auditory nerve, and intracochlear resistance. Figure 4.5 shows the relationships between electrode-specific sQP thresholds and (A) the polarity effect, (C) electrode-to-modiolus distance, and (E) intracochlear resistance. Again, individual data are distinguished by color and shape. The right-hand panels of Figure 4.5 (B, D, and F) show the best-fit lines for each individual. Repeated measures correlations indicated significant relationships between focused thresholds and each of the three main predictors: 1) electrode-to-modiolus distance: $r_{rm(140)} = 0.51$, 95% CI [0.38, 0.63], $P < 0.001$; 2) intracochlear resistance: $r_{rm(141)} = -0.37$, 95% CI [-0.51, -0.22], $P < 0.001$; and 3) the polarity effect: $r_{rm(140)} = 0.27$, 95% CI [0.11, 0.42], $P = 0.001$. Each relationship survived Bonferroni adjustment for multiple comparisons (adjusted $\alpha = 0.017$).

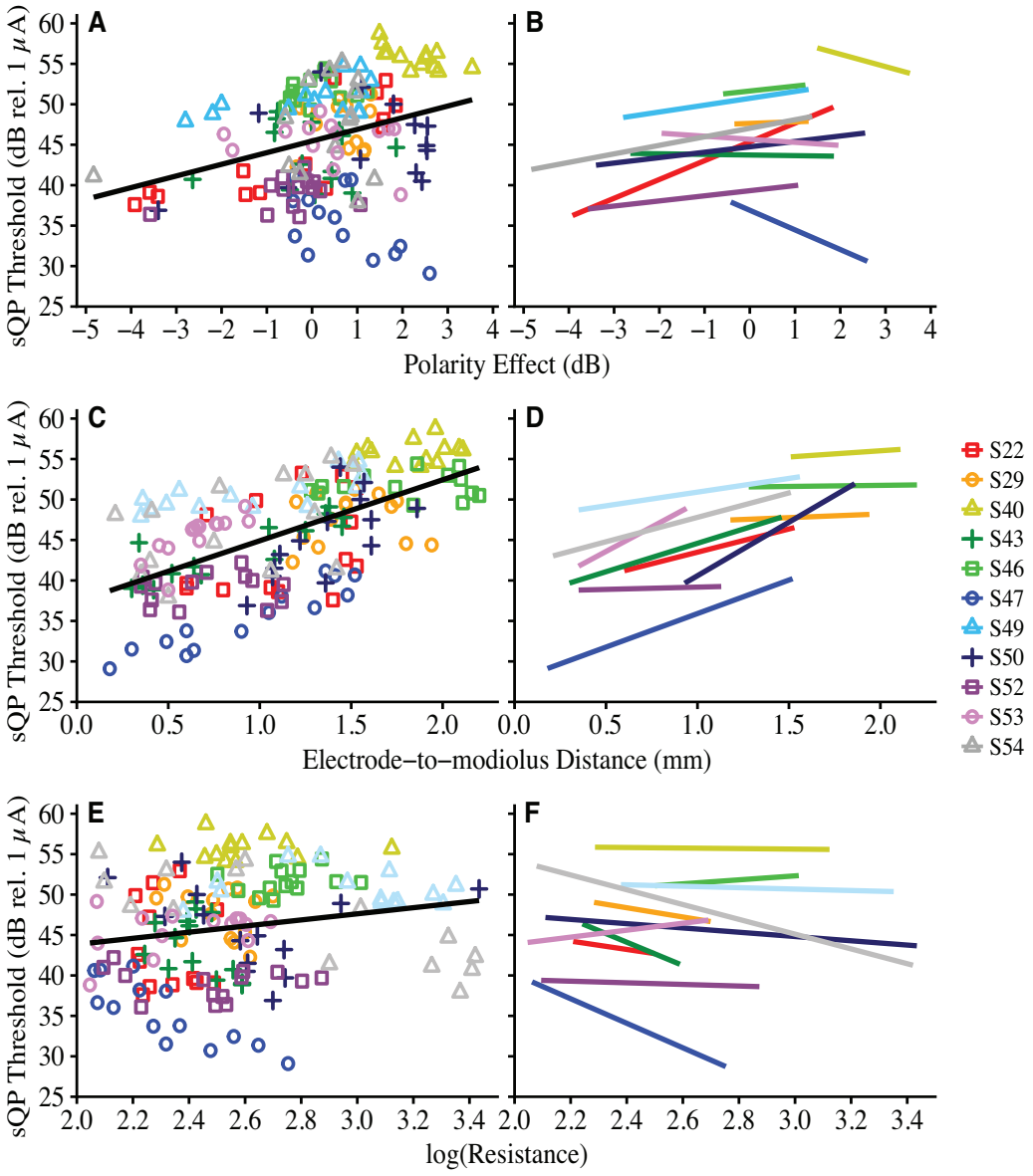

Figure 4.5. Focused (sQP) thresholds (in dB relative to 1 μA) as a function of A,B) polarity effect (in dB), C,D) electrode-to-modiolus distance (in mm), and E,F) log-transformed intracochlear resistance values. Individual subjects are represented by different colors and shapes. In panels A, C, and E, a group regression line is shown in black for ease of visualization. However, note that the black regression line does not account for non-independence of within-subject data. Panels B, D, and F show best-fit lines for individual subjects.

A linear mixed-effects analysis was performed to assess whether the polarity effect remained a significant predictor of sQP thresholds after controlling for electrode position and intracochlear resistance. To determine whether each variable improved the overall model fit, an Akaike information criterion with a bias correction for small sample sizes (AICc) was used for model selection (Hurvich and Tsai 1989). Statistical models with lower AICc values are more parsimonious relative to those with higher AICc. First, we specified an empty model with only subjects as random effects to predict sQP thresholds (AICc = 877.62). Next, we consecutively added each of the following fixed effects: electrode-to-modiolus distance (AICc = 824.33), scalar location (AICc = 808.72), intracochlear resistance (AICc = 803.49), and the polarity effect (AICc = 792.99). The model fit improved with the addition of each predictor, and the lowest AICc value was associated with the model that included all four predictors. So, the final model specified electrode-to-modiolus distance, scalar location, intracochlear resistance, and the polarity effect as independent variables. The dependent variable was sQP threshold.

Traditional R^2 values are not valid for linear mixed-effects models. However, Nakagawa and Schielzeth (2013) propose two types of pseudo-R^2 values that can provide an indication of the variability explained by a multilevel model: 1) marginal R^2 (R^2_{marginal}), which represents the proportion of the total variance explained by the fixed effects, and 2) conditional R^2 ($R^2_{\text{conditional}}$), which represents the proportion of the variance explained by both the fixed and random effects. The difference between the R^2_{marginal} and $R^2_{\text{conditional}}$ reflects the variability in the random effects; here, this represents across-subject variability.

Results from the linear mixed-effects analysis ($R^2_{\text{marginal}} = 0.27$, $R^2_{\text{conditional}} = 0.80$) showed that the polarity effect ($\beta = 0.73$, $F_{(1,\ 138.54)} = 14.83$, $P < 0.001$), electrode-to-modiolus distance ($\beta = 5.46$, $F_{(1,144.60)} = 57.36$, $P < 0.001$), scalar location (β = -1.18 for intermediate, 3.52 for SV, $F_{(2,}$

$_{141.61)}$ = 4.97, P = 0.01), and intracochlear resistance (β = -2.42, $F_{(1, 144.99)}$ = 4.27, P = 0.04) were all significantly predictive of sQP thresholds. After adjustment for multiple comparisons (Tukey), results showed that thresholds were higher for electrodes located in SV relative to those located in the intermediate position ($t_{(141.69)}$ = 2.91, P = 0.01). There were no significant differences in sQP threshold between electrodes located in SV compared to ST (P = 0.08) or in ST compared to the intermediate position (P = 0.21).

Note that the group regression line in Figure 4.5(E-F), which depicts the relationship between sQP thresholds and R_{long}, appears to have a modest positive trajectory; however, the β coefficient for the R_{long} predictor is -2.42 and the repeated measures correlation coefficient (r_{rm}) is -0.37. This suggests that higher sQP thresholds are associated with lower R_{long} values, demonstrating the importance of statistically accounting for clustered data.

Overall, the results indicate that, across subjects, relatively high sQP thresholds are associated with large, positive polarity effects, distant electrode position relative to the modiolus, and low intracochlear resistance. Electrodes with high sQP thresholds are also more likely to be translocated to the SV than electrodes with low sQP thresholds. Moreover, the polarity effect significantly predicts sQP thresholds, even after controlling for electrode-to-modiolus distance, electrode scalar location, and intracochlear resistance.

Despite these results, it is evident from Figures 4.3-4.5 that the within-subject relationships between variables are not the same for every participant. Table 4.3 shows within-subject correlations between sQP thresholds and electrode-to-modiolus distance (threshold-EMD), the polarity effect (threshold-PE), and R_{long} (threshold- R_{long}) for each individual subject. It was noted that five out of 11 subjects (S47, S43, S53, S49, and S50) had strong, positive correlations between focused thresholds and electrode-to-modiolus distance, with correlation

coefficients (*r*) ranging from 0.71 to 0.94 (Cohen 1988). Each of those five threshold-EMD correlations was statistically significant (*p*s < 0.05). This suggests that the variation in sQP thresholds for those five subjects is largely explained by variation in electrode position. The remaining six subjects had weak-to-moderate threshold-EMD correlations (*r* = 0.06 to 0.48) that were not statistically significant (*p*s > 0.05). For that group, electrode position does not account for much of the variability in sQP thresholds.

Table 4.3. Individual correlation coefficients (*r*) and *p*-values for correlations between sQP thresholds (dB rel. 1 μA) and each of the following variables: electrode-to-modiolus distance (EMD; in mm), polarity effect (PE; in dB), and intracochlear resistance (R_{long}; in Ohms); Data are arranged in descending order by strength of threshold-EMD correlation. Significant correlations ($p < 0.05$) are indicated by bold font. Pearson correlations are shown for the threshold-PE and threshold-EMD comparisons. Non-parametric Spearman correlations are shown for the threshold-R_{long} comparisons.

	Threshold-EMD		Threshold-PE		Threshold-R_{long}	
ID	*r*	*p*	*r*	*p*	*r*	*p*
S47	**0.94**	**< 0.001**	**- 0.58**	**0.03**	**- 0.82**	**0.001**
S43	**0.87**	**< 0.001**	- 0.02	0.94	- 0.40	0.08
S53	**0.79**	**< 0.001**	- 0.17	0.55	0.09	0.24
S49	**0.74**	**0.002**	**0.54**	**0.04**	- 0.23	0.41
S50	**0.71**	**0.01**	0.24	0.43	- 0.39	0.61
S54	0.48	0.08	0.28	0.33	**- 0.78**	**< 0.001**
S22	0.34	0.23	**0.82**	**< 0.001**	- 0.24	0.29
S40	0.23	0.44	**- 0.68**	**0.01**	0.01	0.91
S52	0.09	0.77	0.34	0.24	- 0.13	0.96
S29	0.07	0.81	0.04	0.90	- 0.21	0.49
S46	0.06	0.83	0.23	0.43	0.40	0.49

Subjects were separated into two groups based on their threshold-EMD correlations for further analysis. Subjects with threshold-EMD correlation coefficients larger than 0.70 were in the "strong threshold-EMD" group (*N* = 5), whereas those below the 0.70 cut-off were in the "weak-to-moderate threshold-EMD" group (*N* = 6). Figure 4.6 shows the relationship between the polarity effect and sQP thresholds for (A) the five subjects with strong and statistically

significant threshold-EMD correlations, and (B) the six subjects with weak-to-moderate, non-significant threshold-EMD correlations. Repeated measures correlations were performed to determine the strength of the relationship between sQP thresholds and the polarity effect within each group. Overall, the group with strong threshold-EMD correlations did not demonstrate a significant relationship between sQP thresholds and the polarity effect ($r_{rm(63)} = 0.03$, 95% CI [-0.22, 0.28], $P = 0.80$). However, the relationship between the polarity effect and sQP thresholds was significant for the group with weak-to-moderate threshold-EMD correlations ($r_{rm(76)} = 0.48$, 95% CI [0.28, 0.63], $P < 0.001$). These results emphasize that sQP thresholds can reflect either electrode position or neural integrity (as estimated by the polarity effect). Relationships between sQP thresholds and neural integrity may be more likely to emerge when the variation in sQP thresholds cannot be explained by variation in electrode position.

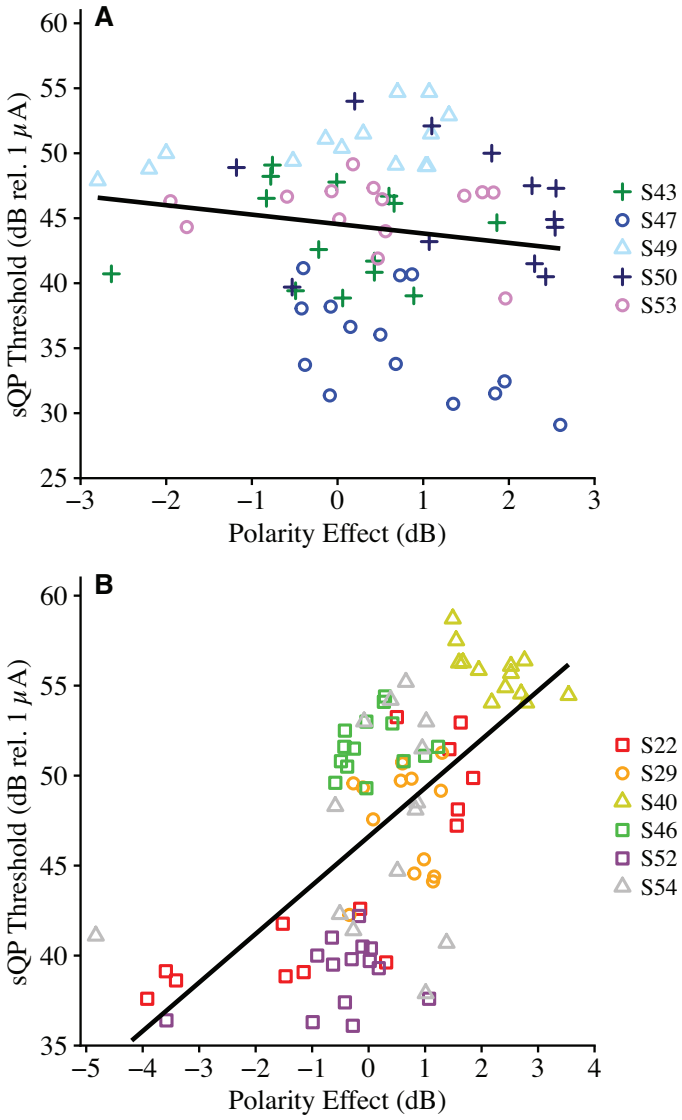

Figure 4.6. Focused (sQP) thresholds (in dB relative to 1 μA) as a function of polarity effect (in dB) for two groups of subjects that are grouped based on the strength of their within-subject correlations between electrode-to-modiolus distance (in mm) and sQP thresholds. A) Subjects that have a very strong correlation ($r = 0.71$ to 0.94) between electrode-to-modiolus distance and sQP thresholds. B) Subjects that have a weak-to-moderate correlation ($r = 0.06$ to 0.48) between electrode-to-modiolus distance and sQP thresholds. Individual subjects are represented by different colors and shapes.

4.4.3 *Polarity Sensitivity and Duration of Deafness*

Finally, we performed a preliminary analysis to quantify the relationship between the polarity effect and duration of deafness, a common implicit assessment of neural integrity. Figure 4.7 shows the relationship between duration of deafness and the across-site average polarity effect. For this analysis, the polarity effect was averaged across all available electrodes for each subject. Duration of deafness was defined as the time, in years, between diagnosis of severe-to-profound sensorineural hearing loss and CI activation. A linear regression analysis indicated that duration of deafness was significantly correlated with the across-site average polarity effect ($R^2 = 0.38$, $R^2_{adjusted} = 0.32$, $F_{(1,9)} = 5.62$, $P = 0.04$). Specifically, individuals that experienced relatively long durations of deafness prior to receiving a CI also tended to have relatively large, positive polarity effects.

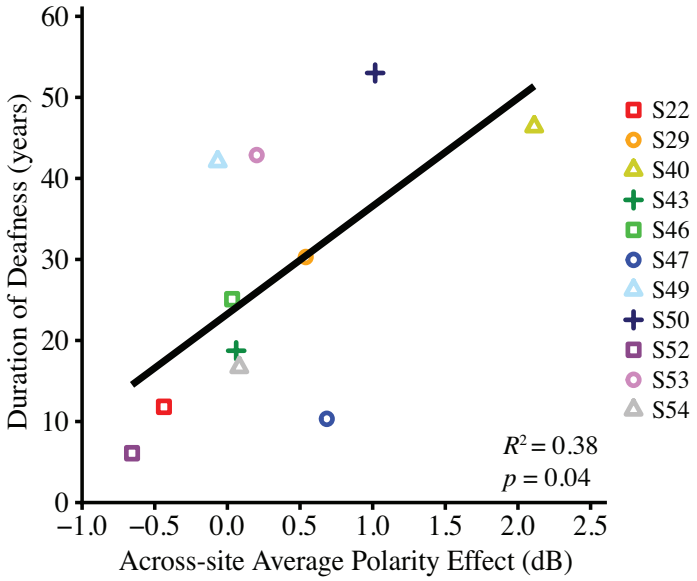

Figure 4.7. The relationship between duration of deafness (in years) and across-site average polarity effect (in dB) is shown ($R^2 = 0.38$, $P = 0.04$). Individual subjects are represented by different colors and shapes.

4.5 DISCUSSION

The present study evaluated the theory that polarity sensitivity reflects neural status in CI listeners. An ideal estimate of neural integrity should vary independently of other factors that influence the quality of the CI electrode-neuron interface, such as electrode position and tissue impedances. Our primary results support these tenets; specifically, the polarity effect at threshold was subject- and electrode-dependent and varied independently of CT-estimated electrode position and intracochlear resistance. The polarity effect was also positively correlated with focused behavioral thresholds, which are believed to reflect a combination of local neural status, electrode position, and intracochlear bone and tissue growth. Importantly, the polarity effect remained a significant predictor of focused thresholds after statistically controlling for electrode position and intracochlear resistance. Taken together, these results support the theory that polarity sensitivity may reflect neural health in CI listeners.

4.5.1 *Polarity Sensitivity Varies Independently of Electrode Position and Intracochlear Resistance*

Psychophysical polarity sensitivity at threshold varied across- and within-subjects. These findings are consistent with previous investigations that demonstrated subject- and electrode-dependent polarity effects at threshold (Macherey et al. 2017; Carlyon et al. 2018). However, previous reports did not rule out the possibility that channel-to-channel variability in the polarity effect was influenced by non-physiological factors. It is possible that either the physical distance of an electrode to its target neurons or the location of the electrode relative to the central axons could influence polarity sensitivity measurements.

The results of the present study demonstrate that the polarity effect at threshold is independent of CT-estimated electrode-to-modiolus distance and electrode scalar location. These

findings may be explained by the nature of the polarity effect measurement, which reflects a difference score rather than an absolute threshold response. Theoretically, excitability (i.e., absolute threshold) of degenerated neurons depends on the physical distance between the electrode and the soma (Rattay et al. 2001b). At a single electrode site, the effect of physical distance on absolute threshold response to each polarity should cancel out when a difference score (i.e., polarity effect) is calculated.

Moreover, recall that modeling work suggests that anodic and cathodic polarities have different sites of spike initiation, wherein depolarization occurs near the central axon for anodic stimuli and more peripherally for cathodic stimuli (Rattay et al. 2001a,b; Joshi et al. 2017; Resnick et al. 2018). When the peripheral processes have degenerated, depolarization in response to cathodic current would occur near the unmyelinated cell body, which is difficult to excite in humans (Rattay 1999; Rattay et al. 2001a). Conversely, for anodic stimulation, action potentials are expected to be generated near the central axon, and therefore do not need to overcome the unmyelinated soma. In turn, when the peripheral processes have degenerated, thresholds in response to cathodic stimuli will be higher than those in response to anodic stimuli (i.e., positive polarity effect).

Conceivably, then, electrode position relative to the central axon could influence polarity sensitivity. However, basic principles of human cochlear anatomy and CI electrode placement would suggest that a functioning CI electrode must be located within the cochlear compartments, distal/peripheral to the soma. In humans, SGN somata are located within Rosenthal's canal; each cell body extends a peripheral process toward the organ of Corti and a central process into the auditory nerve (Nayagam et al. 2011). Since it is unlikely that a viable CI electrode would be located proximal/central to the soma, the difference in threshold response to anodic versus

cathodic stimulation should be independent of the position of the electrode relative to the modiolus.

In addition to electrode position, intracochlear bone and fibrous tissue growth are believed to vary within- and across-subjects (Spelman et al. 1982; Bierer et al. 2015b; Kamakura and Nadol 2016). The present results showed that the polarity effect varies independently of EFI-estimated longitudinal intracochlear resistance. Again, these findings are consistent with the polarity effect measurement as a difference score between threshold responses to two stimuli. Presumably, responses to anodic and cathodic polarities would be affected in similar ways by the impedance environment near a recording electrode; thus, effects of intracochlear resistance on threshold measurements should cancel out when calculating the difference between responses to each polarity at a given site.

In summary, the polarity effect at threshold varies independently of electrode position relative to the modiolus, electrode scalar location, and intracochlear resistance. This may be related to the nature of the polarity effect measurement (i.e., difference score rather than absolute threshold response) and to the necessary position of functioning CI electrodes in humans (i.e., somewhat distal to the SGN cell bodies).

4.5.2 *Across Subjects, the Polarity Effect is Related to Focused Behavioral Thresholds*

Several lines of evidence suggest that focused behavioral thresholds are related to electrode position within the cochlea, intracochlear resistance, and estimates of neural integrity (e.g., Bierer 2007; Bierer and Faulkner 2010; Goldwyn et al. 2010; Bierer et al. 2011; Bierer and Nye 2014; Bierer et al. 2015b; Long et al. 2014; DeVries et al. 2016). Thus, if polarity sensitivity reflects peripheral degeneration in CI listeners, then it should explain some of the variation in

focused behavioral thresholds, even after accounting for electrode position and intracochlear resistance. The present results confirmed this hypothesis.

Specifically, electrodes with relatively high focused behavioral thresholds also tended to have relatively large, positive polarity effects. This relationship held after statistically controlling for CT-estimated electrode position and EFI-estimated intracochlear resistance, which are known to partially explain variation in focused thresholds (Long et al. 2014; Bierer et al. 2015b; DeVries et al. 2016; DeVries and Arenberg 2018a). These findings agree with modeling data showing that electrodes near regions with degenerated or demyelinated neurons have higher thresholds than electrodes near regions with healthy spiral ganglion populations (Goldwyn et al. 2010; Joshi et al. 2017; Resnick et al. 2018). The present data are also consistent with Carlyon et al. (2018), who found a modest, but significant, correlation between the polarity effect and the average of ACA and CAC monopolar thresholds in a sample of eight adults with CIs. Taken together, these findings provide support for the theory that polarity sensitivity may reflect neural health in CI listeners.

Consistent with previous investigations, we also observed a strong relationship between CT-estimated electrode position and focused thresholds (Long et al. 2014; DeVries et al. 2016; DeVries and Arenberg 2018a). Specifically, electrodes that were located far from their target neurons, or that were translocated to SV, had relatively high focused thresholds. We further demonstrated that lower intracochlear resistance values are predictive of higher focused thresholds. The negative relationship between focused thresholds and intracochlear resistance can be explained in the context of Ohm's Law, wherein the amount of current necessary to achieve a criterion voltage (i.e., threshold level) is inversely related to the resistance in the

system. These results are consistent with those of Bierer et al. (2015b), who demonstrated that lower monopolar and tripolar thresholds are associated with higher impedance values.

However, despite the overall relationship between the polarity effect and focused thresholds, Figure 4.5B and Table 4.3 show that positive and significant within-subject correlations were not always observed. Examining the threshold-PE correlations in the context of the individual correlations between focused thresholds and electrode-to-modiolus distance (threshold-EMD) revealed a possible explanation for this finding. Five subjects had strong and significant threshold-EMD correlations (ranging from $r = 0.71$ to 0.94). In those individuals, the variation in focused thresholds was largely explained by variation in electrode position. In fact, the across-subject correlation between the polarity effect and focused thresholds was driven by individuals with weak or moderate threshold-EMD relationships (Figure 4.6). This observation emphasizes the importance of developing in vivo neural health measures that vary independently of confounding factors such as electrode position. In isolation, behavioral thresholds cannot provide a reliable indication of the integrity of local SGNs. Furthermore, it is likely that an ideal assessment of a CI listener's electrode-neuron interface involves a comprehensive evaluation of both electrode position and neural health.

Of note, it is possible that correlations between the polarity effect and focused thresholds could improve with the use of equivalent stimulation rates to measure each response. Stimulation rate is known to influence psychophysical thresholds, wherein thresholds tend to decrease with increasing pulse rate (e.g., Pfingst et al. 2011; Zhou et al. 2012). For the present study, the stimuli used to measure focused thresholds and the polarity effect were selected in keeping with previous literature. Moreover, given that the polarity effect was represented by a difference score, the effect of stimulation rate on absolute thresholds is not expected to substantially

contribute to the outcome measure. However, potential interactions between stimulation rate and polarity effect measurements remain to be investigated.

4.5.3 *Clinical Implications and Future Directions*

Overall, the present results support the theory that the psychophysical polarity effect at threshold may reflect local neural health in CI listeners. Results also indicated that individuals with relatively long durations of deafness prior to implantation tend to have relatively large, positive polarity effects. Although duration of deafness is merely an implicit correlate of neural health, this finding aligns with temporal bone analyses showing that low total SGN counts are associated with long periods of auditory deprivation (Nadol et al. 1989).

Individual- and electrode-specific differences in the magnitude of the polarity effect suggest that this measurement has the potential to assist in developing individualized programming recommendations. However, if polarity sensitivity reflects local neural health in CI listeners, it remains to be determined what magnitude of polarity effect is meaningful. It may be that only extreme positive or negative values provide useful insight into the health of local neurons. In fact, Resnick et al. (2018) predicted that only extreme demyelination results in pathological current spread and recruitment. Future studies with larger samples should investigate the cumulative contributions of diverse aspects of peripheral health to auditory perception with a CI.

Ideally, a combination of neural health and electrode position estimates would be used to optimize the electrode-neuron interface for an individual subject. DeVries and Arenberg (2018b) found that implementing current focusing on electrodes that are located far from the modiolus may help to reduce channel interaction. Some CI listeners also experience speech perception benefit when electrodes that are estimated to interface poorly with the auditory nerve are

deactivated (Noble et al. 2015; Bierer and Litvak 2016; Zhou 2017). Together, assessments of neural health and electrode position could be used to comprehensively characterize neural function near each electrode site, ultimately leading to improved patient-specific interventions. Future work should determine potential uses of polarity sensitivity in individualized CI programming adjustments.

CHAPTER 5. POLARITY SENSITIVITY IN CHILDREN AND ADULTS WITH COCHLEAR IMPLANTS

5.1 ABSTRACT

Modeling data suggest that sensitivity to the polarity of an electrical stimulus may reflect the health of the peripheral processes in cochlear implant (CI) listeners. Specifically, better sensitivity to anodic (positive) current than to cathodic (negative) current may indicate peripheral process degeneration or demyelination. The goal of the present study was to characterize polarity sensitivity in a sample of CI listeners (41 ears) with diverse hearing histories, including children and adults. Relationships between electrode-specific polarity sensitivity at threshold and (a) polarity sensitivity at supra-threshold levels, (b) chronological age, (c) pre-implantation duration of deafness, and (d) phoneme perception were determined. Polarity sensitivity at threshold was defined as the difference in electrode-specific behavioral thresholds measured in response to each of two triphasic pulses, where the central high-amplitude phase was either cathodic (ACA) or anodic (CAC). Positive polarity effects, or lower (i.e., better) anodic thresholds, may suggest peripheral process degeneration. On the majority of electrodes tested, threshold and supra-threshold sensitivity was better for anodic than for cathodic stimulation; however, dynamic range often remained larger for cathodic stimulation. Polarity sensitivity at threshold did not differ between children and adults. Adults with long pre-implantation durations of deafness tended to have large, positive polarity effects on channels that were estimated to interface poorly with the auditory nerve; this was not observed in children. Across subjects, only duration of deafness predicted phoneme perception performance. Subject- and electrode-dependent differences in polarity sensitivity may assist in developing customized CI programming interventions for children and adults.

5.2 INTRODUCTION

Physiological and psychophysical estimates of auditory acuity vary considerably across stimulation sites within individual cochlear implant (CI) listeners (e.g., Pfingst & Xu 2004; Zhu et al. 2012; DeVries et al. 2016; DeVries & Arenberg 2018). Some of this variability may, in part, result from within- and across-subject variation in spiral ganglion neuron (SGN) health. Human post-mortem temporal bone studies demonstrate that SGN density varies widely across individuals and across the length of the cochlea within an individual ear (Otte et al. 1978; Hinojosa & Marion 1983; Nadol et al. 1989; Nadol 1997; Makary et al. 2011). In those temporal bone analyses, variability in SGN counts is partially explained by demographic variables such as chronological age, duration of deafness, and hearing loss etiology. Animal studies also indicate that long-term auditory deprivation is associated with reduced SGN survival relative to normal (e.g., Hall 1990; Shepherd & Javel 1997). However, histological studies in humans have not found consistent relationships between post-mortem SGN density and speech perception scores obtained during an individual's lifetime (Otte et al. 1978; Nadol et al. 2001; Khan et al. 2005; Fayad & Linthicum 2006).

In vivo estimates of neural status may improve our ability to study how the health of the auditory nerve relates to auditory perception with a CI during life. Over the years, several indirect measures of SGN density have been proposed and evaluated in animals and humans. In animal models, characteristics of evoked potential responses differ as a function of SGN density; for instance, electrodes near cochlear regions with relatively few surviving SGNs tend to have relatively small evoked potential amplitudes, high thresholds, and shallow amplitude growth functions (AGFs; e.g., Hall 1990; Shepherd & Javel 1997; Ramekers et al. 2014; Pfingst et al.

2015a). Moreover, psychophysical temporal multipulse integration abilities may depend, in part, on local SGN density (Pfingst et al. 2011; Zhou et al. 2015).

In human CI listeners, evoked potential and multipulse integration responses vary widely across recording sites (e.g., Brown et al. 1990; Eisen & Franck 2004; Cafarelli Dees et al. 2005; Bierer et al. 2011; Zhou & Pfingst 2014; DeVries et al. 2016; Schvartz-Leyzac & Pfingst 2016). Some investigators have noted that younger participants have larger evoked potential amplitudes and steeper AGF slopes than older participants (Cafarelli Dees et al. 2005; Brown et al. 2010), and that shallower AGF slopes are associated with longer durations of hearing loss (Schvartz-Leyzac & Pfingst 2016). Moreover, there is some evidence that better speech perception scores are associated with larger evoked potential amplitudes and steeper AGF slopes (Brown et al. 1990; Kim et al. 2010; DeVries et al. 2016; Scheperle 2017). In bilateral CI listeners, between-ear differences in phoneme perception are partially explained by between-ear differences in evoked potential responses (Schvartz-Leyzac & Pfingst 2018) and multipulse integration abilities (Zhou & Pfingst 2014).

Although indirect estimates of SGN density, especially evoked potential measures, have been studied extensively in humans, the number of remaining SGNs constitutes only one aspect of neural health. Conceivably, the integrity of the peripheral processes could also influence the fidelity of electrical stimulation by a CI. Recent computational modeling evidence suggests that sensitivity to the polarity of an electrical stimulus may reflect local peripheral process integrity (Rattay et al. 2001a,b; Joshi et al. 2017; Resnick et al. 2018). The primary goal of the present study was to characterize polarity sensitivity in a large group of CI listeners with diverse hearing histories.

Polarity sensitivity refers to the difference in psychophysical or physiological responses to positive (anodic) and negative (cathodic) electrical current. Modeling data suggest that better sensitivity to the anodic polarity than to the cathodic polarity may indicate peripheral process degeneration or demyelination (Rattay et al. 2001a,b; Joshi et al. 2017; Resnick et al. 2018). Differential sensitivity to each polarity is thought to reflect differences in the site of spike initiation in response to anodic and cathodic pulse shapes. Specifically, injecting positive (anodic) current into the extracellular space results in depolarization near the central axon, whereas negative (cathodic) current depolarizes more distal regions of the neuron, near the peripheral processes. When the peripheral processes have degenerated, higher current levels for cathodic relative to anodic polarities are required in order for cathodic stimuli to overcome the unmyelinated cell body and generate an action potential near the central axon (Rattay et al. 2001a,b; Joshi et al. 2017; Macherey et al. 2017; Resnick et al. 2018).

The polarity sensitivity theory, based largely on data from computational modeling studies, has gained increasing popularity in the human CI literature. Physiological and psychophysical evidence in CI listeners suggests that polarity sensitivity has the potential to provide insight into the status of the electrode-neuron interface (Macherey et al. 2006; van Wieringen et al. 2008; Undurraga et al. 2010; Undurraga et al. 2013; Spitzer & Hughes 2017; Hughes et al. 2017; Macherey et al. 2017; Hughes et al. 2018; Carlyon et al. 2018; Jahn & Arenberg 2019). At suprathreshold stimulation levels, evoked potential amplitudes are generally larger (Macherey et al. 2008; Undurraga et al. 2010; Bahmer & Baumann 2013; Hughes et al. 2017; Hughes et al. 2018), and most comfortable listening levels are generally lower (Macherey et al. 2017), for anodic compared to cathodic stimulation. These findings using suprathreshold

stimulation levels suggest that anodic stimulation may be a more effective stimulus, in general, than cathodic stimulation in human CI listeners.

On the other hand, recent evidence using low-level stimulation shows that polarity sensitivity at threshold is subject- and electrode-dependent in post-lingually deafened adults (Macherey et al., 2017; Carlyon et al. 2018; Jahn & Arenberg 2019). Moreover, Jahn and Arenberg (2019) demonstrated that the psychophysical polarity effect at threshold varies independently of electrode position relative to the modiolus and intracochlear resistance. Taken together, these studies provide increasing evidence that polarity sensitivity may reflect neural health in CI listeners, and that the measure is relatively independent of other factors that influence the quality of the electrode-neuron interface in humans.

In order to comprehensively characterize polarity sensitivity in CI listeners and to determine its utility in clinical interventions, it is important to evaluate polarity sensitivity in individuals with diverse hearing histories and to determine whether it relates to CI outcomes. To date, polarity sensitivity has been studied in small samples of largely post-lingually deafened adults. Children and adults with CIs typically present with different demographic characteristics that may influence SGN integrity. For instance, adults are older and often experience longer durations of pre-implantation auditory deprivation than children who are implanted early in life. Children and adults with CIs also tend to have different hearing loss etiologies. Human histological studies demonstrate that chronological age, duration of deafness, and hearing loss etiology are related to SGN density (Otte et al., 1978; Nadol et al., 1989; Nadol, 1997; Makary et al., 2011). The primary goal of the present study was to expand upon previous literature by characterizing polarity sensitivity and speech perception performance in a relatively large sample of CI listeners with diverse hearing histories, including children and adults.

The primary outcome measure is the polarity effect at threshold, defined as the difference in electrode-specific behavioral thresholds measured in response to anodic and cathodic polarities (cathodic threshold minus anodic threshold; Carlyon et al. 2018; Jahn & Arenberg 2019). The polarity effect at threshold was chosen as the primary outcome measure because it has been shown to vary independently of electrode position and tissue impedances in CI listeners (Jahn & Arenberg 2019). In the present study, we also assessed the polarity effect at suprathreshold levels, by estimating individuals' most comfortable listening levels (MCLs) for each stimulus and calculating the polarity effect at MCL (cathodic MCL minus anodic MCL) and for dynamic range (cathodic DR minus anodic DR).

Consistent with prior investigations, we predicted that the polarity effect at threshold would be subject- and electrode-dependent, but that the polarity effect at MCL would be largely positive in magnitude (Macherey et al. 2017; Carlyon et al. 2018; Jahn & Arenberg 2019;). We expected variability in polarity sensitivity to persist across the diverse sample of pediatric and adult CI listeners included in this dataset. Furthermore, we predicted that: 1) Long periods of pre-implantation auditory deprivation would be associated with large, positive polarity effects (i.e., more peripheral degeneration); 2) Adults would have larger, more positive, polarity effects (i.e., more peripheral degeneration) than children; 3) Relatively poor speech perception scores would be associated with relatively large, positive polarity effects (i.e., more peripheral degeneration). The results of this investigation will provide important insight into the characteristics of polarity sensitivity in children and adults with CIs and may assist in developing hypothesis-driven recommendations for the application of polarity sensitivity to CI programming interventions.

5.3 METHODS

5.3.1 *Subjects*

Demographic information for all subjects and ears tested in this study is presented in Table 5.1. Data were obtained from a total of 41 ears (27 individual subjects, 13 males) implanted with Advanced Bionics HiRes 90K devices. Twenty ears (11 individual subjects) were deafened and implanted during childhood (prior to age 18 years). At the time of testing, subjects in the child-implanted group ranged in age from 13 to 18 years (M = 15.2 years, SD = 1.4 years). Nine of the 11 child-implanted subjects were bilaterally implanted, and data were collected from each ear. Subjects P11 and P12 are fraternal twins. No other subjects are related to one another. Hereafter, this group of subjects will be referred to as the "children", to signify that they were implanted during childhood and largely tested as children (one subject, P06, was 18 years old at the time of testing). In all figures, data from the children are denoted by green symbols.

Table 5.1. Demographic information for all participants including: hearing loss etiology (if known), chronological age at time of testing (in years), age of implantation for implanted each ear (in years), duration of deafness for each implanted ear (in years), and electrode array for each implanted ear. Duration of deafness is defined as the time between diagnosis of severe-to-profound sensorineural hearing loss and cochlear implant activation. Note that subjects S47 and S59 are bilaterally implanted, but their second-implanted ears were not tested as part of this study. EVA: enlarged vestibular aqueduct; DFNB1: genetic non-syndromic hearing loss. HF1J: HiFocus 1J electrode array. MS: Mid-Scala electrode array

			First-implanted Ear			Second-implanted Ear		
ID	Etiology	Age (years)	Age Implanted (years)	Duration of Deafness (years)	Electrode Array	Age Implanted (years)	Duration of Deafness (years)	Electrode Array
Children								
P02	EVA	13.9	1.1	1.1	HF1J	3.1	3.1	HF1J
P03	Unknown	14.7	1.4	1.4	HF1J	5.6	5.6	HF1J
P04	Unknown	15.2	1.7	1.7	HF1J	4.7	4.7	HF1J
P06	Unknown	18.8	4.3	1.8	HF1J	10.9	8.5	HF1J
P07	Unknown	15.4	1.9	1.9	HF1J	4.9	4.9	HF1J
P09	Unknown	14.9	2.6	1.3	HF1J	3.9	2.7	HF1J
P11	DFNB1	15.3	1.4	1.2	HF1J	10.2	10.0	HF1J
P12	DFNB1	15.3	1.7	1.4	HF1J	10.2	10.0	HF1J
P13	EVA	13.4	9.2	6.4	HF1J	--	--	--
P16	DFNB1	14.6	1.0	1.0	HF1J	4.5	4.5	HF1J
P17	Unknown	15.5	1.3	1.3	HF1J	--	--	--
	Mean	15.2	2.5	1.9		6.5	6.0	
	(*SD*)	(*1.4*)	(*2.4*)	(*1.5*)		(*3.1*)	(*2.8*)	
Adults								
S22	Unknown	78.2	66.7	11.8	1J Helix	--	--	--
S23	Unknown	73.4	62.0	3.9	1J Helix	64.6	6.5	HF1J
S29	Noise exposure	87.8	76.8	30.3	HF1J	85.7	39.2	MS
S39	Genetic	54.4	30.1	8.0	HF1J	40.1	18.0	HF1J
S40	EVA	56.2	50.4	46.4	HF1J	--	--	--
S43	Noise exposure	72.5	67.9	18.7	MS	--	--	--
S45	Genetic	65.4	54.0	11.0	HF1J	61.0	18.0	MS
S46	Unknown	69.4	64.2	25.1	HF1J	--	--	--
S47	Unknown	40.4	36.4	10.3	MS	--	--	--
S49	Unknown	45.8	43.5	42.1	MS	44.2	42.8	MS
S50	Unknown	76.5	71.0	53.0	HF1J	--	--	--
S52	Unknown	71.2	66.0	6.1	HF1J	--	--	--
S53	Meningitis	56.0	44.1	42.9	1J Helix	--	--	--
S54	EVA	27.8	23.7	16.7	MS	--	--	--
S59	Ototoxicity	32.1	30.9	18.9	MS	--	--	--
S60	Meningitis	22.5	19.2	19.1	MS	--	--	--
	Mean	59.9	50.4	22.8		59.1	24.9	
	(*SD*)	(*18.8*)	(*18.3*)	(*15.6*)		(*18.2*)	(*15.5*)	

Twenty-one ears (16 individual subjects) were implanted during adulthood (age 18 or older). Four of the adult-implanted subjects (S40, S49, S53, and S60) were diagnosed with severe-to-profound sensorineural hearing loss as children, and the remaining subjects became deaf as adults. At the time of testing, adult-implanted participants ranged in age from 22 to 87 years (M = 59.9 years, SD = 18.8 years). Seven of the 16 adult-implanted participants presented with bilateral implants; however, due to time constraints, only five of the bilaterally implanted adults were tested in both ears. Hereafter, this group of subjects will be referred to as the "adults", to signify that they were implanted and tested as adults. In all figures, data from the adults are denoted by blue symbols.

All subjects primarily used spoken language to communicate, and all but one subject were native American English speakers. Subject S54 learned English as a second language during early childhood. Each child provided written informed assent, and their parents or legal guardians provided written informed consent. Each adult provided written informed consent. All procedures were approved by the University of Washington Human Subjects Division.

5.3.2 *Electrical Stimuli*

Electrical stimuli were controlled by the Bionic Ear Data Collection System (BEDCS) version 1.18.315 (Advanced Bionics, Valencia, CA) and custom MATLAB scripts (MathWorks, Inc., Natick, MA). Stimuli were presented directly to the internal device. Prior to testing, electrical stimuli were verified using a reference implant and a digital storage oscilloscope.

5.3.3 *Selection of Channels for Polarity Testing*

Advanced Bionics implants have 16 electrode contacts. Due to time and attention constraints, it was not feasible to measure the polarity effect on every electrode in each participant, especially

for the children. Instead, four channels per ear were selected for polarity effect testing. Within a subject, the four channels were selected based on the relative within-subject magnitude of electrode-specific behavioral thresholds measured in response to a spatially-focused electrode configuration. Focused behavioral thresholds are believed to reflect the overall quality of the electrode-neuron interface; within a subject, higher-threshold channels are thought to interface poorly with the auditory nerve relative to lower-threshold channels (for review, see Bierer 2010). For instance, channels with relatively high focused thresholds are often located farther from their target neurons (Long et al. 2014; DeVries et al. 2016; DeVries & Arenberg 2018) and have smaller evoked potential amplitudes (DeVries et al. 2016) than lower-threshold channels.

Several prior investigations have used relative focused behavioral threshold levels to select a subset of channels for experimental testing (Bierer & Faulkner 2010; Bierer et al. 2011; Bierer & Nye 2014; Bierer et al. 2015c). In the present study, the two lowest-threshold channels and the two highest-threshold channels were selected for polarity effect assessment. None of the four channels were directly adjacent to one another. Theoretically, selecting low- and high-threshold channels within a subject allows for assessment of a subset of electrodes that vary in the quality with which they interface with the auditory nerve; low- and high-threshold channels represent “good” and “poor” electrode-neuron interfaces, respectively.

Single-channel focused behavioral thresholds were assessed using a modified Békésy-style sweep procedure **(**Sek et al. 2005; Bierer et al. 2015a**).** Using current steering, stimuli were swept across the electrode array by dividing the electrical current between two adjacent intracochlear electrodes and varying the proportion of current directed to each electrode. The sweep procedure enables attainment of single-channel behavioral thresholds across the electrode

array in a manner that is four times faster than would be possible with traditional adaptive forced-choice methods (Bierer et al. 2015a).

Stimuli were biphasic, cathodic-leading pulse trains (102 μs/phase, 0-μs interphase gap, 200.4 ms duration, 997.9 pps) presented using a steered quadrupolar (sQP) stimulation mode. A channel was comprised of four adjacent intracochlear electrodes. The two middle electrodes served as active electrodes, and the two outermost electrodes served as return electrodes. The current focusing coefficient (σ), was set to 0.9, indicating that 90% of the return current was delivered through the intracochlear return electrodes (45% to each electrode), and the remaining 10% was delivered through an extracochlear ground. Current focusing coefficients can range from 0 to 1, with 1 representing the highest possible degree of current focusing and, consequently, resulting in the most spatially restrictive electrical field. The higher the current focusing coefficient, the greater the observed channel-to-channel variability in focused thresholds (Bierer & Faulkner 2010). A highly-focused coefficient of 0.9 was selected to capture as much within-subject variability in focused thresholds as possible, while remaining below the voltage compliance limits of the device.

The modified sweep procedure has been described in detail in many other studies from our laboratory (e.g., Bierer et al., 2015b; DeVries et al., 2016; DeVries & Arenberg, 2018a; Jahn & Arenberg 2019). A brief review of the sweep procedure is provided here. To sweep stimuli across the electrode array, current was steered between the two active electrodes by varying the steering coefficient, alpha (α). When α = 0, all current is delivered through the more apical of the active electrode pair. Conversely, when α = 1, all current is delivered through the more basal active electrode. Because sQP stimulation requires four adjacent intracochlear electrodes, focused thresholds can only be obtained for electrodes 2-15. Per convention, on channels 3-15,

integer channel numbers refer to the number of the basal active electrode when $\alpha = 1$; for channel 2, an α value of 0 is used to center the current on electrode 2.

The upper limit of stimulation on each electrode was set to each listener's electrode-specific MCL, which corresponded to a loudness rating of "6", or "most comfortable", on the Advanced Bionics clinical loudness scale (Advanced Bionics, Valencia, CA). Pulse trains were presented starting at a level 6 dB below each listener's MCL and swept across the electrode array by increasing alpha from 0 to 1 in step sizes of 0.1. The listener was instructed to continuously depress the spacebar on a standard computer keyboard when he or she could hear the stimulus, and to release the spacebar when he or she could not hear the stimulus. The participants completed one forward sweep that progressed basally (channels 2 to 15) and one reverse sweep that progressed apically (channels 15 to 2). Final single-channel focused threshold estimates were calculated as the weighted average of consecutive current levels at integer channel numbers along the forward and reverse sweeps (Bierer et al. 2015a).

Following the threshold measurement, the channels with the two lowest focused thresholds and those with the two highest focused thresholds were identified for each ear. If any of those channels were adjacent to one another, the channel with the next-lowest or next-highest non-adjacent threshold was identified. These four non-adjacent channels (two low-threshold and two high-threshold) were selected for subsequent polarity effect testing.

5.3.4 *Polarity Effect Measurement*

Polarity sensitivity was assessed on four non-adjacent channels within each ear: the two channels with the lowest focused thresholds, and the two channels with the highest focused thresholds. To assess polarity sensitivity, single-channel behavioral thresholds were measured in response to each of two triphasic pulses. The triphasic pulses had a central high-amplitude phase that was

twice the amplitude of the first and third phases. The polarity of the central high-amplitude phase was either anodic (CAC) or cathodic (ACA). Stimuli were 99 pulse-per-second (pps) trains presented in a monopolar stimulation mode (43 μs/phase, 0-μs interphase gap, 400 ms duration). These stimuli concentrate the charge of the polarity of interest into a brief time window, while maintaining the requisite charge balance for use in humans. Asymmetric pulse shapes have been shown to be particularly effective in measuring polarity sensitivity in human psychophysical experiments (Carlyon et al. 2013; Macherey et al. 2006, 2008, 2017). The stimuli were identical to those used by Carlyon et al. (2018) and Jahn and Arenberg (2019).

The polarity effect (in dB) on each tested channel was defined as the ACA threshold minus the CAC threshold (ACA – CAC). A positive polarity effect indicated that CAC thresholds were lower (i.e., better) than ACA thresholds. Based on modeling data, a positive polarity effect (i.e., lower thresholds in response to the anodic polarity) may indicate some degree of peripheral process degeneration (Rattay et al., 2001a,b; Joshi et al. 2017; Resnick et al. 2018). A negative polarity effect indicated higher (i.e., worse) CAC thresholds compared to ACA thresholds, and may reflect healthier peripheral processes relative to a channel with a positive polarity effect (Rattay et al. 2001a,b; Joshi et al. 2017; Resnick et al. 2018).

To obtain supra-threshold polarity data and to set the upper limit of stimulation for polarity assessment, MCLs were obtained on each of the four channels in response to each polarity. To measure MCL, the current level was gradually increased from a subthreshold level of 50 microamps (μA) up until the subject reported a loudness rating of "6", or "most comfortable" on the Advanced Bionics clinical loudness scale (Advanced Bionics, Valencia, CA). For each channel and polarity, the corresponding MCL was set as the upper limit of stimulation for the threshold measurement procedure.

For 27 out of the 328 (8%) total channel/polarity combinations tested, MCL could not be reached at stimulation levels below the voltage compliance limits of the device. This tended to occur for certain subjects and was not related to CI channel or polarity, as follows: P12 (both implanted ears, all electrode/polarity combinations), P13 (first/only-implanted ear, both polarities on channel 15), P17 (first/only-implanted ear, all electrode/polarity combinations except for the anodic polarity on channel 2), and S29 (second-implanted ear, cathodic polarity on channels 8 and 13). In those cases, the upper limit of stimulation was set to the highest current level that could be achieved without exceeding voltage compliance limits. In each case, the upper stimulation level was equivalent to a subjective listening level of either 4 ("medium soft") or 5 ("medium"), which was sufficiently high for the subject to accurately perform the threshold measurements. However, those 27 measurements were excluded from any subsequent MCL and DR analyses.

An adaptive one-up/one-down staircase tracking procedure was used to measure single-channel behavioral detection thresholds for each polarity on each of the four channels. For each adaptive track, the initial presentation level was set to 90% of MCL; for channel/polarity combinations where MCL could not be reached, the initial presentation level was set to 98% of the upper stimulation level. For subsequent tracks, the initial presentation level was set anywhere from 50 to 98% of the upper stimulation level. A lower starting level was used on electrodes with large dynamic ranges to reduce the amount of time necessary to estimate threshold. Higher starting levels were maintained for electrodes with small dynamic ranges to ensure that the subject could comfortably hear the stimulus before the first reversal.

The subject was instructed to press the spacebar on the computer keyboard one time whenever he or she heard a sound. The presentation level decreased if the subject responded

within three seconds after stimulus presentation and increased if the subject did not respond within three seconds. The initial step size was 0.5 dB. After the first reversal, the step size was reduced to 0.2 dB. Random delays of 0.1 to 0.6 seconds were incorporated prior to each stimulus presentation. After eight reversals, the adaptive procedure terminated. Threshold was estimated as the average of the final six reversals.

The order of channels and polarities tested was randomized for each subject. Two adaptive threshold tracks were completed for each polarity on each channel. The two threshold estimates were averaged together to calculate a final threshold value. A third and fourth run were completed if the thresholds estimated on the first two runs differed by 1 decibel (dB) or more. In those cases, threshold estimates from each of the four runs were averaged together.

5.3.5 *Speech Perception*

Speech perception was assessed using medial vowel and consonant recognition tasks. Phonemes were chosen as the speech perception tasks because they are particularly sensitive to spectral and temporal distortions resulting from CI processing and poor electrode-neuron interfaces (Shannon et al. 2004; Xu et al. 2005; Nie et al. 2006; DiNino et al. 2016). Vowel stimuli were a closed set of 10 recorded vowels in /hVd/ context (/i/, “heed”; /ɪ/, “hid”; /eɪ/, “hayed”; /ɛ/,”head”; /æ/,”had”; /ɑ/, “hod”; /u/, “who’d”; /ʊ/, “hood”; /oʊ/, “hoed”; /ʌ/, “hud”) that were spoken by one female talker native to the Pacific Northwest region of the United States. Consonant stimuli were a closed set of 16 recorded consonants presented in /aCa/ context (/p/, “aPa”; /t/, “aTa”; /k/, “aKa”; /b/, “aBa”; /d/, “aDa”; /g/, “aGa”; /f/, “aFa”; /θ/, “aTHa”; /s/, “aSa”; /ʃ/, “aSHa”; /v/, “aVa”; /z/, “aZa”; /dʒ/, “aJa”; /m/, “aMa”; /n/, “aNa”; /l/, “aLa”) and spoken by one male talker (stimuli were the same as those used by Shannon et al. 1999). Testing was performed in a double-walled sound-treated booth (IAC RE-243). Stimuli were presented through an external

A/D device (SIIF USB SoundWave 7.1) and a Crown D75 amplifier at a calibrated level of 60 dB-A through a Bose 161 speaker placed at 0º azimuth and 1 meter from the participant's head. Custom software (ListPlayer2 version 2.2.11.52, Advanced Bionics, Valencia, CA) was used to present the stimuli and to record responses.

Participants were tested with one ear at a time, using their everyday listening programs. Unilateral CI users wore an earplug in the non-implanted ear during speech perception testing. After each speech token was presented, a graphical user interface with the possible phoneme choices was displayed on a computer screen. The participant selected his or her response using a computer mouse. Participants completed one practice run consisting of three repetitions of each speech token prior to beginning the experiment. Performance feedback was provided during the practice run. During the experiment, two runs consisting of three repetitions of each speech token were conducted, resulting in a total of six presentations of each speech token. Feedback was not provided during the experiment. Stimuli were pseudo-randomly interleaved within each run. If scores on the two runs differed by more than 10%, a third run consisting of three additional repetitions was presented. Scores from each run were averaged together to achieve a final percent correct.

5.3.6 *Statistical Analyses*

Data were analyzed using R Version 3.3.1 (R Core Team 2016). Linear mixed-effects models were employed for all analyses to account for clustering of electrode-specific data within ears, and/or for clustering of two ears within the same listener. "Subject" and/or "ear" were included as random effects in the models, where appropriate. Models were fit using restricted maximum likelihood (REML) parameter estimates to minimize small sample estimation bias (McNeish 2017). An unstructured covariance matrix was specified for each model. An Aikaike information

criterion with a bias correction for small samples (AICc) was used for model selection (Hurvich & Tsai 1989).

Note that traditional R^2 values are invalid for multilevel models. Instead, two pseudo-R^2 values, described by Nakagawa and Schielzeth (2013), are presented where applicable: 1) marginal R^2 (R^2_{marginal}), representing the proportion of the total variance explained by the fixed effects, and 2) conditional R^2 ($R^2_{\text{conditional}}$), representing the proportion of the variance explained by both the fixed and random effects. The difference between the R^2_{marginal} and $R^2_{\text{conditional}}$ reflects the variability in the random effects; here, this would represent across-subject variability. The lmerTest (Kuznetsova et al. 2017), MuMIn (Bartón 2018), and Lattice (Sarkar 2008) R packages were used to perform statistical analyses and to assess the validity of model assumptions. Bonferroni corrections for multiple comparisons were applied and are noted where appropriate.

5.4 RESULTS

5.4.1 *Electrode Array Considerations*

Subjects presented with a variety of electrode array types (HiFocus 1J, 1J Helix, and Mid-Scala; Table 5.1). Different electrode arrays are designed to achieve different positions in the cochlea relative to the modiolus (Dhanasingh & Jolly 2018) and can influence absolute threshold measurements (Long et al. 2014; DeVries et al. 2016; DeVries & Arenberg 2018a). However, Jahn and Arenberg (2019) showed that the polarity effect varies independently of electrode position relative to the inner wall of the cochlea. This is likely because the polarity effect is a difference score, rather than an absolute threshold measurement. The same stimuli and analysis methods used in Jahn and Arenberg (2019) were used in the present study. We confirmed that the polarity effect was not influenced by electrode array type ($F(2, 36.31) = 0.63$, $p = 0.63$) or

electrode cochlear location ($F(1, 129.83) = 0.03$, $p = 0.86$) in this sample of subjects. Electrode position is not considered further.

5.4.2 *Characterization of the Polarity Effect at Threshold and at Supra-threshold Levels*

The first analysis served to characterize the polarity effect at threshold and at supra-threshold levels in a relatively diverse sample of CI listeners, including children and adults. Figure 5.1(A-D) shows individual site-specific thresholds and MCLs measured in response to the ACA and CAC stimuli for two children (panels A and B) and two adults (panels C and D). Black squares represent responses to the ACA stimulus and red circles represent responses to the CAC stimulus. Solid lines connect the threshold responses and dashed lines connect the MCLs. Lower threshold or MCL responses to the CAC stimulus compared to the ACA stimulus indicate positive polarity effects. Based on modeling data, positive polarity effects (i.e., lower thresholds or MCLs for anodic compared to cathodic polarities) may reflect more peripheral process degeneration compared to negative polarity effects (Rattay et al. 2001a,b; Joshi et al. 2017; Resnick et al. 2018).

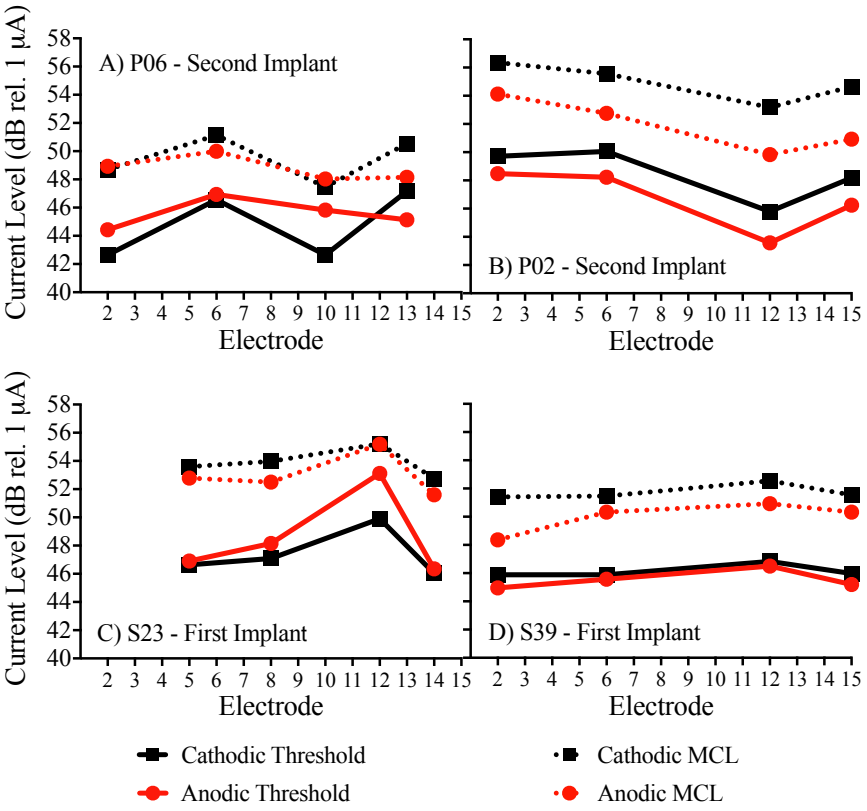

Figure 5.1. Individual site-specific thresholds and most comfortable listening levels (MCLs) measured in response to the cathodic (ACA) and anodic (CAC) pulse shapes for two children (panels A and B) and two adults (panels C and D). Black squares represent responses to the ACA pulse shape and red circles represent responses to the CAC pulse shape. Solid lines connect threshold measurements and dotted lines connect MCL measurements. Lower threshold responses to the CAC pulse shape (red) compared to the ACA pulse shape (black) indicate positive polarity effects.

Polarity effect magnitude at threshold and at MCL varied across- and within-subjects. Across electrodes, the polarity effect at threshold ranged from -4.82 dB to 3.54 dB (M = 0.25 dB, SD = 1.52 dB) and 102 out of the 164 electrodes (62.20%) had positive polarity effects at threshold. The polarity effect at MCL was calculated on 149 out of the 164 electrodes tested. At MCL, the polarity effect ranged from -2.13 dB to 4.83 dB (M = 1.12 dB, SD = 1.24 dB) and 133 out of the 149 electrodes (89.26%) demonstrated positive polarity effects at MCL. An electrode

with a positive polarity effect at threshold did not necessarily have a positive polarity effect at MCL, and vice versa.

Assessing the polarity effect at threshold and at MCL allowed us to calculate the difference in DR between the two polarities (i.e., DR polarity effect). DR was calculated as the difference between MCL and threshold for each polarity and each tested electrode. The DR polarity effect was calculated as the difference in DR for the cathodic (ACA) polarity versus the anodic (CAC) polarity (ACA – CAC). A positive DR polarity effect would indicate that the DR in response to the cathodic (ACA) polarity was larger than that in response to the anodic (CAC) polarity. Although a positive polarity effect at threshold and at MCL reflects better sensitivity to the anodic polarity, a positive DR polarity effect suggests the inverse (i.e., a larger DR for the cathodic polarity compared to the anodic polarity).

The DR polarity effect was assessed on 149 electrodes. The DR polarity effect varied from -2.05 dB to 5.31 dB (M = 0.87 dB, SD = 1.25 dB) and 115 out of 149 electrodes (77.18%) demonstrated positive DR polarity effects. Like threshold and MCL, the DR polarity effect was subject- and electrode-dependent. Despite the finding that most electrodes had better sensitivity to the anodic polarity at threshold and at MCL, the majority of electrodes exhibited larger DRs for the cathodic polarity than for the anodic polarity.

Relationships between polarity sensitivity at threshold and at suprathreshold levels were evaluated to determine whether polarity effects at low current levels are predictive of those at higher current levels across this sample of CI listeners. Initially, “age group” was included in the models as an independent variable to account for potential differences between children and adults; however, in each case, more parsimonious model fits (i.e., lower AICc values) were obtained when age group was excluded. Thus, the relationships between polarity sensitivity at

threshold and at suprathreshold levels did not differ between children and adults, and "age group" was not included in the final models. To elucidate this finding, data from children and adults are denoted by separate colors in each figure (green and blue symbols, respectively).

Figure 5.2(A-C) shows electrode-specific data for the relationships between A) polarity effect at threshold and at MCL, B) polarity effect at threshold and for DR, and C) polarity effect at MCL and for DR. Dashed lines split each panel into four quadrants at y = 0 and x = 0. Data points that fall in the upper right-hand quadrants and in the lower left-hand quadrants have the same sign (positive or negative, respectively) for both of the measures represented in the figure.

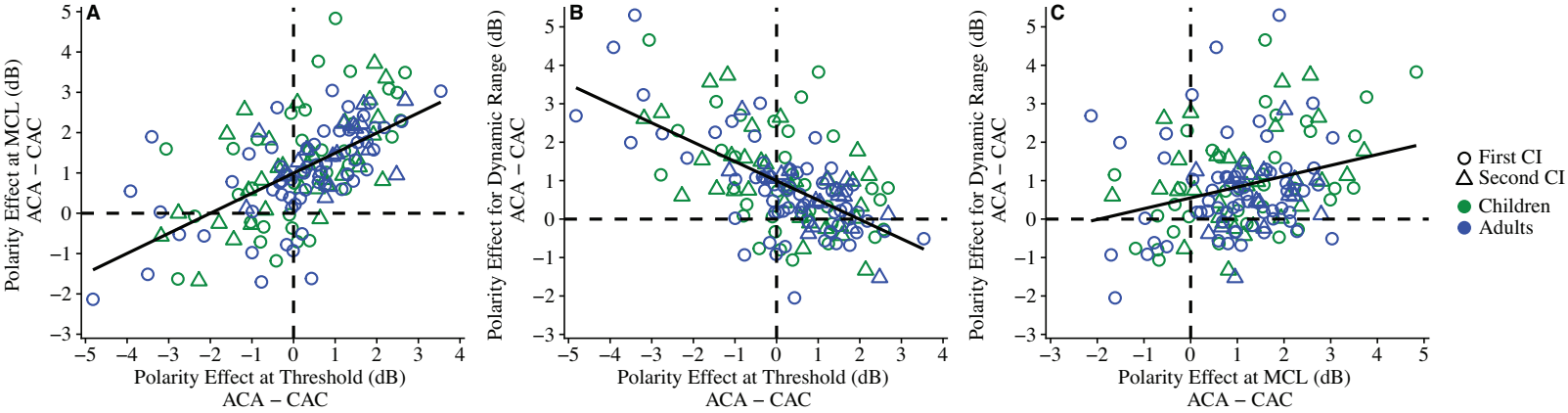

Figure 5.2. Electrode-specific data for the relationships between A) polarity effect at threshold and at most comfortable listening level (MCL), B) polarity effect at threshold and for dynamic range (DR), and C) polarity effect at MCL and for DR. Dashed lines split each panel into four quadrants at y = 0 and x = 0. Data points that fall in the upper right-hand quadrants and in the lower left-hand quadrants have the same sign (positive or negative, respectively) for both of the measures represented in the figure. Circles indicate data from first-implanted ears and triangles represent data from second-implanted ears. Green symbols indicate data from children, whereas blue symbols indicate data from adults. CI: cochlear implant.

Polarity effects at threshold, MCL and DR were highly correlated. Therefore, to statistically analyze the relationships between each measure, it was necessary to specify separate

mixed-effects models. A Bonferroni adjustment for multiple comparisons was applied (adjusted $\alpha = 0.017$). The polarity effect at threshold was positively correlated with the polarity effect at MCL ($R^2_{\text{marginal}} = 0.42$, $R^2_{\text{conditional}} = 0.67$, $F(1,139.27) = 132.78$, $p < 0.001$), wherein large, positive polarity effects at threshold (i.e., lower thresholds for the anodic polarity) were associated with large, positive polarity effects at MCL (i.e., lower MCLs for the anodic polarity). This suggests that, in general, electrodes that had better threshold sensitivity to the anodic polarity also had better suprathreshold sensitivity to the anodic polarity.

Furthermore, the polarity effect at threshold was negatively correlated with the DR polarity effect ($R^2_{\text{marginal}} = 0.27$, $R^2_{\text{conditional}} = 0.60$, $F(1,139.27) = 74.22$, $p < 0.001$). Specifically, larger polarity effects at threshold (i.e., lower thresholds for the anodic polarity) were associated with smaller DR polarity effects (i.e., larger DR for the anodic polarity). This suggests that, on average, electrodes with better sensitivity (i.e., lower thresholds) to the anodic polarity also had larger DRs for anodic than for cathodic pulse shapes. However, many data points (42.28%) fall in the upper right-hand quadrant of Figure 5.2B. Electrodes in the upper right-hand quadrant have larger DRs for the cathodic polarity (i.e., positive DR polarity effect), despite having lower (i.e., better) thresholds for the anodic polarity.

Finally, the polarity effect at MCL was positively correlated with the DR polarity effect ($R^2_{\text{marginal}} = 0.06$, $R^2_{\text{conditional}} = 0.23$, $F(1,119.02) = 8.33$, $p = 0.005$). Large polarity effects at MCL (i.e., lower MCLs for the anodic compared to the cathodic polarity) were associated with large DR polarity effects (i.e., smaller DRs for the anodic polarity compared to the cathodic polarity). The DR in response to each polarity was influenced by both the threshold and the MCL. However, better sensitivity at threshold or MCL for a particular polarity did not necessarily mean

that the DR was larger in response to that polarity. On some electrodes, low MCLs for the anodic polarity may restrict the anodic DR relative to the cathodic DR.

5.4.3 *Polarity Sensitivity as a Function of Channel Classification*

The second analysis evaluated differences in polarity sensitivity as a function of channel classification (low- versus high-threshold). Recall that the polarity effect was measured on two non-adjacent low-threshold channels and two non-adjacent high-threshold channels in each ear. Channels were selected based on the relative within-subject magnitude of electrode-specific focused behavioral thresholds. Once again, during the model selection procedure, it was determined that polarity sensitivity as a function of channel classification did not differ between children and adults and that including "age group" in the models resulted in poorer fits (i.e., higher AICc values). Thus, the final models for this analysis did not include "age group" as an independent variable.

Figure 5.3 shows the electrode-specific polarity effect as a function of channel classification (low-threshold versus high-threshold) for A) the polarity effect at threshold, B) the polarity effect at MCL, and C) the DR polarity effect. Since the polarity effects at threshold, MCL and DR are highly correlated, separate mixed-effects models were specified to assess differences in each measure as a function of channel classification. A Bonferroni adjustment for multiple comparisons was applied (adjusted $\alpha = 0.017$). On high-threshold channels, the polarity effect at threshold ranged from -3.20 dB to 2.90 dB ($M = 0.61$ dB, $SD = 1.21$ dB). On low-threshold channels, the polarity effect at threshold ranged from -4.82 dB to 3.54 dB ($M = -0.11$ dB, $SD = 1.71$ dB). High-threshold channels had significantly larger polarity effects, on average, than low-threshold channels (Figure 5.3A; $R^2_{\text{marginal}} = 0.07$, $R^2_{\text{conditional}} = 0.29$, $F(1,122) = 12.97$, $p < 0.001$).

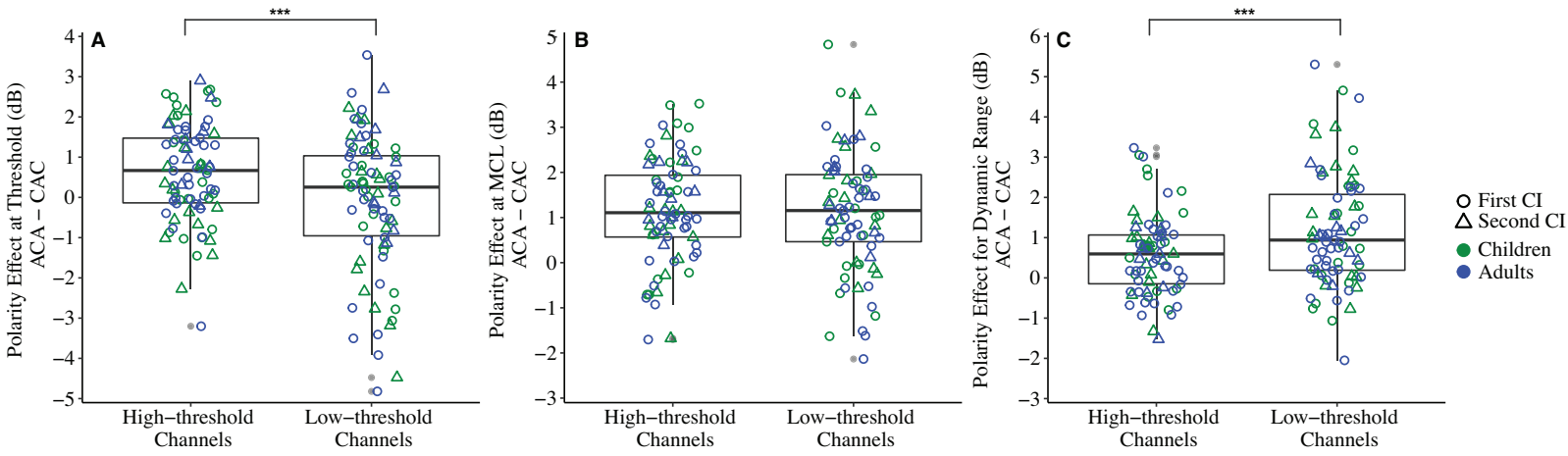

Figure 5.3. Electrode-specific polarity effect as a function of channel classification (high-focused-threshold versus low-focused-threshold) for A) the polarity effect at threshold, B) the polarity effect at most comfortable listening level (MCL), and C) the polarity effect for dynamic range (DR). Circles indicate data from first-implanted ears and triangles represent data from second-implanted ears. Green symbols indicate data from children, whereas blue symbols indicate data from adults. CI: cochlear implant. *** denotes a statistically significant difference in polarity effect between high- and low-threshold channels at the $p < 0.001$ level.

However, the polarity effect at MCL did not differ between high- and low-threshold channels (Figure 5.3B; $R^2_{marginal} < 0.01$, $R^2_{conditional} = 0.44$, $F(1,110.71) = 0.05$, $p = 0.83$). On high-threshold channels, the polarity effect at MCL ranged from -1.70 dB to 3.52 dB ($M = 1.14$ dB, $SD = 1.16$ dB). On low-threshold channels, the polarity effect at MCL ranged from -2.13 dB to 4.83 dB ($M = 1.11$ dB, $SD = 1.33$ dB).

Finally, the DR polarity effect was larger for low-threshold channels than for high-threshold channels (Figure 5.3C; $R^2_{marginal} = 0.05$, $R^2_{conditional} = 0.30$, $F(1,110.4) = 11.11$, $p = 0.001$). In other words, low-threshold channels tended to have larger DRs for the cathodic polarity than for the anodic polarity. On high-threshold channels, the DR polarity effect ranged from -1.52 dB to 3.23 dB ($M = 0.58$ dB, $SD = 1.00$ dB). On low-threshold channels, the DR

polarity effect ranged from -2.04 dB to 5.30 dB (M = 1.15 dB, SD = 1.40 dB). Although the polarity effect at threshold and the DR polarity effect differed significantly between high- and low-threshold channels, note that there is substantial variability in both outcome measures, irrespective of channel classification.

5.4.4 *Across-site Average Polarity Effect, Demographics, and Speech Perception*

The final analyses assessed the relationships between the across-site average polarity effect at threshold, demographic information (age and duration of deafness), and speech perception. The across-site average polarity effect was calculated by averaging the polarity effects at threshold across the four tested electrodes within each ear. This across-site averaging method has been used in several studies to quantify and relate electrode-specific measures to demographic characteristics (e.g., DeVries et al. 2016; Schvartz-Leyzac & Pfingst 2016, 2018; Scheperle 2017; Jahn & Arenberg 2019). During the model selection procedure, it was determined that more parsimonious model fits (i.e., lower AICc values) were obtained when "age group" (children versus adults) was included in the model instead of "chronological age". This is likely because chronological age was bimodally distributed in this sample.

Figure 5.4 shows the across-site average polarity effects at threshold for the children and adults. Table 5.2 shows the across-site average polarity effects for each ear tested. A mixed-model analysis ($R^2_{marginal}$ = 0.04, $R^2_{conditional}$ = 0.24) revealed that the polarity effect at threshold did not vary as a function of age group ($F(1, 27.00) = 0.03$, $p > 0.05$) or duration of deafness ($F(1, 32.14) = 0.99$, $p > 0.05$). There was substantial variability in the across-site average polarity effect for both groups of subjects. For the children, the polarity effect at threshold ranged from -4.48 dB to 2.68 dB (M = 0.13 dB, SD = 1.51 dB). For the adults, the polarity effect at threshold ranged from -4.82 dB to 3.54 dB (M = 0.36 dB, SD = 1.53 dB).

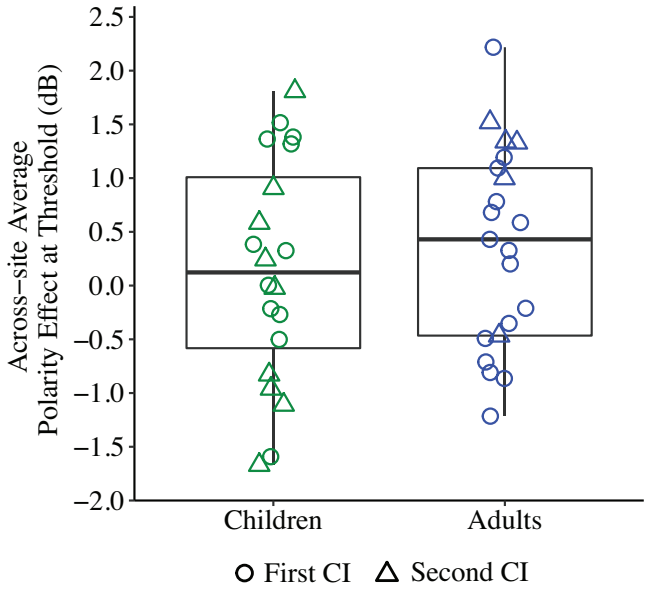

Figure 5.4. Across-site average polarity effects at threshold (in dB) for the children and adults. Circles indicate data from first-implanted ears and triangles represent data from second-implanted ears. CI: cochlear implant.

Table 5.2. Across-site average polarity effects at threshold (in dB) for all ears tested. Average polarity effects are shown for the two low-threshold channels, the two high-threshold channels, and all four channels combined. Low-threshold channels refer to the two non-adjacent channels with the lowest focused behavioral thresholds within an individual ear. High-threshold channels refer to the two non-adjacent channels with the highest focused behavioral thresholds within an individual ear. Focused thresholds were measured with a steered quadrupolar electrode configuration (focusing coefficient = 0.9). CI: cochlear implant

	First CI			Second CI		
ID	Low-threshold Channels M (*SD*)	High-threshold Channels M (*SD*)	All Channels M (*SD*)	Low-threshold Channels M (*SD*)	High-threshold Channels M (*SD*)	All Channels M (*SD*)
Children						
P02	0.80 (*0.29*)	1.93 (*0.80*)	1.36 (*0.81*)	2.08 (*0.19*)	1.53 (*0.42*)	1.81 (*0.42*)
P03	0.56 (*0.93*)	2.47 (*0.15*)	1.51 (*1.23*)	1.36 (*0.25*)	0.45 (*1.59*)	0.91 (*1.07*)
P04	0.86 (*0.67*)	-0.21 (*0.83*)	0.32 (*0.87*)	-0.06 (*0.99*)	-1.86 (*0.59*)	-0.96 (*1.23*)
P06	1.02 (*0.32*)	-1.01 (*0.02*)	0.00 (*1.19*)	-2.49 (*0.99*)	0.83 (*1.70*)	-0.82 (*2.22*)
P07	-2.05 (*1.03*)	1.05 (*0.53*)	-0.50 (*1.91*)	-2.18 (*0.82*)	-0.04 (*0.32*)	-1.11 (*1.34*)
P09	-0.57 (*0.21*)	0.03 (*0.09*)	-0.27 (*0.37*)	1.01 (*1.29*)	-1.05 (*0.05*)	-0.02 (*1.40*)
P11	-2.72 (*0.49*)	-0.46 (*0.57*)	-1.59 (*1.37*)	-0.30 (*1.23*)	1.47 (*0.95*)	0.58 (*1.36*)
P12	0.43 (*0.11*)	2.34 (*0.43*)	1.38 (*1.13*)	-3.41 (*1.51*)	0.07 (*0.90*)	-1.67 (*2.25*)
P13	0.23 (*0.04*)	-0.66 (*1.11*)	-0.21 (*0.83*)	--	--	--
P16	0.15 (*0.18*)	2.49 (*0.27*)	1.32 (*1.36*)	-0.07 (*0.74*)	0.55 (*0.29*)	0.24 (*0.58*)
P17	0.36 (*0.05*)	0.41 (*0.61*)	0.38 (*0.35*)	--	--	--
Mean (*SD*)	-0.08 (*1.22*)	0.76 (*1.35*)	0.34 (*0.99*)	-0.45 (*1.87*)	0.21 (*1.11*)	-0.12 (*1.12*)
Adults						
S22	-2.70 (*1.73*)	0.97 (*0.66*)	-0.87 (*2.37*)	--	--	--
S23	-0.69 (*0.54*)	-1.74 (*2.07*)	-1.22 (*1.37*)	-0.98 (*0.22*)	0.05 (*0.37*)	-0.47 (*0.64*)
S29	0.41 (*1.06*)	0.95 (*0.50*)	0.68 (*0.74*)	-0.03 (*0.20*)	2.69 (*0.30*)	1.33 (*1.58*)
S39	0.55 (*0.32*)	0.62 (*0.44*)	0.59 (*0.31*)	1.27 (*0.32*)	1.41 (*0.30*)	1.34 (*0.27*)
S40	2.86 (*0.96*)	1.58 (*0.13*)	2.22 (*0.93*)	--	--	--
S43	-0.03 (*0.66*)	-0.39 (*0.54*)	-0.21 (*0.53*)	--	--	--
S45	0.21 (*0.06*)	1.36 (*0.06*)	0.78 (*0.67*)	2.19 (*0.71*)	0.85 (*0.13*)	1.52 (*0.87*)
S46	0.28 (*0.47*)	0.12 (*0.23*)	0.20 (*0.32*)	--	--	--
S47	2.22 (*0.54*)	0.17 (*0.79*)	1.19 (*1.31*)	--	--	--
S49	-2.45 (*0.42*)	1.03 (*0.38*)	-0.71 (*2.03*)	0.37 (*0.71*)	1.63 (*0.26*)	1.00 (*0.85*)
S50	-1.97 (*2.04*)	0.98 (*1.10*)	-0.49 (*2.16*)	--	--	--
S52	-0.64 (*0.51*)	-0.06 (*0.14*)	-0.35 (*0.45*)	--	--	--
S53	1.26 (*0.99*)	0.93 (*1.06*)	1.09 (*0.86*)	--	--	--
S54	-1.91 (*4.12*)	0.29 (*0.53*)	-0.81 (*2.71*)	--	--	--
S59	-0.98 (*3.56*)	1.84 (*0.11*)	0.43 (*2.62*)	--	--	--
S60	1.22 (*0.16*)	-0.57 (*0.59*)	0.33 (*1.09*)	--	--	--
Mean (*SD*)	-0.15 (*1.61*)	0.50 (*0.91*)	0.17 (*0.92*)	0.56 (*1.21*)	1.33 (*0.98*)	0.94 (*0.81*)

Notably, duration of deafness varied widely for the adults (range = 3.9 to 53.0 years), and less so for the children (range = 1.0 to 10.1 years). We also previously showed that the polarity effect at threshold differs between low- and high-threshold channels. So, we subsequently evaluated the relationship between duration of deafness and the across-site average polarity effect separately for each age group and for each channel classification.

Figure 5.5(A-B) shows the relationship between duration of deafness and the across-site average polarity effect on high-threshold channels for A) the children, and B) the adults. On high-threshold channels, the average polarity effect increased with increasing durations of deafness for the adults ($R^2_{marginal} = 0.28$, $R^2_{conditional} = 0.46$; $F(1, 15.53) = 7.31$, $p = 0.016$; Bonferroni-adjusted $\alpha = 0.025$), but not for the children ($R^2_{marginal} = 0.02$, $R^2_{conditional} = 0.15$; $F(1, 13.43) = 0.50$, $p = 0.49$). On low-threshold channels, the polarity effect did not vary as a function of duration of deafness for either group (ps > 0.05).

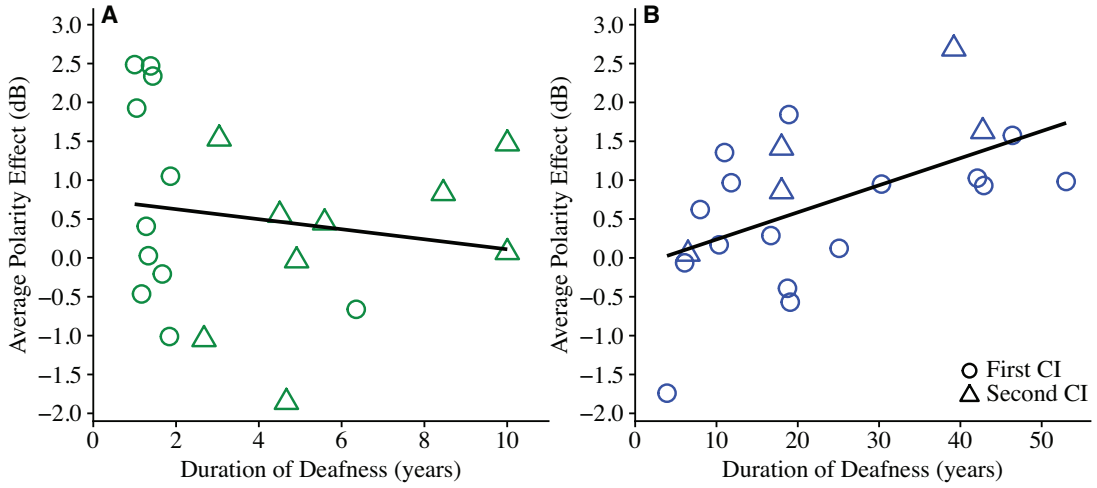

Figure 5.5. Across-site average polarity effect (in dB) as a function of duration of deafness (in years) on high-focused-threshold channels for A) the children, and B) the adults. Circles indicate data from first-implanted ears and triangles represent data from second-implanted ears. CI: cochlear implant.

Finally, relationships between speech perception, the across-site average polarity effect at threshold, and demographic variables were evaluated. Speech perception scores, in percent correct, are presented in Table 5.3. Percent correct scores were converted to rationalized arcsine units (RAUs) prior to statistical analysis to normalize error variance (Studebaker 1985). The mixed-effects models predicting phoneme perception included fixed effects for across-site average polarity effect, age group, and duration of deafness (vowels: $R^2_{marginal} = 0.23$, $R^2_{conditional} = 0.74$; consonants: $R^2_{marginal} = 0.22$, $R^2_{conditional} = 0.71$). Neither vowel nor consonant perception were predicted by the across-site average polarity effect (ps > 0.05; vowels: $F(1, 26.96) = 2.22$; consonants: $F(1, 26.24) = 1.29$) or age group (ps > 0.05; vowels: $F(1, 27.21) = 1.83$; consonants: $F(1, 24.52) = 2.12$). However, duration of deafness was inversely related to vowel ($F(1, 33.82) = 9.93$, $p = 0.003$) and consonant ($F(1, 30.74 = 9.36$, $p = 0.005$) perception. Figure 5.6(A-B) shows A) vowel perception, and B) consonant perception as a function of duration of deafness. Both vowel and consonant perception decreased with increasing duration of pre-implantation auditory deprivation. As before, relationships between speech perception and the across-site average polarity effect were also assessed separately for high- and low-threshold channels; however, the relationship between speech perception and polarity sensitivity did not differ as a function of channel classification (ps > 0.05).

Table 5.3. Vowel and consonant perception scores (in % correct) for all ears tested. Stimuli were presented in quiet at a level of 60 dB-A. CI: cochlear implant

	Vowel Scores (% correct)		Consonant Scores (% correct)	
ID	First CI	Second CI	First CI	Second CI
Children				
P02	97	100	79	84.5
P03	93.5	100	82	82
P04	96.5	97	77	86.5
P06	100	93	--	--
P07	98.5	96	95	72
P09	83	91.5	83	80
P11	63.5	22	60.5	17
P12	53.5	21.5	52	21.7
P13	98.5	--	77	--
P16	90	95	95	75
P17	93.5	--	63.3	--
Mean	88.0	79.4	76.5	64.9
(*SD*)	(*15.5*)	(*32.8*)	(*14.3*)	(*28.4*)
Adults				
S22	96.5	--	80	--
S23	95	87.7	74	75
S29	92	92.3	79	74
S39	100	95	92	91
S40	48	--	35	--
S43	67.7	--	80	--
S45	100	100	80	80
S46	55	--	31	--
S47	100	--	90	--
S49	41	88	41	44
S50	53.3	--	51	--
S52	82	--	55	--
S53	90	--	81	--
S54	98.5	--	85.5	--
S59	90	--	77	--
S60	45	--	41	--
Mean	78.4	92.6	67.0	72.8
(*SD*)	(*22.5*)	(*5.1*)	(*20.9*)	(*17.5*)

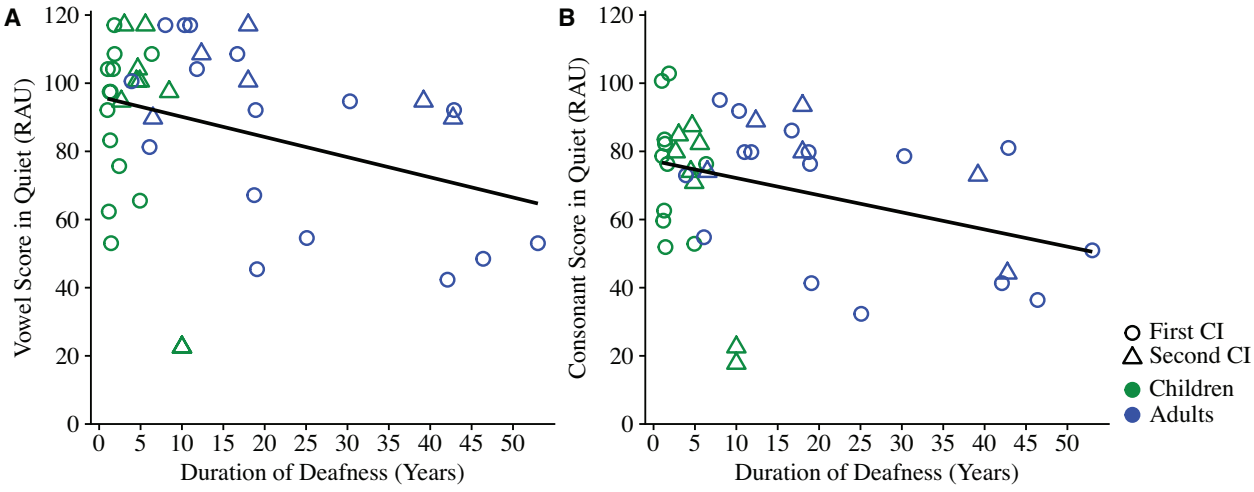

Figure 5.6. A) vowel perception (RAUs), and B) consonant perception (RAUs) as a function of duration of deafness (in years). Circles indicate data from first-implanted ears and triangles represent data from second-implanted ears. Green symbols indicate data from children, whereas blue symbols indicate data from adults. CI: cochlear implant

5.5 Discussion

Modeling evidence suggests that sensitivity to electrical stimulus polarity may reflect the health of the peripheral processes in CI listeners (Rattay et al. 2001a,b; Joshi et al. 2017; Resnick et al. 2018). Specifically, better sensitivity to anodic (positive) current than to cathodic (negative) current may indicate some degree of peripheral process degeneration. The primary aim of this study was to characterize polarity sensitivity in a diverse sample of CI listeners, including children and adults, and to determine the relationship between polarity sensitivity and traditional CI outcome measures. Interestingly, although most electrodes showed better sensitivity to the anodic polarity at threshold and at MCL, the psychophysical DR of the cathodic polarity was often larger than that of the anodic polarity. Polarity sensitivity varied widely within- and across-listeners and did not differ between children and adults. Across subjects, phoneme perception performance was predicted by duration of deafness, but not by polarity sensitivity. Moreover,

polarity sensitivity at threshold was related to duration of deafness in the adults, but not in the children. Subject- and electrode-dependent differences in polarity sensitivity may be useful in customizing programming interventions for CI listeners with a variety of hearing histories.

5.5.1 *Polarity Sensitivity at Threshold and at Supra-threshold Levels*

The primary outcome measure in this study was the psychophysical polarity effect at threshold, which has been hypothesized to reflect local peripheral process integrity (Macherey et al. 2017; Carlyon et al. 2018; Jahn & Arenberg 2019) and to vary independently of electrode position and intracochlear resistance in CI listeners (Jahn & Arenberg 2019). The polarity effect was defined as the difference in electrode-specific behavioral thresholds measured in response to cathodic (ACA) and anodic (CAC) pulse shapes (ACA – CAC). Our data suggest that the polarity effect at threshold is subject- and electrode-dependent in a large sample of CI listeners (n = 41 ears) with diverse hearing histories, including children and adults. These findings are consistent with previous studies in small samples of post-lingually deafened adults (Macherey et al. 2017; Carlyon et al. 2018; Jahn & Arenberg 2019).

In the present sample, the majority of electrodes (62.20%) showed better threshold sensitivity to the anodic polarity than to the cathodic polarity (i.e., positive polarity effects). Based on modeling data, the proportion of electrodes with better threshold sensitivity to the anodic polarity than to the cathodic polarity would reflect the proportion of fibers with some degree of peripheral process degeneration or demyelination (Rattay et al. 2001a,b; Joshi et al. 2017; Resnick et al. 2018). This theory assumes that the site of spike initiation differs for anodic and cathodic current. At low current levels, maximum depolarization occurs near the periphery in response to cathodic stimulation, leading to relative hyperpolarization in more central regions

of the neuron. The inverse occurs for anodic stimulation, wherein maximal depolarization occurs closer to the central axon.

When the peripheral processes have demyelinated or degenerated, cathodic stimulation must overcome the unmyelinated cell body and a region of central hyperpolarization in order to generate an action potential. Thus, high current levels are necessary in order to generate an action potential in response to cathodic stimulation in a degenerated neuron. Conversely, thresholds in response to anodic stimulation should remain lower than those in response to cathodic stimulation in a peripherally-degenerated neuron. Relatively low thresholds in response to the anodic polarity are expected because the action potential would not need to overcome the unmyelinated cell body or a region of strong hyperpolarization to excite the central axon (Rattay et al. 2001a,b; Joshi et al. 2017; Resnick et al. 2018). If polarity sensitivity does reflect peripheral process integrity in humans, then our data indicate that some degree of peripheral degeneration is likely to occur near most electrode sites in CI listeners with profound deafness.

Our results also indicated that the polarity effect at threshold is larger (i.e., more positive) on channels with relatively high focused behavioral thresholds compared to those with lower behavioral focused thresholds. Focused thresholds are believed to reflect the overall quality of the electrode-neuron interface, which is influenced by electrode position (Long et al. 2014; DeVries et al. 2016; DeVries & Arenberg 2018a), intracochlear bone and tissue growth (Spelman, 1982; Jahn & Arenberg 2019), and the integrity of the auditory neurons (Goldwyn et al. 2010). Channels with high focused thresholds are believed to interface relatively poorly with the auditory nerve, as they are often located far from target neurons (Long et al., 2014; DeVries et al., 2016; DeVries & Arenberg, 2018a; Jahn & Arenberg 2019) and have small evoked potential amplitudes and steep growth functions (Bierer et al. 2011; DeVries et al. 2016).

It is unlikely that the polarity effect at threshold was influenced by electrode position relative to the modiolus or intracochlear resistance. In a sample of 11 adult CI listeners, Jahn and Arenberg (2019) demonstrated that the electrode-specific polarity effect at threshold varies independently of electrode position relative to the modiolus and intracochlear resistance. They also showed that, across listeners, the polarity effect at threshold predicted focused behavioral thresholds (sQP; focusing coefficient = 0.9), wherein relatively high focused thresholds were associated with relatively large, positive polarity effects.

The present results agree with those of Jahn and Arenberg (2019), demonstrating that high-threshold channels are more likely, on average, to have large, positive polarity effects than low-threshold channels. We also show that this finding is consistent across a relatively large group of participants with diverse hearing histories. However, it should be noted that although the polarity effect at threshold differed significantly between high- and low-threshold channels, there was substantial variability in the magnitude of the polarity effect, irrespective of channel classification.

Some of the observed variability in polarity sensitivity likely results from the channel selection procedure. Channels were selected based on the relative magnitude of within-subject focused thresholds; that is, two low-threshold channels and two high-threshold channels were selected for polarity effect testing in each ear. It is likely that focused thresholds on many of the selected electrodes were low or high as a result of electrode position and/or intracochlear bone and tissue growth, and not necessarily because of the local status of the auditory nerve (Long et al. 2014; DeVries et al., 2016; DeVries & Arenberg 2018a; Jahn & Arenberg 2019). Regardless, our results still show that channels that are estimated to interface poorly with the auditory nerve are more likely to have large, positive polarity effects than channels with better interfaces. This

provides additional evidence that polarity sensitivity reflects an underlying characteristic of the electrode-neuron interface that may be related to SGN integrity in children and adults with CIs.

If polarity sensitivity reflects peripheral process degeneration, it may have utility in customizing CI programming parameters. Taken together, the results from the present study and from Jahn and Arenberg (2019) imply that a comprehensive approach that considers electrode position and polarity sensitivity may help in selecting channels for deactivation or current focusing. DeVries and Arenberg (2018b) demonstrated that some listeners receive speech perception benefit when a subset of electrodes that are located far from their target neurons are stimulated using a spatially-focused electrode configuration; however, some listeners did not benefit, or performed worse, with that type of listening strategy. Others have shown that deactivating channels that are estimated to interface poorly with the auditory nerve improves speech perception scores for some listeners, but not others (Bierer & Litvak 2016; Noble et al. 2013, 2014, 2016; Zhou 2017).

An individualized CI programming approach that considers estimates of electrode position and neural health may be ideal. For example, it may be desirable to implement current focusing on an electrode that is located far from its target neurons, but that has a small, or negative, polarity effect at threshold (possibly indicating that the target neurons are healthy). On the other hand, it may be best to deactivate or employ an anodic pulse shape on an electrode with a large, positive polarity effect at threshold (possibly indicating local peripheral degeneration). Our results, and others (e.g., Noble et al. 2016), indicate that this combined programming approach could be assessed in both children and adults with CIs.

In addition to the primary outcome measure (polarity effect at threshold), we also assessed the polarity effect at MCL and differences in DR as a function of polarity. A vast majority of electrodes tested (89.26%) had a positive polarity effect at MCL, or better sensitivity to the anodic than to the cathodic polarity. This is consistent with prior studies showing that MCLs are often lower for anodic than for cathodic pulse shapes in post-lingually deafened adults (Carlyon et al. 2013; Macherey et al. 2006, 2008, 2017). These findings also align with modeling data suggesting a peripheral-to-central shift in the site of spike initiation for cathodic stimulation at high current levels (Rattay et al., 2001a,b; Joshi et al. 2017; Resnick et al. 2018). The present results further demonstrate that variability in the polarity effect at MCL is observed in both children and adults with CIs.

If the majority of electrodes are more sensitive at threshold and at MCL to the anodic polarity than to the cathodic polarity, it may be assumed that the DR is simply shifted downward for anodic stimulation. However, although correlated, the magnitude and sign of the polarity effect at threshold did not necessarily correspond to that at MCL. This suggests that DR may also differ between anodic and cathodic polarities in an electrode-dependent manner. In fact, despite generally lower sensitivity for anodic stimuli at threshold and at MCL, DR remained larger for cathodic pulse shapes on most electrodes (77.18%). Macherey et al. (2017) demonstrated that loudness tends to grow less steeply as a function of current level for cathodic pulse shapes than for anodic pulse shapes. Thus, if loudness grows less steeply for cathodic than for anodic stimulation, larger DRs would generally be expected for cathodic pulse shapes.

Electrode-dependent differences in DR as a function of polarity may have applications to CI programming. There is evidence that CI listeners programmed with larger electrical DRs have better speech perception scores (Zeng & Galvin 1999; Fu & Shannon 2000; Loizou et al. 2000;

Bento et al. 2005) and better binaural sensitivity (Todd et al. 2017) than those with smaller electrical DRs. It is possible that a pulse shape that maximizes DR on an electrode-specific basis may assist in optimizing programming recommendations for individual CI listeners. For instance, anodic pulse shapes could be implemented on channels with large anodic DRs, and cathodic pulse shapes on electrodes with large cathodic DRs. Our results suggest that novel programming interventions based on polarity sensitivity may be attempted in individuals with a variety of hearing histories, including children and adults.

5.5.2 *Polarity Sensitivity as a Function of Age and Duration of Deafness*

Another primary hypothesis of the present study was that children would have smaller (i.e., more negative) polarity effects at threshold than adults. This prediction was based on human temporal bone literature, and limited behavioral and electrophysiological evidence. Post-mortem temporal bone studies demonstrate a reduction in SGN density with increasing age and duration of hearing loss (Otte et al. 1978; Nadol et al. 1989; Nadol 1997; Makary et al. 2011). Histopathological data also show that hearing loss etiology is a strong predictor of SGN density in humans (Otte et al. 1978; Nadol et al. 1989; Nadol 1997). Etiology often differs between individuals who are deafened during childhood, and those who are deafened as adults. Available behavioral and electrophysiological evidence supports the temporal bone findings, suggesting that children with CIs have lower focused behavioral thresholds (DiNino et al. 2019) and steeper evoked potential amplitude growth functions (Brown et al. 2010) than adults. For these reasons, we predicted that children with CIs would experience less peripheral process degeneration than adult CI listeners and that this would be reflected in larger, more positive polarity effects in the adults.

However, results demonstrated that the polarity effect at threshold did not differ between the children and adults in this study. Instead, substantial variability in the polarity effect was observed across all subjects and electrodes. If polarity sensitivity does reflect peripheral process integrity, this may suggest that both children and adults with CIs experience some degree of peripheral degeneration, even if they are implanted early in life. This finding is consistent with the fact that all participants presented with a damaged auditory system secondary to severe-to-profound sensorineural hearing loss. SGN degeneration begins at the peripheral processes and progresses centrally, so some degree of peripheral degeneration should be expected in individuals with profound deafness (Johnsson 1974). Moreover, the temporal bone studies and the limited in vivo evidence that informed the initial hypothesis evaluated SGN density rather than peripheral process integrity. It is possible that peripheral process degeneration occurs to some degree in both groups, but that SGN density has not declined as much in the children. Future studies will investigate this distinction.

We also hypothesized that individuals with longer periods of auditory deprivation prior to implantation would have larger, more positive polarity effects than those with shorter durations of deafness. This hypothesis was confirmed on high-threshold channels for adults, but not for children. Duration of deafness did not relate to polarity sensitivity on low-threshold channels in either group of subjects. This finding is somewhat consistent with Jahn and Arenberg (2019), who demonstrated that the across-site average polarity effect was larger in adults with relatively long pre-implantation durations of deafness. However, in that study, the polarity effect was averaged across all 16 electrodes in each ear. In the present study, the polarity effect was only assessed on four electrodes per ear. It is likely that high-threshold channels reflect greater degradation in the quality of the electrode-neuron interface relative to low-threshold channels

(reviewed by Bierer 2010). This may explain why polarity sensitivity on low-threshold channels was not associated with duration of deafness.

It is possible that the children in the present study did not vary widely enough in duration of deafness to capture its relationship with polarity sensitivity. Many of the pediatric ears were implanted early in life and the longest duration of deafness in that group was 10.1 years. In contrast, the adults ranged in duration of deafness from 3.9 to 53 years. However, despite the children's limited range of pre-implantation auditory deprivation, they still presented with substantial variability in polarity sensitivity. It may be that hearing loss etiology is a more important predictor of polarity sensitivity than age or duration of deafness, as etiology is strongly associated with SGN survival in human temporal bone analyses (Otte et al. 1978; Nadol et al. 1989; Nadol 1997). Unfortunately, the majority of our participants presented with unknown etiologies, so the effect of etiology on polarity sensitivity could not be evaluated here. Future investigations should attempt to recruit participants with known hearing loss etiologies.

5.5.3 *Phoneme Perception is Related to Duration of Deafness, but not to Polarity Sensitivity*

A final goal of the present study was to evaluate the relationship between polarity sensitivity and phoneme perception scores. We hypothesized that individuals with large, positive polarity effects at threshold would have poorer phoneme perception scores than individuals with smaller, more negative polarity effects at threshold. Contrary to this prediction, the across-site average polarity effect at threshold was not related to either vowel or consonant perception. Instead, phoneme perception was predicted by duration of deafness. Individuals with relatively short pre-implantation periods of auditory deprivation tended to have better phoneme perception scores than individuals with longer durations of deafness. The observed relationship between duration

of deafness and speech perception is consistent across many investigations (e.g., Green et al. 2007; Lazard et al. 2012; Blamey et al. 2013; Holden et al. 2013). Changes in the central auditory system as a consequence of auditory deprivation that are not captured by peripheral measures likely play an important role in CI outcomes.

Importantly, relationships between indirect estimates of SGN health and speech perception are largely inconsistent across studies. Histopathological studies have failed to demonstrate consistent, positive relationships between post-mortem SGN density and speech perception scores assessed during life (Otte et al. 1978; Nadol et al. 2001; Khan et al. 2005; Fayad & Linthicum 2006). A few evoked potential analyses have demonstrated that larger peak amplitudes (DeVries et al. 2016; Scheperle 2017) and steeper growth function slopes (Brown et al. 1990; Kim et al. 2010) are associated with better speech perception scores. For bilateral CI listeners, between-ear differences in evoked potential measures (Schvartz-Leyzac & Pfingst 2018) and in multipulse integration abilities (Zhou & Pfingst 2014) may be predictive of between-ear differences in speech perception abilities. However, there are also many studies that have not observed relationships between evoked potential measures and speech perception outcomes (e.g., Franck & Norton 2001; Turner et al. 2002; Cosetti et al. 2010).

If SGN integrity plays a role in CI performance, the relationship is likely complex and extends beyond measuring speech perception scores. In fact, modeling data suggest that speech perception tasks may not be the optimal psychophysical tools for assessing the effects of modest peripheral degeneration on auditory perception with a CI. Resnick et al. (2018) proposed that mild to moderate peripheral degeneration would not influence perception of relevant speech features, which are generally longer than 20 ms in duration. Instead, modest demyelination is expected to alter coding of fine temporal cues, such as those needed to detect interaural timing

differences (ITDs). An ITD-based sound localization task might be more appropriate than speech perception for probing the behavioral implications of peripheral degeneration.

Moreover, if polarity sensitivity reflects peripheral degeneration in CI listeners, it is still unclear what magnitude of polarity effect would be detrimental to auditory perception. Only extreme demyelination leads to pathological current spread and recruitment in some biophysical models (Resnick et al. 2018). In humans, substantial peripheral demyelination might be necessary to incur a measurable impact on auditory perception. In the presence of mild to moderate degeneration, neural status alone may be insufficient for explaining perceptual CI outcomes.

5.5.4 *Concluding Remarks*

The wide variability in CI outcomes is likely due, in part, to within- and between-listener variation in the quality of the electrode-neuron interface. SGN integrity may contribute to the efficacy with which a CI electrode interfaces with the auditory nerve; however, it is difficult to estimate neural health in humans. The present study characterized polarity sensitivity, a proposed estimate of peripheral process integrity, in children and adults with CIs. We demonstrated that, if polarity sensitivity reflects neural health in CI listeners, then both children and adults with CIs likely experience some degree of peripheral degeneration, even if implanted early. Future endeavors to apply polarity sensitivity to the study of individualized programming strategies should incorporate both pediatric and adult listeners.

Subsequent investigations may attempt to use polarity sensitivity, in conjunction with estimates of electrode position, to select appropriate CI electrodes for deactivation and current focusing. It may also be possible to selectively stimulate electrode sites with pulse shapes that

optimize a listener's DR, using differences in DR as a function of stimulus polarity as a guide. We also demonstrated that polarity sensitivity may not predict phoneme perception scores for CI listeners. Instead, future studies, especially those that intend to implement programming adjustments, should consider psychophysical tasks that assess one's ability to process fine temporal cues.

CHAPTER 6. CONCLUSION

Overall, the results of these experiments suggest that some aspects of estimated SGN integrity differ as a function of hearing history in younger and older CI recipients. Since CIs are designed to directly stimulate SGNs, these findings implicate that optimal CI programming interventions may differ for children and adults with CIs. The results of each experiment have laid the groundwork for future investigation into improved patient-specific programming interventions that may benefit CI listeners with diverse hearing histories.

Experiments 1 and 2 demonstrated that young CI listeners who were deafened and implanted during childhood likely have denser populations of viable SGNs than older listeners who were deafened and implanted as adults. Differences in estimated SGN density were consistent across two populations of CI listeners with different device types: Cochlear Ltd. (Experiment 1) and Advanced Bionics (Experiment 2). If children and young adults have relatively dense global SGN populations, they may benefit from CI programming strategies that employ current focusing to reduce channel interaction. In fact, reducing channel interaction through current focusing may be particularly important for pediatric CI listeners. A recent study by Jahn et al. (2019) showed that children with normal hearing receive greater speech perception benefit than adults when simulated channel interaction is reduced.

Furthermore, Experiment 2 demonstrated that the ECAP may be used to identify CI channels within an ear that have relatively good and poor electrode-neuron interfaces. Prior investigations have demonstrated that deactivating channels with relatively poor electrode-neuron interfaces improves speech perception for some adults with CIs (Garadat et al. 2013; Noble et al. 2013, 2014; Bierer & Litvak 2016; Zhou 2017). Only one investigation has assessed a site selection programming intervention in pediatric CI listeners (Noble et al. 2016). Using CT-

estimated metrics of electrode position, Noble et al. (2016) showed that some children benefitted when poorly positioned electrodes were deactivated.

However, the clinical utility of site selection methods used in prior studies is limited, especially in the pediatric population. Due to time or attention constraints, it is often not clinically feasible to assess complex psychophysical percepts on every available electrode. Moreover, CT imaging can be cost prohibitive and necessitates exposure to radiation. The present experiments showed that the ECAP may provide a more clinically feasible objective method for identifying channels to use in site selection programming interventions. Importantly, results suggested that the ECAP is effective at identifying channels with good and poor electrode-neuron interfaces in both pediatric and adult CI listeners. Future studies should investigate the efficacy of site selection programs in children and adults using ECAP measures.

Experiments 3 and 4 assessed estimates of peripheral process integrity (i.e., the polarity effect) in children and adults with CIs. The results of Experiment 3 provided important evidence that the polarity effect varies relatively independently of electrode position within the cochlea and intracochlear resistance in humans. Those findings support the theory that the polarity effect reflects neural health in CI listeners. Accordingly, Experiment 4 evaluated polarity sensitivity in a large sample of children and adults with diverse hearing histories. The results of Experiment 4 demonstrated that, on average, polarity sensitivity does not differ between children and adults with CIs. If polarity sensitivity does reflect the health of the peripheral processes, this could indicate that children with CIs may experience some degree of peripheral degeneration, even if they are implanted early. That conclusion is supported by human temporal bone evidence showing that damage to the dendrites is common in cochlear implantees (Linthicum et al. 1991). Furthermore, because SGN degeneration begins at the dendrites and progresses centrally

(Johnsson 1974), it is likely that many individuals with severe to profound hearing impairment experience some degree of peripheral degeneration.

Thus, the results of Experiment 4 suggest that CI programming interventions based on single-channel polarity effect data should include both children and adults. Experiment 4 also provided insight into potential programming adjustments that should be studied based on channel-to-channel variation in the polarity effect. For instance, results demonstrated that some channels had larger dynamic ranges for anodic stimulation than for cathodic stimulation. In such cases, it is possible that stimulation with an anodic pulse shape instead of a traditional cathodic pulse shape may assist in maximizing a channel's dynamic range. It is also possible that both children and adults can benefit from site selection strategies that deactivate channels with relatively large, positive polarity effects.

The experiments in this dissertation have provided a foundation for future investigation into optimal CI programming strategies for children and adults with CIs. Results demonstrated that young CI listeners who were deafened and implanted during childhood likely have denser populations of SGNs than older adults who were deafened and implanted later in life. However, it is possible that some degree of peripheral degeneration occurs in deaf individuals, regardless of their hearing history. Future studies should build upon the knowledge gained in these experiments by assessing novel current focusing and site selection CI programming strategies that are tailored a listener's hearing history and local characteristics of his or her electrode-neuron interface.

BIBLIOGRAPHY

[1] Abbas, P.J., Brown, C.J., Shallop, J.K., et al. (1999). Summary of results using the Nucleus CI24M implant to record the electrically evoked compound action potential. *Ear Hear, 20*, 45-59.

[2] Bahmer, A., Baumann, U. (2013). Effects of electrical pulse polarity shape on intra cochlear neural responses in humans: Triphasic pulses with cathodic second phase. *Hear Res*, *306*, 123–130.

[3] Bakdash, J.Z., Marusich, L.R. (2017). Repeated measures correlation. *Front Psychol, 8*, 1-13.

[4] Bakdash, J.Z., Marusich, L.R. (2018). rmcorr: Repeated measures correlation. R package version 0.3.0. https://CRAN.R-project.org/package=rmcorr

[5] Bartón, K. (2018). MuMIn: Multi-model inference. R package version 1.42.1. Retrieved August 15, 2018, from http://cran.r-project.org/package=MuMIn

[6] Bates, D., Maechler, M., Bolker, B., et al. (2015). Fitting linear mixed-effects models using lme4. *J Statistical Softw, 67*, 1-48.

[7] Bento, R.F., Neto, R.V.D.B., Castilho, A.M., et al. (2005). Psychoacoustic dynamic range and cochlear implant speech-perception performance in Nucleus 22 users. *Cochlear Implants Int, 6*(sup1), 31-34.

[8] Berenstein, C.K., Mens, L.H.M., Mulder, J.J.S., et al. (2008). Current steering and current focusing in cochlear implants: Comparison of monopolar, tripolar, and virtual electrode configurations. *Ear Hear, 29*, 250-260.

[9] Bierer, J.A. (2007). Threshold and channel interaction in cochlear implant users: Evaluation of the tripolar electrode configuration. *J Acoust Soc Am, 121*, 1642-1653.

[10] Bierer, J.A. (2010). Probing the electrode-neuron interface with focused cochlear implant stimulation. *Trends Amplif, 14*, 84–95.

[11] Bierer, J.A., Faulkner, K.F. (2010). Identifying cochlear implant channels with poor electrode-neuron interface: Partial tripolar, single-channel thresholds and psychophysical tuning curves. *Ear Hear, 31*, 247–258.

[12] Bierer, J.A., Faulkner, K.F., Tremblay, K.L. (2011). Identifying cochlear implant channels with poor electrode-neuron interfaces: Electrically evoked auditory brain stem responses measured with the partial tripolar configuration. *Ear Hear 32*, 436–444.

[13] Bierer, J.A., Nye, A.D. (2014). Comparisons between detection threshold and loudness perception for individual cochlear implant channels. *Ear Hear, 35*, 641–65.

[14] Bierer, J.A., Bierer, S.M., Kreft, H.A., et al. (2015a). A fast method for measuring psychophysical thresholds across the cochlear implant array. *Trends Hear, 19*, 1-12.

[15] Bierer, S.M., Shea-Brown, E., Bierer, J.A. (2015b). Current spread in the cochlea: Insights from CT and electrical field imaging. Poster presented at the Conference on Implantable Auditory Prostheses, Tahoe, CA.

[16] Bierer, J.A., Deeks, J.M., Billig, A.J., et al. (2015c). Comparison of signal and gap -detection thresholds for focused and broad cochlear implant electrode configurations. *J Assoc Res Otolaryngol*, *16*(2), 273–284.

[17] Bierer, J.A., Litvak, L. (2016). Reducing channel interaction through cochlear implant programming may improve speech perception: Current focusing and channel deactivation. *Trends Hear, 20*, 1-12.

[18] Blamey, P., Artieres, F., Baskent, D., et al. (2013). Factors affecting auditory performance of postlinguistically deaf adults using cochlear implants: An update with 2251 patients. *Audiol Neurotol, 18*, 36-47.

[19] Briare, J.J., Frijns, J.H.M. (2000). Field patterns in a 3D tapered spiral model of the electrically stimulated cochlea. *Hear Res, 148*, 18-30.

[20] Brown, C.J., Abbas, P.J., Gantz, B. (1990). Electrically evoked whole-nerve action potentials: Data from human cochlear implant users. *J Acoust Soc Am*, *88*(3), 1385–1391.

[21] Brown, C.J., Abbas, P.J., Etler, C.P., et al. (2010). Effects of long-term use of a cochlear implant on the electrically evoked compound action potential. *J Am Acad Audiol*, *21*(1), 5–15.

[22] Cafarelli Dees, D., Dillier, N., Lai, W.K., et al. (2005). Normative findings of electrically evoked compound action potential measurements using the neural response telemetry of the Nucleus CI24M cochlear implant system. *Audiol Neurotol*, *10*(2), 105–116.

[23] Carlyon, R.P., Deeks, J.M., Macherey, O. (2013). Polarity effects on place pitch and loudness for three cochlear-implant designs and at different cochlear sites. *J Acoust Soc Am, 134*, 503-509.

[24] Carlyon, R.P., Cosentino, S., Deeks, J.M., et al. (2018). Effect of stimulus polarity on detection thresholds in cochlear implant users: Relationships with average threshold, gap detection, and rate discrimination. *J Assoc Res Otolaryngol*. doi: 10.1007/s10162-018 -0677-5

[25] Cohen, J. (1988). Set correlation and contingency tables. *Appl Psychol Meas, 12*, 425 -434.

[26] Cosetti, M.K., Shapiro, W.H., Green, J.E., et al. (2010). Intraoperative neural response telemetry as a predictor of performance. *Otol Neurotol, 31*(7), 1095-1099.

[27] Cords, S.M., Reuter, G., Issing, P.R., et al. (2000). A silastic positioner for a modiolus -hugging position of intracochlear electrodes: Electrophysiologic effects. *Am J Otol, 21*(2), 212-217.

[28] DeVries, L., Scheperle, R., Bierer, J.A. (2016). Assessing the electrode-neuron interface with the electrically-evoked compound action potential, electrode position, and behavioral thresholds. *J Assoc Res Otolaryngo,l 17*, 237–252.

[29] DeVries, L., Arenberg, J.G. (2018a). Psychophysical tuning curves as a correlate of electrode position in cochlear implant listeners. *J Assoc Res Otolaryngol, 19*, 571-587.

[30] DeVries, L., Arenberg, J.G. (2018b). Current focusing to reduce channel interaction for distant electrodes in cochlear implant programs. *Trends Hear*. doi: 10.1177/2331216518813811

[31] Dhanasingh, A., Jolly, C. (2017). An overview of cochlear implant electrode array designs. *Hear Res, 356*, 93-103.

[32] Dietz, A., Wennström, M., Lehtimäki, A., et al. (2016). Electrode migration after cochlear implant surgery: More common than expected? *Eur Arch Otorhinolaryngol, 273*, 1411-1418.

[33] DiNino, M., Wright, R.A., Winn, M.B., et al. (2016). Vowel and consonant confusions from spectrally manipulated stimuli designed to simulate poor cochlear implant electrode-neuron interfaces. *J Acoust Soc Am*, *140*(6), 4404–4418.

[34] DiNino, M., O'Brien, G.E., Bierer, S.M., et al. (2019). The estimated electrode-neuron interface in cochlear implant listeners is different for early-implanted children and late -implanted adults. *J Assoc Res Otolaryngol*, DOI: 10.1007/s10162-019-00716-4.

[35] Eisen, M.D., Franck, K.H. (2004). Electrically evoked compound action potential amplitude growth functions and HiResolution programming levels in pediatric CII implant subjects. *Ear Hear*, *25*(6), 528–538.

[36] Fayad, J.N., Linthicum, F.H. (2006). Multichannel cochlear implants: Relation of histopathology to performance. *Laryngoscope, 116*, 1310-1320.

[37] Finke, M., Büchner, A., Ruigendijk, E., et al. (2016). On the relationship between auditory cognition and speech intelligibility in cochlear implant users: An ERP study. *Neuropsychologia, 87*, 169-181.

[38] Firszt, J.B., Wackym, P.A., Gaggl, W., et al. (2003). Electrically evoked auditory brainstem responses for lateral and medial placement of the Clarion HiFocus electrode. *Ear Hear, 24*, 184-190.

[39] Franck, K.H., Norton, S.J. (2001). Estimation of psychophysical levels using the electrically evoked compound action potential measured with the neural response telemetry capabilities of Cochlear Corporation's CI24M device. *Ear Hear, 22*, 289-299.

[40] Friedland, D.R., Runge-Samuelson, C., Baig, H., et al. (2010). Case-control analysis of cochlear implant performance in elderly patients. *Arch Otolaryngol Head Neck Surg, 136*, 432-438.

[41] Friesen, L.M., Shannon, R.V., Baskent, D., et al. (2001). Speech recognition in noise as a function of the number of spectral channels: comparison of acoustic hearing and cochlear implants. *J Acoust Soc Am, 110*(2), 1150-1163.

[42] Fu, Q.-J., Shannon, R.V. (2000). Effects of dynamic range and amplitude mapping on phoneme recognition in Nucleus 22 cochlear implant users. *Ear Hear, 21*, 227-235.

[43] Garadat, S.N., Zwolan, T.A., Pfingst, B.E. (2013). Using temporal modulation sensitivity to select stimulation sites for processor MAPs in cochlear implant listeners. *Audiol Neurootol, 18*(4), 247-260.

[44] Goldwyn, J.H., Bierer, S.M., Bierer, J.A. (2010). Modeling the electrode-neuron interface of cochlear implants: Effects of neural survival, electrode placement, and the partial tripolar configuration. *Hear Res, 268,* 93-104.

[45] Gordon, K.A., Papsin, B.C., Harrison, R.V. (2004). Toward a battery of behavioral and objective measures to achieve optimal cochlear implant stimulation levels in children. *Ear Hear, 25*, 447-463.

[46] Green, K.M.J., Bhatt, Y.M., Mawman, D.J., et al. (2007). Predictors of audiological outcome following cochlear implantation in adults. *Cochlear Implants Int, 8*(1), 1-11.

[47] Hall, R.D. (1990). Estimation of surviving spiral ganglion cells in the deaf rat using the electrically evoked auditory brainstem response. *Hear Res, 45*, 123-136.

[48] He, S., Teagle, H.F.B., Buchman, C.A. (2017). The electrically evoked compound action potential: From laboratory to clinic. *Front Neurosci, 11*, 1-20.

[49] Heydebrand, G., Hale, S., Potts, L., et al. (2007). Cognitive predictors of improvements in adults' spoken word recognition six months after cochlear implantation. *Audiol Neurootol, 12*, 254-264.

[50] Hinojosa, R., Marion, M. (1983). Histopathology of profound sensorineural deafness. *Ann N Y Acad Sci*, *405*(1), 459–484.

[51] Holden, L.K., Finley, C.C., Firzst, J.B., et al. (2013). Factors affecting open-set word recognition in adults with cochlear implants. *Ear Hear, 34*, 342-360.

[52] Hughes, M.L., Vander Werff, K.R., Brown, C.J., et al. (2001). A longitudinal study of electrode impedance, the electrically evoked compound action potential, and behavioral measures in Nucleus 24 cochlear implant users. *Ear Hear, 22*, 471-486.

[53] Hughes, M.L. (2012). Objective measures in cochlear implants. http://ebookcentral.proquest.com. Accessed 15 January 2019

[54] Hughes, M.L., Goehring, J.L., Baudhuin, J.L. (2017). Effects of stimulus polarity and artifact reduction method on the electrically evoked compound action potential. *Ear Hear 38*, 332-343.

[55] Hughes, M.L., Sangsook, C., Glickman, E. (2018). What can stimulus polarity and interphase gap tell us about auditory nerve function in cochlear-implant recipients? *Hear Res, 359*, 50-63.

[56] Hurvich, C.M., Tsai, C. (1989). Regression and time series model selection in small samples. *Biometrika, 76*, 297-307.

[57] Jahn, K.N., DiNino, M., Arenberg, J.G. (2019). Reducing simulated channel interaction reveals differences in phoneme identification between children and adults with normal hearing. *Ear Hear, 40*(2), 295-311.

[58] Jahn, K.N., Arenberg, J.G. (2019). Evaluating psychophysical polarity sensitivity as an indirect estimate of neural status in cochlear implant listeners. *J Assoc Res Otolaryngol*, DOI: 10.1007/s10162-019-00718-2.

[59] Johnsson, L.-G. (1974). Sequence of degeneration of corti's organ and its first-order neurons. *Ann Otol, 83*, 294-303.

[60] Jolly, C.N., Spelman, F.A., Clopton, B.M. (1996). Quadrupolar stimulation for cochlear prostheses: modeling and experimental data. *IEEE Trans Biomed Eng, 43*, 857-865.

[61] Joshi, S.N., Dau, T., Epp, B. (2017). A model of electrically stimulated auditory nerve fiber responses with peripheral and central sites of spike generation. *J Assoc Res Otolaryngol, 18*, 323-342.

[62] Kamakura, A., Nadol, J.B. (2016). Correlation between word recognition score and intracochlear new bone and fibrous tissue after cochlear implantation in the human. *Hear Res, 339*, 132-141.

[63] Khan, A.M., Handzel, O., Burgess, B.J., et al. (2005). Is word recognition correlated with the number of surviving spiral ganglion cells and electrode insertion depth in human subjects with cochlear implants? *Laryngoscope*, *115*(4), 672–677.

[64] Kim, J-R., Abbas, P.J., Brown, C.J., et al. (2010). The relationship between electrically evoked compound action potential and speech perception: A study in cochlear implant users with short electrode array. *Otol Neurotol, 31*, 1041-1048.

[65] Koles, Z.J., Rasminsky, M. (1972). A computer simulation of conduction in demyelinated nerve fibers. *J Physiol, 227*(2), 351-364.

[66] Kujawa, S.G., Liberman, M.C. (2006). Acceleration of age-related hearing loss by early noise exposure: Evidence of a misspent youth. *J Neurosci, 26*(7), 2115-2123.

[67] Kujawa, S.G., Liberman, M.C. (2009). Adding insult to injury: Cochlear nerve degeneration after "temporary" noise-induced hearing loss. *J Neurosci, 29*(45), 14077 -14085.

[68] Kuznetsova, A., Brokhoff, P.B., Christensen, R.H.B. (2017). lmerTest Package: Tests in linear mixed effects models. *J Statistical Softw, 82*, 1-26.

[69] Kral, A., Hartmann, R., Mortazavi, D., et al. (1998). Spatial resolution of cochlear implants: The electrical field and excitation of auditory afferents. *Hear Res, 121*, 11-28.

[70] Lazard, D.S., Vincent, C., Venail, F., et al. (2012). Pre-, per- and postoperative factors affecting performance of postlinguistically deaf adults using cochlear implants: A new conceptual model over time. *PLoS One, 7*, e48739.

[71] Leake, P.A., Hradek, G.T., Rebscher, S.J., et al. (1991). Chronic intracochlear electrical stimulation induces selective survival of spiral ganglion neurons in neonatally deafened cats. *Hear Res, 54*, 251-271.

[72] Leake, P.A., Snyder, R.L., Hradek, G.T., et al. (1992). Chronic intracochlear electrical stimulation in neonatally deafened cats: Effects of intensity and stimulating electrode location. *Hear Res, 64*, 99-117.

[73] Leake, P.A., Hradek, G.T., Snyder, R.L. (1999). Chronic electrical stimulation by a cochlear implant promotes survival of spiral ganglion neurons after neonatal deafness. *J Comp Neurol, 412*, 543-562.

[74] Lenth, R. (2018). emmeans: Estimated Marginal Means, aka Least-Squares Means. R package version 1.3.0. https://CRAN.R-project.org/package=emmeans

[75] Linthicum, F.H., Fayad, J., Otto, S.R., et al. (1991). Cochlear implant histopathology. *Am J Otol, 12*, 245-311.

[76] Loizou, P.C., Dorman, M., & Fitzke, J. (2000). The effect of reduced dynamic range on speech understanding: Implications for patients with cochlear implants. *Ear Hear, 21*(1), 25-31.

[77] Long, C.J., Holden, T.A., McClelland, G.H., et al. (2014). Examining the electro-neural interface of cochlear implant users using psychophysics, CT scans, and speech understanding. *J Assoc Res Otolaryngol, 15*, 293-304.

[78] Lousteau, R.J. (1987). Increased spiral ganglion cell survival in electrically stimulated, deafened guinea pig cochleae. *Laryngoscope, 97*, 836-842.

[79] Macherey, O., van Wieringen, A., Carlyon, R.P., et al. (2006). Asymmetric pulses in cochlear implants: Effects of pulse shape, polarity, and rate. *J Assoc Res Otolaryngol, 7*, 253-266.

[80] Macherey, O., Carlyon, R.P., van Wieringen, A., et al. (2008). Higher sensitivity of human auditory nerve fibers to positive electrical currents. *J Assoc Res Otolaryngol, 9*, 241-251.

[81] Macherey, O., Carlyon, R.P., Chatron, J., et al. (2017). Effect of pulse polarity on thresholds and on non-monotonic loudness growth in cochlear implant users. *J Assoc Res Otolaryngol, 18*, 513-527.

[82] Makary, C.A., Shin, J., Kujawa, S.G., et al. (2011). Age-related primary cochlear neuronal degeneration in human temporal bones. *J Assoc Res Otolaryngol*, *12*(6), 711 -717.

[83] McNeish, D. (2017). Small sample methods for multilevel modeling: A colloquial elucidation of REML and the Kenward-Roger correction. *Multivariate Behav Res, 52*, 661-670.

[84] Miller, C.A., Abbas, P.J., Robinson, B.K. (1994). The use of long-duration current pulses to assess nerve survival. *Hear Res, 78*, 11-26.

[85] Molisz, A., Zarowski, A., Vermeiren, A., et al. (2015). Postimplantation changes of electrophysiological parameters in patients with cochlear implants. *Audiol Neurootol, 20*, 222-228.

[86] Nadol, J.B., Young, Y.S., Glynn, R.J. (1989). Survival of spiral ganglion cells in profound sensorineural hearing loss: Implications for cochlear implantation. *Ann Otol Rhinol Laryngol, 98*, 411-416.

[87] Nadol, J.B. (1997). Patterns of neural degeneration in the human cochlea and auditory nerve: Implications for cochlear implantation. *Otolaryngol Head Neck Surg, 117*, 220 -228.

[88] Nadol, J.B., Burgess, B.J., Gantz, B.J., et al. (2001). Histopathology of cochlear implants in humans. *Ann Otol, Rhinol Laryngol*, *110*(9), 883–891.

[89] Nakagawa, S., Schielzeth, H. (2013). A general and simple method for obtaining R^2 from generalized linear mixed-effects models. *Methods Ecol Evol, 4*, 133-142.

[90] Nayagam, B.A., Muniak, M.A., Ryugo, D.K. (2011). The spiral ganglion: Connecting the peripheral and central auditory systems. *Hear Res, 278*, 2-20.

[91] Nehme, A., El Zir, E., Moukarzel, N., et al. (2014). Measures of the electrically evoked compound action potential threshold and slope in HiRes 90K users. *Cochlear Implants Int, 15(*1), 53-60.

[92] Nie, K., Barco, A., Zeng, F.-G. (2006). Spectral and temporal cues in cochlear implant speech perception. *Ear Hear*, *27*(2), 208–217.

[93] Niparko, J.K., Tobey, E.A., Thal, D.J., et al. (2010). Spoken language development in children following cochlear implantation. *JAMA, 303*(15), 1498-1506.

[94] Noble, J.H., Labadie, R.F., Gifford, R.H., et al. (2013). Image-guidance enables new methods for customizing cochlear implant stimulation strategies. *IEEE Trans Neural Syst Rehabil Eng, 21*(5), 820-829.

[95] Noble, J. H., Gifford, R. H., Hedley-Williams, A. J., et al. (2014). Clinical evaluation of an image-guided cochlear implant programming strategy. *Audiol Neurootol*, *19*(6), 400 -411.

[96] Noble, J.H., Hedley-Williams, A.J., Sunderhaus, L., et al. (2016). Initial results with image-guided cochlear implant programming in children, *Otol Neurotol, 37*(2), e63-e69.

[97] Otte, J.M.D., Schuknecht, H.F.M.D., Kerr, A.G.M B. (1978). Ganglion cell populations in normal and pathological human cochleae: Implications for cochlear implantation. *Laryngoscope*, *88*(8).

[98] Pelliccia, P., Venail, F., Bonafe, A., et al. (2014). Cochlea size variability and implications in clinical practice. *Acta Otorhinolaryngol Ital, 34*, 42-49.

[99] Pfingst, B.E., Xu, L., Thompson, C.S. (2004). Across-site threshold variation in cochlear implants: Relation to speech recognition. *Audiol Neurootol*, *9*, 341–352.

[100] Pfingst, B.E., Xu, L. (2004). Across-site variation in detection thresholds and maximum comfortable loudness levels for cochlear implants. *J Assoc Res Otolarnygol, 5*(1), 11–24.

[101] Pfingst, B.E., Colesa, D.J., Hembrador, S., et al. (2011). Detection of pulse trains in the electrically stimulated cochlea: effects of cochlear health. *J Acoust Soc Am, 130*, 3954 -3968.

[102] Pfingst, B.E., Zhou, N., Colesa, D.J., et al. (2015a). Importance of cochlear health for implant function. *Hear Res*, *322*, 77–88.

[103] Pfingst. B.E., Hughes, A.P., Colesa, D.J., et al. (2015b). Insertion trauma and recovery of function after cochlear implantation: Evidence from objective functional measures. *Hear Res, 330*, 98-105.

[104] Prado-Guitierrez, P., Fewster, L.M., Heasman, J.M., et al. (2006). Effect of interphase gap and pulse duration on electrically evoked potentials is correlated with auditory nerve survival. *Hear Res, 215*, 47-55.

[105] R Core Team (2016). R: A language and environment for statistical computing. R Foundation for Statistical Computing. https://www.R-project.org/.

[106] Rader, T., Baumann, U., Stöver, T., et al. (2016). Management of cochlear implant electrode migration. *Otol Neurotol, 37*, e341-e348.

[107] Ramekers, D., Versnel, H., Strahl, S.B., et al. (2014). Auditory-nerve responses to varied inter-phase gap and phase duration of the electric pulse stimulus as predictors for neuronal degeneration. *J Assoc Res Otolarnygol*, *15*(2), 187–202.

[108] Rattay, F. (1999). The basic mechanism for the electrical stimulation of the nervous system. *Neuroscience, 89*(2), 335-346.

[109] Rattay, F., Lutter, P., Felix, H. (2001a). A model of the electrically excited human cochlear neuron I. Contribution of neural substructures to the generation and propagation of spikes. *Hear Res, 153*, 43-63.

[110] Rattay, F., Lutter, P., Felix, H. (2001b). A model of the electrically excited human cochlear neuron II. Influence of the three-dimensional cochlear structure on neural excitability. *Hear Res, 153*, 64-79.

[111] Resnick, J.M., O'Brien, G.E., Rubinstein, J.T. (2018). Simulated auditory nerve axon demyelination alters sensitivity and response timing to extracellular stimulation. *Hear Res, 361*, 121-137.

[112] Robb, R.A. (2001). The biomedical imaging resource at Mayo Clinic. *IEEE Trans Med Imaging, 20*, 854–867.

[113] Sarkar, D. (2008). *Lattice: Multivariate data visualization with R*. Springer, New York.

[114] Scheperle, R.A. (2017). Suprathreshold compound action potential amplitude as a measure of auditory function in cochlear implant users. *J Otol, 12*, 18-28.

[115] Schvartz-Leyzac, K.C., Pfingst, B.E. (2016). Across-site patterns of electrically evoked compound action potential amplitude-growth functions in multichannel cochlear implant recipients and the effects of the interphase gap. *Hear Res*, *341*, 50–65.

[116] Schvartz-Leyzac, K.C., Pfingst, B.E. (2018). Assessing the relationship between the electrically evoked compound action potential and speech recognition abilities in bilateral cochlear implant recipients. *Ear Hear, 39*, 344-358.

[117] Sék, A., Alcantara, J., Moore, B.C.J., et al. (2005). Development of a fast method for determining psychophysical tuning curves. *Int J Audiol. 44*, 408–420.

[118] Seyyedi, M., Viana, L.M., Nadol, J.B. (2014). Within-subject comparison of word recognition and spiral ganglion cell count in bilateral cochlear implant recipients. *Otol Neurotol, 35*(8), 1446-1450.

[119] Shannon, R.V., Jensvold, A., Padilla, et al. (1999). Consonant recordings for speech testing. *J Acoust Soc Am*, *106*(6), L71-74.

[120] Shannon, R., Fu, Q.-J., Galvin Iii, J. (2004). The number of spectral channels required for speech recognition depends on the difficulty of the listening situation. *Acta Oto Laryngol*, *124*, 50–54.

[121] Shepherd, R.K., Hatsushika, S., Clark, G.M. (1993). Electrical stimulation of the auditory nerve: The effect of electrode position on neural excitation. *Hear Res, 66*, 108-120.

[122] Shepherd, R.K., Javel, E. (1997). Electrical stimulation of the auditory nerve. I. Correlation of physiological responses with cochlear status. *Hear Res*, *108*(1–2), 112 -144.

[123] Shepherd, R.K., Javel, E. (1999). Electrical stimulation of the auditory nerve: II. Effect of stimulus waveshape on single fiber response properties. *Hear Res, 130*(1-2), 171-188.

[124] Skinner, M.W., Holden, T.A., Whiting, B.R., et al. (2007). In vivo estimates of the position of Advanced Bionics electrode arrays in the human cochlea. *Ann Otol Rhinol Laryngol, 197*, 1-24.

[125] Smith, L., Simmons, F.B. (1983). Estimating eighth nerve survival by electrical stimulation. *Ann Otol Rhinol Laryngol*, *92*, 19–23.

[126] Spelman, F.A., Clopton, B.M., Pfingst, B.E. (1982). Tissue impedance and current flow in the implanted ear. Implications for the cochlear prosthesis. *Ann Otol Rhinol Laryngol Suppl, 98,* 3–8.

[127] Spitzer, E.R., Hughes, M.L. (2017). Effect of stimulus polarity on physiological spread of excitation in cochlear implants. *J Am Acad Audiol*, *28*(9), 786–798.

[128] Srinivasan, A.G., Padilla, M., Shannon, R.V., et al. (2013). Improving speech perception in noise with current focusing in cochlear implant users. *Hear Res, 299*, 29-36.

[129] Studebaker, G.A. (1985). A "rationalized" arcsine transform. *J Speech Hear Res, 28*, 455-462.

[130] Tasaki, I. (1955). New measurements of the capacity and the resistance of the myelin sheath and the nodal membrane of the isolated frog nerve fiber. *Am J Physiol, 181*, 639 -650.

[131] Teymouri, J., Hullar, T.E., Holden, T.A., et al. (2011). Verification of computed tomographic estimates of cochlear implant array position: A micro-CT and histologic analysis. *Otol Neuroto,l 32*, 980-986.

[132] Todd, A.E., Goupell, M.J., Litovksy, R.Y. (2017). The relationship between intensity coding and binaural sensitivity in adults with cochlear implants. *Ear Hear, 38*(2), e128 -e141.

[133] Turner, C., Mehr, M., Hughes, M., et al. (2002). Within-subject predictors of speech recognition in cochlear implants: A null result. *Acoust Res Lett Online, 3*(3), 95-100.

[134] Undurraga, J.A., van Wieringen, A., Carlyon, R.P., et al. (2010). Polarity effects on neural responses of the electrically stimulated auditory nerve at different cochlear sites. *Hear Res, 269*, 146-161.

[135] Undurraga, J.A., Carlyon, R.P., Wouters, J., et al. (2013). The polarity sensitivity of the electrically stimulated human auditory nerve measured at the level of the brainstem. *J Assoc Res Otolaryngol, 14*, 359-377.

[136] Vaerenberg, B., Smits, C., De Ceulaer, G., et al. (2014). Cochlear implant programming: A global survey on the state of the art. *Sci World J*, *2014*, 1–12.

[137] van Eijl, R.H.M., Buitenhuis, P.J., Stegeman, I., et al. (2017). Systematic review of compound action potentials as predictors for cochlear implant performance. *Laryngoscope, 127*, 476-487.

[138] Vanpoucke, F.J., Zarowski, A.J., Peeters, S.A. (2004). Identification of the impedance model of an implanted cochlear prosthesis from intracochlear potential measurements. *IEEE Trans Biomed Eng, 51*, 2174–2183.

[139] van Wieringen, A., Macherey, O., Carlyon, R.P., et al. (2008). Alternative pulse shapes in electrical hearing. *Hear Res, 242*, 154-163.

[140] Voie, A.H., Burns, D.H., Spelman, F.A. (1993). Orthogonal-plane fluorescence optical sectioning: Three-dimensional imaging of macroscopic biological specimens. *J Microsc, 170*, 229-236.

[141] Xu, L., Thompson, C.S., Pfingst, B.E. (2005). Relative contributions of spectral and temporal cues for phoneme recognition. *J Acoust Soc Am*, *117*(5), 3255–3267.

[142] Young, N.M., Grohne, K.M. (2001). Comparison of pediatric Clarion recipients with and without the electrode positioner. *Otol Neurotol, 22*, 195-199.

[143] Zeng, F.-G., Galvin, J.J. (1999). Amplitude mapping and phoneme recognition in cochlear implant listeners. *Ear Hear, 20*(1), 60-74.

[144] Zhou, N., Xu, L., Pfingst, B.E. (2012). Characteristics of detection thresholds and maximum comfortable loudness levels as a function of pulse rate in human cochlear implant users. *Hear Res, 284*, 25-32.

[145] Zhou, N., Pfingst, B.E. (2014). Relationship between multipulse integration and speech recognition with cochlear implants. *J Acoust Soc Am, 136*, 1257-1268.

[146] Zhou, N., Kraft, C.T., Colesa, D.J., et al. (2015). Integration of pulse trains in humans and guinea pigs with cochlear implants. *J Assoc Res Otolarnygol*, *16*(4), 523–534.

[147] Zhou, N. (2017). Deactivating stimulation sites based on low-rate thresholds improves spectral ripple and speech reception thresholds in cochlear implant users. *J Acoust Soc Am, 141*, EL243-EL248.

[148] Zhu, Z., Tang, Q., Zeng, F.-G., et al. (2012). Cochlear-implant spatial selectivity with monopolar, bipolar and tripolar stimulation. *Hear Res*, *283*(1–2), 45–58.

[149] Zilberstein, Y., Liberman, M.C., Corfas, G. (2012). Inner hair cells are not required for survival of spiral ganglion neurons in the adult cochlea. *J Neurosci, 32*(2), 405-410.